In this issue

Front Cover

New Caledonia and (inset) Tropical Cyclone Erica:– see articles on pages 2 and 7. © Thierry Lefort.

Editorial

On page 2 Thierry Lefort (Météo-France) outlines the progress that forecasters have made in medium-range forecasting for New Caledonia using ECMWF and other forecast products, while on page 7 François Lalaurette gives an update on recent developments at ECMWF in predicting tropical cyclones in the early medium-range, and describes some new products available on the web site. The difficult practical decisions that forecasters have to make when faced with the threat of severe weather are discussed on page 15 by members of the Turkish Weather Service. The article on page 16 by Martin Leutbecher and colleagues describes some experiments to assess the usefulness of making additional targeted observations in areas that are considered likely to be sensitive for the subsequent forecast. Details of the improvements made to the Integrated Forecasting System in two recent cycles – Cycle 26r3 (operational on 7 October 2003) and Cycle 28r1 (operational on 9 March 2004) – are given by Jean-Noël Thépaut and colleagues on page 26. Finally, on page 36 John Hennessy looks back into the early history of the Centre and describes the problems involved in producing the first operational forecasts 25 years ago.

Peter White

Changes to the operational weather prediction system

28 September 2004 – Cycle 28r3 was introduced. This included changes to the:

◆ **Physics** – Revised numerics of the convection scheme and the calling of the cloud scheme; use of the tangent linear and adjoint of vertical diffusion in the first minimization of 4D-Var; reduction of the radiation frequency to one hour in the high-resolution forecasts; improved numerics of surface tile coupling; post-processing of total-column liquid water and ice.

◆ **Use of satellite data** – RTTOV-8; minor revisions to ATOVS and AIRS usage; assimilation of MSG clear-sky radiances and GOES-9 BUFR AMVs; assimilation of SCIAMACHY ozone products from KNMI; correction of error in AMSU-B usage over land; activation of EARS data.

◆ **Data assimilation** – Blacklist SYNOP humidity data at local night time; increased use of radiosonde humidity (using RS90 to -80°C, RS80 to -60°C, other sensors to -40°C); proper cycling of the information from the wave altimeter and the surface data analyses (first-guess forecasts moved from 00 and 12 UTC to 06 and 18 UTC).

◆ **EPS** – Gaussian sampling for extratropical singular vectors instead of selection and rotation; revision of initial–condition perturbations for tropical cyclones (initial condition perturbations extended to latitude belts 40°S and 40°N from 25°S and 25°N, and tropical singular vectors are computed in the subspace orthogonal to the leading 25 extratropical singular vectors); new algorithm to determine optimisation regions based on predicted tropical cyclone tracks from previous EPS run (the Caribbean remains an optimisation region if no tropical cyclone is in the vicinity); orthonormalisation applied to the set of all tropical singular vectors).

7 October 2004 – Monthly forecasts run operationally on a weekly basis (Thursdays).

18 October 2004 – The bias correction for AMSU-A and AIRS satellites was harmonised. The bias correction for AMSU-B and HIRS was simplified to use two predictors.

9 November 2004 – All four BC-project analyses used background fields generated from the latest operational 4D-Var analysis

François Lalaurette

Starting up medium-range forecasting for New Caledonia in the South-West Pacific Ocean – a not so boring tropical climate

New Caledonia is located 1500km east of Queensland, Australia, between 18°S and 23°S. Its surface is 19,000km^2. The main island or Grande Terre is 400km long and 50km wide, with a mountain range roughly parallel to the coasts that reaches 1000 to 1600m in altitude. Smaller islands are located to the north and to the south. The lagoon is 8000km^2 in area and as much as 65km wide. One hundred kilometres to the east lie the Loyauté islands; these are flat, coral islands (Figure 1).

Photograph © Thierry Lefort
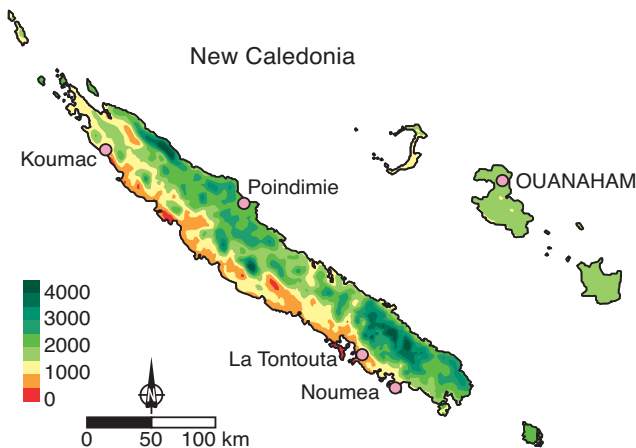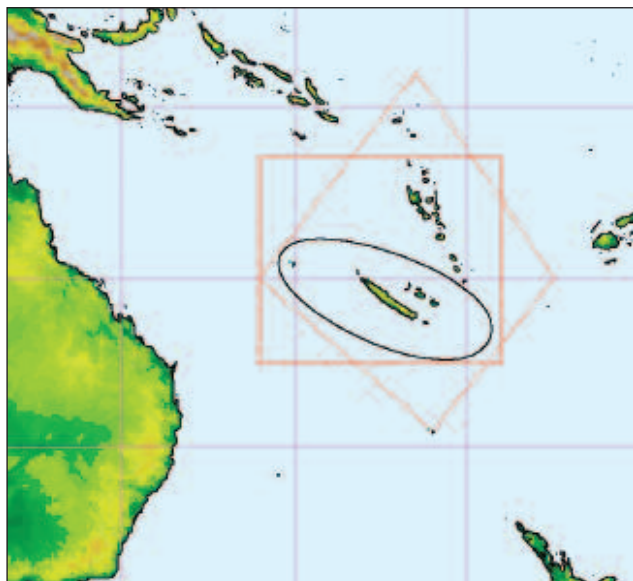
New Caledonia is located just north of the Tropic of Capricorn, but its climate is said to be 'maritime tropical'. The year is divided roughly into two periods. The cool season lasts from May to October: extratropical lows form in the Tasman Sea and we get occasional cold fronts associated with short periods of westerlies. The average low temperature in July is 11.8°C in the western lowlands, so that morning temperatures of less than 10°C are frequent. The lowest temperature recorded in flat areas is 2.3°C on the Grande Terre, and 2.7°C on the Loyauté islands! The hot season lasts from November to April; it is also called the tropical-cyclone or rainy season. Since the elongated Grande Terre is roughly perpendicular to the prevailing easterlies, there is a considerable difference between the east coast, which is humid and green, and the west coast, which is much drier in the lee of the range (Figure 2).

As New Caledonia is a French Territory, Météo-France is in charge of meteorology. The last decade has seen tremendous changes in the working environment of Météo-France forecasters in New Caledonia: the workstation Synergie was installed in 1994; two precipitation radars are now operating, with a third due to be operating soon; and the forecaster is provided with several global models, including the French model ARPEGE TROPIQUE and the ECMWF T511 fields displayed on a 0.5 degree grid at six-hour intervals. Ensemble products are also available from the workstation, the Intranet

Fig. 1 (upper) A map of south-west Pacific Ocean. The oval shows the New Caledonian territory. The square is the domain for tropical cyclone warnings. The diamond-shape is the domain for marine bulletins. (lower) Detail of New Caledonia and the nearby islands.
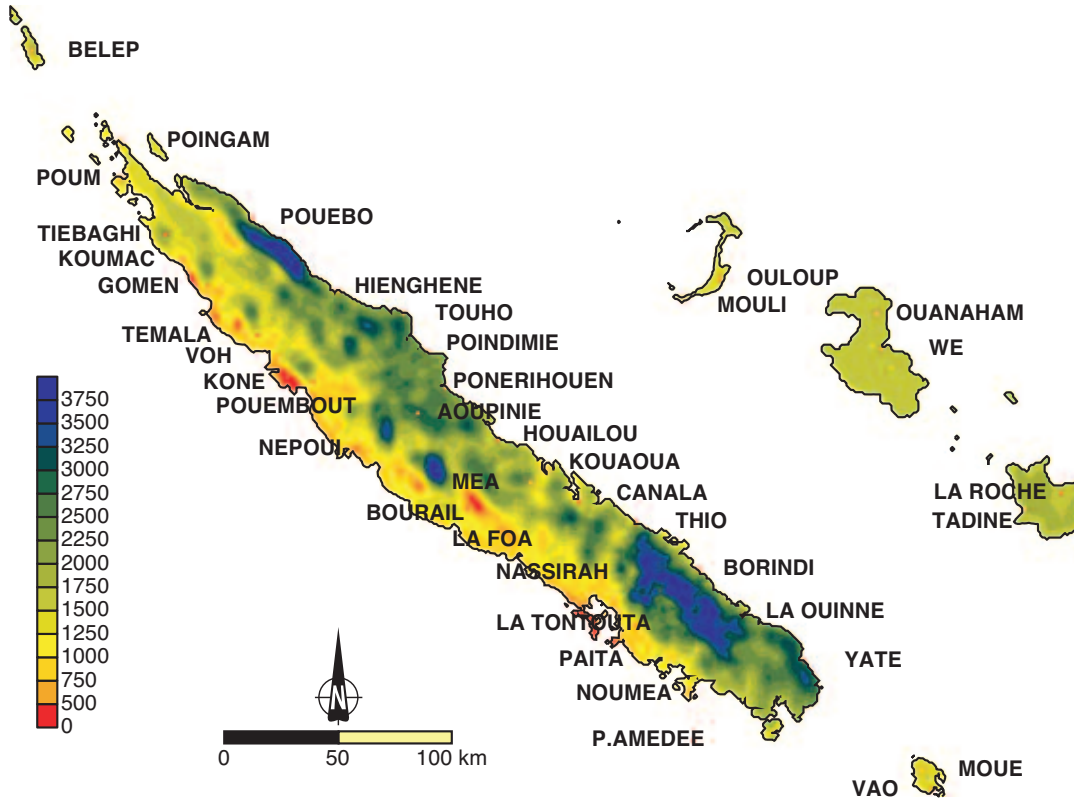
Fig. 2 Reconstruction of the annual precipitation for New Caledonia for the period 1991–2000 using the model Aurelhy (mm).

page of the Predictability Section of Météo-France's Central Forecasting Office, and of course the ECMWF website.

What is predictable?

The current public bulletin issued by Météo-France in New Caledonia covers the period from Day 2 to Day 5 (Day 1 is the day the bulletin is issued).

Over the Atlantic Ocean, *Chessa and Lalaurette* (2001) have shown that a probabilistic forecast of flow patterns (*Ayrault et al.*, 1995) beats climatology, even at Day 9. In 2002, the skill of the ECMWF model for the Southern Hemisphere matched the one for the Northern Hemisphere (*Hollingsworth et al.*, 2003). For the domain covering Australia and New Zealand (including New Caledonia), the Australian Bureau of Meteorology reports that ECMWF produces useful guidance out to at least seven days (François Lalaurette suggested at the 2004 ECMWF users' meeting that 7½ days was more appropriate).

As for the tropics, *Kanamitsu* (1985) pointed out that errors grow very fast there during the first 24 hours compared with those in the extratropics, and then grow more slowly. He added that the choice of parameters to be verified in the tropics needed some discussion. Since that time, however, today's tropical or subtropical forecaster has been provided with very little additional information about improvements in numerical model skill within his domain of interest, except for hurricane tracks.

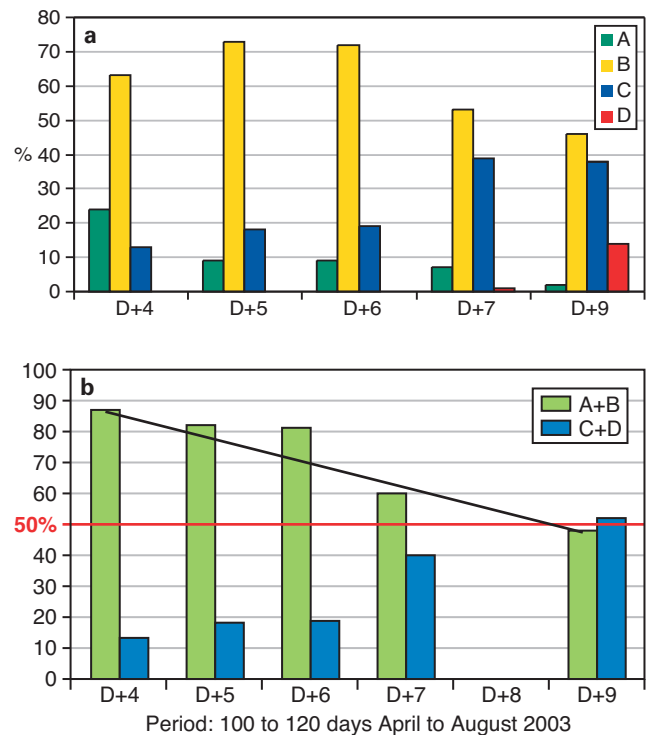**Fig. 3** (a) The percentage of marks A (very good), B (good), C (rather bad), D (very bad) given by the forecaster to the pattern of the ensemble mean forecasts in April to August 2003 during the cool season (influenced by extratropical features). (b) The same marking system and period as (a), but with A and B grouped together and C and D grouped together, showing that good forecasts are possible out to about Day 9.

The Ensemble Prediction System (EPS) provides a useful guidance for the New Caledonian forecaster up to Day 8

We decided to start a subjective evaluation of the EPS for New Caledonia. We used standard charts available at the time: the ensemble means of the 1000 hPa geopotential (Z1000), the 850 hPa temperature (T850) and the 500 hPa geopotential and temperature (ZT500), as well as the precipitation on threshold probability maps over the south-west Pacific domain. Marks were given by one forecaster for the accuracy of forecasts from 108 hours (noon local time on Day 5) to 228 hours (noon on Day 10) according to the following:

A Large-scale and details correct;

B Large-scale correct, but some details wrong;

C Large-scale correct but the flow pattern too wrong around New Caledonia to allow a good forecast;

D Large-scale totally wrong.

The results for a four-month period (mostly during the cool season) are presented in Figures 3(a) and (b). Up to Day 8, the ensemble mean seems to allow the forecaster to predict the type of circulation induced by the movements of the subtropical anticyclones, the position of the intertropical convergence zone (ITCZ), etc.

An additional investigation was to check to see if the EPSgrams had any significant skill in our area. We studied one-year archives for Noumea EPSgrams, kindly provided by the ECMWF staff. We compared the EPSgrams with the description of weather changes and major rain events reported in the monthly weather summary. We defined as major rain events the cases when all or most of the rain gauges registered significant amounts (this includes extreme events); such events explain a large part of the monthly rain amounts and anomalies, especially in the cool season. We found that the EPSgrams are a very powerful product for providing the forecaster with an early warning of changes in weather regimes and of the probability of major rain events. Furthermore, they are surprisingly consistent in the signal, which is sometimes not the case with the deterministic model; Figure 4 illustrates a good example (one among many!). Four consecutive EPSgrams (one per day) are presented and illustrate that the signal of weather change and rain is given as early as seven days in advance, (n.b. the vertical scale for the rainfall varies from one panel to another). It seems that the ensemble gets the signal two days earlier than the deterministic run.

Let's define weather regimes

Previous study has shown that major rain events usually occur with a marked change in weather regime. Reading the fifty-year archives of the monthly weather summary shows that weather regime is not a new concept at all. The most famous and most frequent one throughout the year is the trade-wind regime, called (back in the 1950s) the 'indirect polar maritime air mass'. On the basis of this existing knowledge the present-day forecasters agreed on a classification into seven different weather regimes:

◆ Trade-wind regime;

◆ Large-scale convergence;

◆ Easterly flow;

◆ Northerly flow;

◆ Westerly flow;

◆ Anticyclonic;

◆ Shift of the ITCZ.

Forecaster and climatologist meet

Figure 5 is an example of very good correlation between periods of weather regimes described by the forecasters, and the daily temperature curve presented by the climatologist for a hot-season month. The first six days belong to the anticyclonic weather regime: no wind, moist (dew point 25-27°C) and much hotter than normal day and night in Noumea under 'continental' north-easterlies. These are described by the public-at-large as 'oppressive conditions', and lead to intensive use of air conditioning in offices and houses day and night. The hottest spots of the west coast get highs of 38-39°C in such a situation. The second period is associated with a nine-day easterly flow; hotter than average, but not as extreme. Noumea gets wind in such a situation, so that the comfort index is more acceptable; one can sleep without air conditioning in ventilated houses. Then, a six-day trade-wind period brings near normal temperatures, lower dew-points and sustained wind day and night; this is pleasant summer weather, with reasonably hot days and cool nights (18°C in the bush), when air conditioning is not considered a necessary comfort.

As a summary, the classification based on weather charts such as the 850hPa flow fits well with climatological reports. Thus, predicting weather regimes leads to predicting socio-economical aspects such as energy consumption, health issues, level of tourism activity, etc.

Starting up an experimental, medium-range bulletin

A day-5 to day-8 experimental bulletin has been tested since March 2004. The forecaster uses the deterministic run, the ensemble mean, probability maps, EPSgrams for three locations in New Caledonia, spaghetti plots, EFI, etc. Note that the NCEP ensembles (same thresholds and 24-hour intervals for rain) and the US Navy ensembles are also available on the web. All these data provide us with a 'rich man's' ensemble made of three ensemble systems!

What we try to predict is the most likely type of weather prevailing over the whole country, by emphasising changes in weather regimes or long-lasting periods of the same weather. We have given up the idea of predicting day-to-day timing or geographical details. A first attempt at giving the uncertainty through a two-level confidence index has showed that more work is needed in that domain.

This bulletin is currently issued twice a week: on Monday, covering the following Thursday to Monday; and on Thursday, covering Monday to Thursday. Voluntary identified private customers and Météo-France agents have agreed to evaluate this product, by giving marks A to D, along the lines described earlier. The forecasters also give marks by checking satellite images, SYNOPs, and model analysis over the whole country.

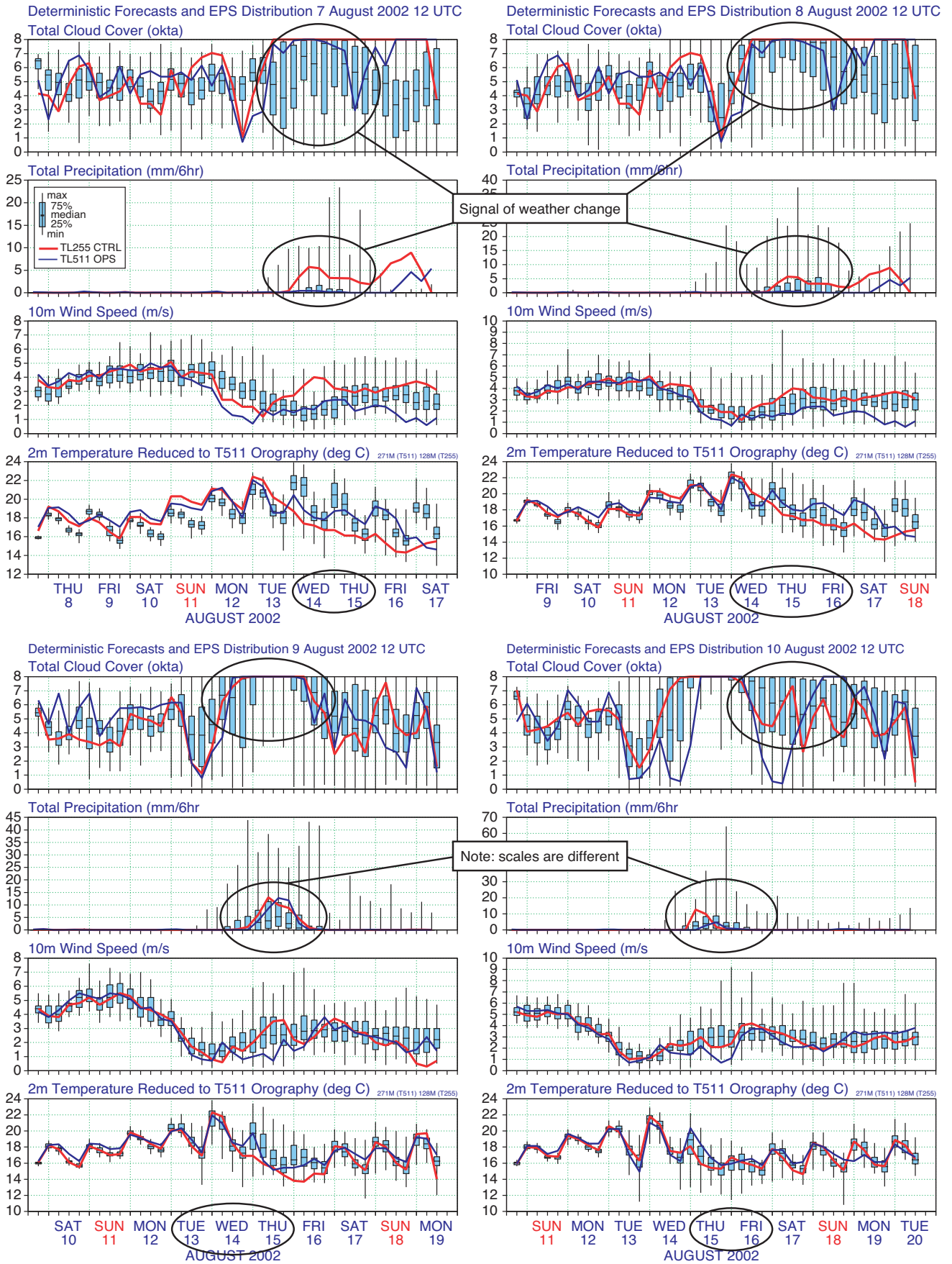**EPS Meteogram – Noumea 22.1°S , 166.3°E**

Fig. 4 EPSgrams for Noumea for 4 consecutive days in August 2002, showing the consistency of forecasts of a change in the weather pattern.
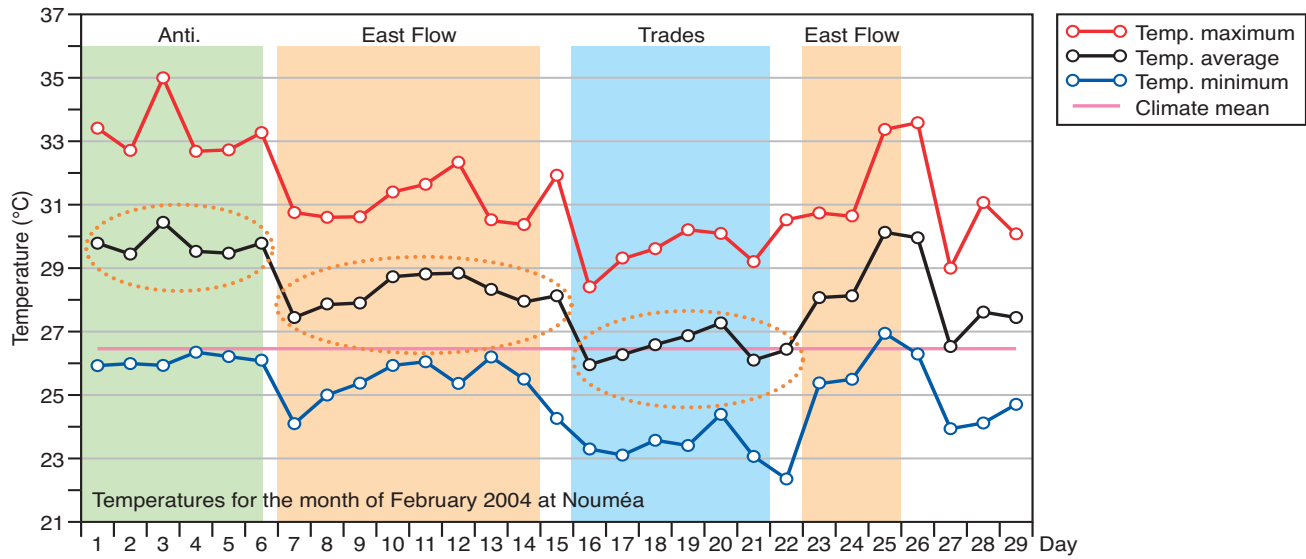
5

Fig. 5 Time-series of daily temperatures in Noumea for February 2004, showing the transitions between different weather regimes (red – maximum temperature; blue – minimum temperature; black – mean temperature; magenta – climatological mean temperature).

Firsts results are very encouraging

After five months, mostly in the cool season, the marks given by forecasters are shown in Figure 6. The A and B scores together represent 75% of the marks. Note that, for half the cases, a change in weather regime occurred during the Day-5 to Day-8 period; the marks were then slightly less good, but still well above 50%. Table 1 is a contingency table for major rain events: hit rate, false-alarm rates and rates of missed events show a good skill. It is important to say that there is a good correlation between the marks given by the forecasters and those given by the end users (not shown), a result which pleases us well.
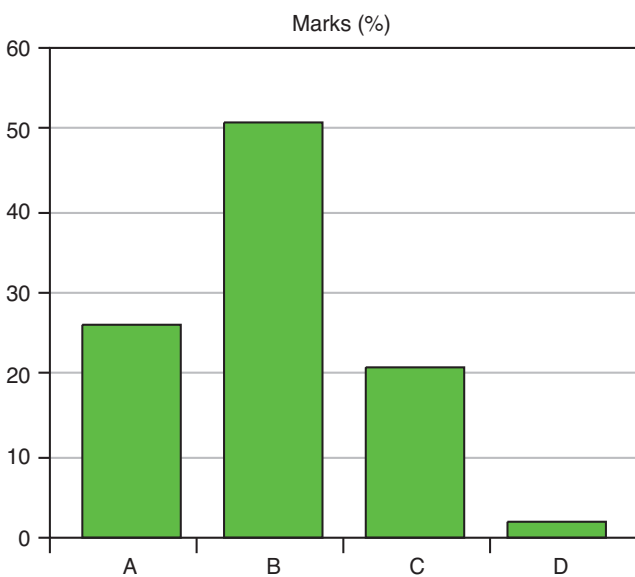

Fig. 6 The percentage of marks given by forecasters to the experimental medium-range bulletin (marking system as in Figure 3).

Perspectives: go for a week-two forecast!

We must now continue this evaluation during the rainy season. Indeed, in summer the predictability of the weather seems to be lower, due to the fact that highly-convective rain events can be driven by small changes in the weather pattern, so that small errors in the flow can lead to large errors for the public. Moreover, the numerical models often encounter problems when dealing with tropical cyclones, which could lead to erroneous large-scale patterns. If more controls were to be developed, an objective classification similar to the one used for the Atlantic Ocean (*Ayrault*, 1995) should be undertaken.

The next few years are very promising in terms of extended medium-range forecasting. First, the upgrading of the ensemble prediction system, with higher resolution, is expected to bring improved accuracy of the Day 7 bulletins. Then, the monthly forecast system shows some skill over the western Pacific Ocean for Week 2, and maybe Week 3. Hovmöller diagrams, which present anomalies averaged over a longitude, might be a powerful tool to predict anomalous blocking situations, or major changes in weather patterns. We should learn how to use them in an efficient way. Finally, tropical cyclone activity in the south–west Pacific Ocean has proven to be very sensitive to the Madden–Julian Oscillation, and a statistical model has just been developed (*Leroy*, 2004) which shows good skill at least for Week 2. All these new products should enable us to extract some valuable information for the second week, at least for a certain category of users. For sure, more work is to come for tropical forecasters!

Forecast		Observed		
		Yes	No	Total
	Yes	6	2	8
	No	3	26	29
	Total	9	28	37

Table 1 Contingency table for the prediction of major rain events.

FURTHER READING

Ayrault, **F.**, **F. Lalaurette**, **A. Joly** and **C. Loo**, 1995: North Atlantic ultra high frequency variability. *Tellus*, **47A**, 671-696

Chessa, **P.A.** and **F. Lalaurette**, 2001: Verification of the ECMWF ensemble prediction system forecasts: A study of large-scale patterns. *Weather and Forecasting*, **16**, 611-619

Hollingsworth, **A.**, **A.J. Simmons**, **A. Ghelli**, **T. Tsuyuki** and **T. Hart**; 2003: Improvements in the skill of numerical weather prediction with global models. *WMO Bulletin*, **52**, 33-39

Kanamitsu, **M.**, 1985: A study of the predictability of the ECMWF operational forecast model in the tropics. *J. Met. Soc. Japan*, **96**, 779-804

Lalaurette, **F.** and **G. Van der Grijn**, 2003: Ensemble forecasts: can they provide useful warnings? *ECMWF Newsletter*, **96**, 10-18

Leroy, **A.**, 2004: 'Statistical prediction of the weekly tropical cyclone activity in the Southern Hemisphere'. *Rapport de stage de fin d'étude*, **939**, Météo-France, Met College-ENM, Toulouse, France

Vitart, **F.**, 2004: Monthly Forecasting. *ECMWF Newsletter*, **100**, 3-13

Thierry Lefort (Météo-France, New Caledonia)

Early medium-range forecasts of tropical cyclones

Tropical cyclones (TCs) are probably the most feared of all weather events. Their dreadful impact on human lives and properties is due to the combined effect of ferocious winds and torrential rains. It is, therefore, no surprise if meteorologists have tried for a long time to provide inhabitants of those countries facing the risk of being hit by TCs with the best possible forecasts.

While the advent of satellite geostationary imagery provided a first spectacular improvement in the monitoring of these events, we are probably currently living a less spectacular, but still important, step in forecasting TCs. With the advent of 4D-Var data assimilation techniques, the massive influx of new satellite observations (both passive radiances and microwave backscatter), increased global resolution and dynamical probabilistic methods (ensemble forecasts), global models are developing a capability of extending the range of useful forecasts for TC tracks into the early medium range. This is raising the prospect of advanced warnings that would undoubtedly help in planning mitigating actions.

Recent model improvements relevant for tropical cyclones

It is certainly difficult to isolate among the numerous important changes made during the past five years or so those that really have had the most important impact on our ability to analyse and forecast TCs. We will try, however, to summarise a few here (a comprehensive list of model changes can be retrieved at www.ecmwf.int/products/data/technical/model_id):

◆ Several changes have been brought to the 4D-Var data assimilation: new formulation and tuning of the background (J_b) and observation (J_o) statistics (in October 1999 and June 2000); nonlinear balance (introduced in January 2003); move from a six to a 12-hour optimisation period (September 2000); new humidity analysis (October 2003);

◆ Many new satellite observations have been activated, among which are SeaWinds from QuikSCAT (January 2002), SSMI winds (October 1999), AMSU (since May 1999) and AIRS (October 2003) radiances. Clear-sky radiances from geostationary satellites have been actively assimilated since July 1999;

◆ Dropsondes (such as those released in or around TCs) have been activated in the data assimilation since July 1999; higher-resolution winds derived from geostationary satellite sequences have also been included in several steps during the period;

◆ Model vertical and horizontal resolution were increased in March and October 1999 and in November 2000;

◆ Several important changes have been made to the microphysics and convection schemes (October 1999, January 2003 and October 2004);

◆ The oceanic wave model was fully (two-way) coupled to the atmospheric model in June 1998, with important consequences to the representation of momentum, heat and humidity fluxes near the sea surface;

◆ The EPS evolved singular vectors were introduced in March 1998 and stochastic physics in October 1998; EPS perturbations targeted at observed TCs were added in January 2002 (*Puri et al.* 2001) and revised in October 2004;

This latest series of changes introduced into the EPS have opened the door to the probabilistic forecast of TC tracks, a crucial development in order to extend the useful validity range of the forecasts. Unlike extratropical EPS perturbations that are computed semi-globally using a very simplified version of the model physics, tropical perturbations use a more comprehensive set of physical parametrizations. Because the natural scale-selection that operates in the extratropics is not present in the tropics, a global selection of unstable modes (singular vectors) cannot be produced in the same way. Rather, the optimisation of the most unstable perturbations is calculated over smaller areas, targeted over observed tropical cyclones (and, when available, their future track as forecast by the previous EPS run). An example of such targets is shown in Figure 1.
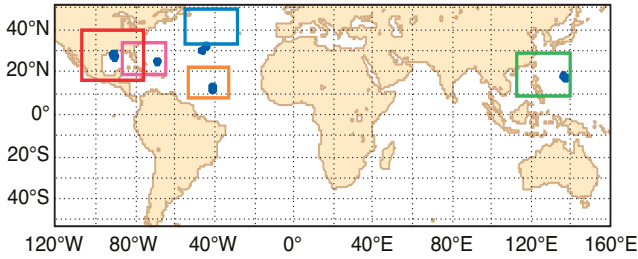
Fig. 1 EPS targeted areas (12 UTC 23 September 2004, pre-operational suite)

To keep a fair balance, it should be remembered that there are still severe limitations in the model's ability to cope with TCs.

◆ Insufficient resolution is obviously one limitation. In no way can the eye of the cyclone (where surface pressure drops to very low values over a short distance) be resolved with an 80 km, or even a 40 km, resolution model. The situation is even worse in terms of the analysis (increments currently have only about a 130 km resolution);

◆ The non-interaction between the atmospheric and oceanic components is another limitation. Indeed the sea surface temperatures (SSTs) are kept constant during the model integration (only the monthly and seasonal forecast models currently have an interactive ocean).

Both of these have important consequences in terms of the ability of our system to predict the intensity of the TCs correctly. Rather than providing a realistic description of the powerful energy cycle that occurs within a TC (for the upper layers of the ocean this is an important component), the model currently only represents a crude approximation of an axisymmetric circulation whose intensity is strongly underestimated compared with most energetic TCs. As is shown later in this article, there is undoubtedly skill in the model forecasts of TC tracks–much more so than ten, or even five, years ago. It is to get an objective evaluation of such a skill that a TC tracker has been developed at ECMWF in recent years, and recently (October 2004) turned into an operational application.

Tracking the cyclone

It is important to stress that the tracker described here is a pure diagnostic of the model's ability to detect (analyse)

and forecast the displacement, growth and decay of TCs. It does not interfere with the model's dynamics. The tracking algorithm simply tries to detect, in the area where the TC has been reported, features in the model fields (pressure, vorticity, temperature) that are characteristic of TCs. If these features are detected, the tracker then tries to follow the system in subsequent forecast steps–for the deterministic model as well as for all EPS members. The tracker finally stores information about cyclone position and intensity in the ECMWF general-purpose meteorological archive facility (MARS). It can then be used for the generation of forecast products or for verification purposes.

Just like the targeting that is described above, the tracking algorithm is fed with TC observation data. The ECMWF TC tracker will, therefore, only run for TCs for which there is an observation available within the data assimilation time window (0300-1500 UTC for a 1200 UTC run, 1500-0300 UTC for a 0000 UTC run). It is important to stress that, at this stage, no identification of TCs that may be generated during the forecast is attempted. A first description of the tracker has been published by van der Grijn (2002); an updated version following improvements suggested by experience is given later in this article.

Figure 2 shows a schematic description of the tracking algorithm currently in use. Once a TC observation is received (black dot), the tracker will try to find this cyclone in the analysis. Several meteorological features need to be present in the analysis before the tracker can successfully detect the cyclone. To start with, the tracker looks for a minimum in mean-sea-level pressure (MSLP) within a radius of 445 km around the observed TC position. A minimum in MSLP is only regarded as a genuine TC if there is also a cyclonic signature and a warm core present in its vicinity. The tracker looks, therefore, for maxima in both the 850 hPa relative vorticity and the 850-200 hPa thickness within a radius of 278 km around the MSLP minimum.

When the TC is found to be genuine, the tracker will then try to follow this in subsequent forecast steps. TC observations no longer being available, the tracker needs a first-guess position; a weighted average of an extrapolation of the past movement and of an advection by the steering flow is used for that purpose.
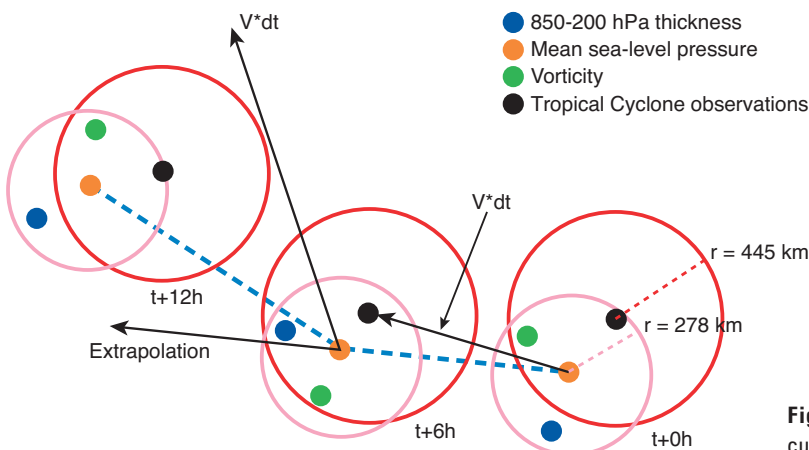

Fig. 2 Graphical summary of the tracking algorithm currently in use at ECMWF.

Parameter	Level	Threshold	Comments
Mean-sea-level pressure	Surface	≤1015 hPa	
Vorticity	850 hPa	≥5 x10^{-5} s^{-1}	≤ -5 x 10^{-5} s^{-1} for Southern Hemisphere
Thickness	850-200 hPa		A maximum in thickness is only required once the TC has become extratropical.
Zonal and meridional wind	850, 700, 500 and 200 hPa	Weighted average defines the steering flow	
10 m wind speed	10 m	≥8 ms^{-1}	Only required over land
Orography	Surface	≤1000 m	Tracker stops if the TC is over high orography (>1000 m) AND its location is more than 278 km away from the tracker first guess

Table 1 Parameters and their respective levels and thresholds that are used in the ECMWF TC tracker.

The ECMWF TC Tracker is a fully automated system designed to follow features in the ECMWF model that are often intense and small scale in the real world. It might be superfluous, but it is important to note that, for this very reason, the tracker is not perfect. Especially in situations when the TC is weak or close to complex orography, there is a risk that the tracker will detect and follow features that have nothing to do with TCs. In order to keep this risk to a minimum there are several other checks that are applied. Table 1 gives an overview of all the model parameters and their respective thresholds that need to be met in order to detect a TC successfully or to continue to track it.

Products on the web

Since June 2004, various TC products can be found on the ECMWF web server (http://www.ecmwf.int/products/forecasts/d/tccurrent) that can be accessed by all ECMWF and WMO [1] Member States. The TC web pages feature forecast guidance products and simple verification maps for active cyclones and historical cyclones since March 2003.

Figure 3 shows a so-called strike-probability map that can be found on the above-mentioned web pages. The definition of strike probability used for here is the probability that a TC will pass within a 120 km radius from a given location during the next 120 hours. This probability is based on the number of EPS members forecasting this event, each member having equal weight.

Users should bear in mind that the strike probability is based on the concept that the foremost information that a forecaster wants to know is whether a TC will hit his area of interest rather then when this will exactly happen. The strike probability is calculated for a five-day window, and it therefore allows for a quick assessment of the high-risk areas in the short-to-medium range. As a consequence, it does not give much guidance about the exact timing of a possible hit.

Figure 4 shows another product that can be viewed on the ECMWF TC web pages. This product, also known as a Lagrangian EPSgram, shows for a specific TC the EPS distribution of the 10 m wind and core pressure as a function of time. In contrast to most conventional probability products,

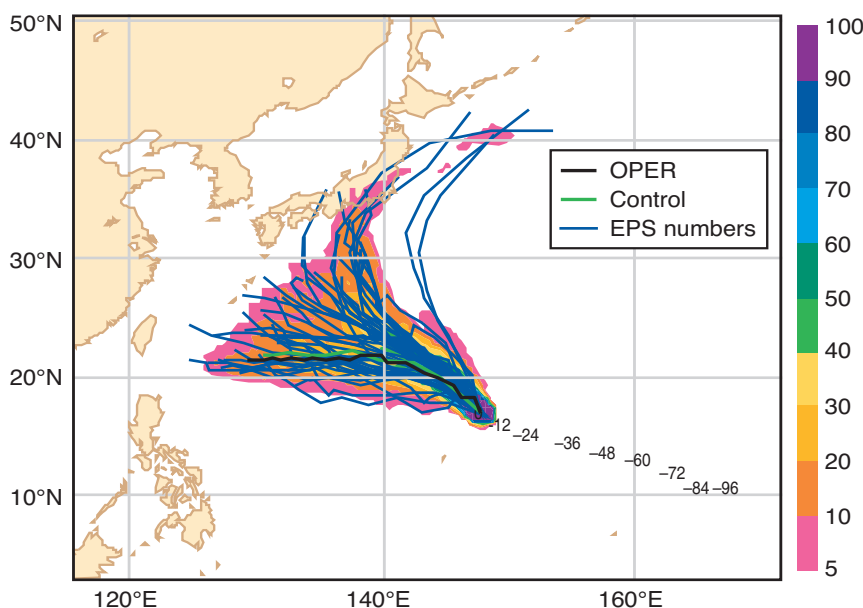**Fig. 3** Strike-probability map for typhoon Songda, valid for the five-day period starting at 12 UTC 31 August 2004; strike probabilities are shaded; high-resolution and low-resolution unperturbed tracks are in black and green, respectively; blue lines are the perturbed EPS member tracks.

[1] Login/passwords can be obtained from ECMWF by request passed on by the WMO Permanent Representative of each country.
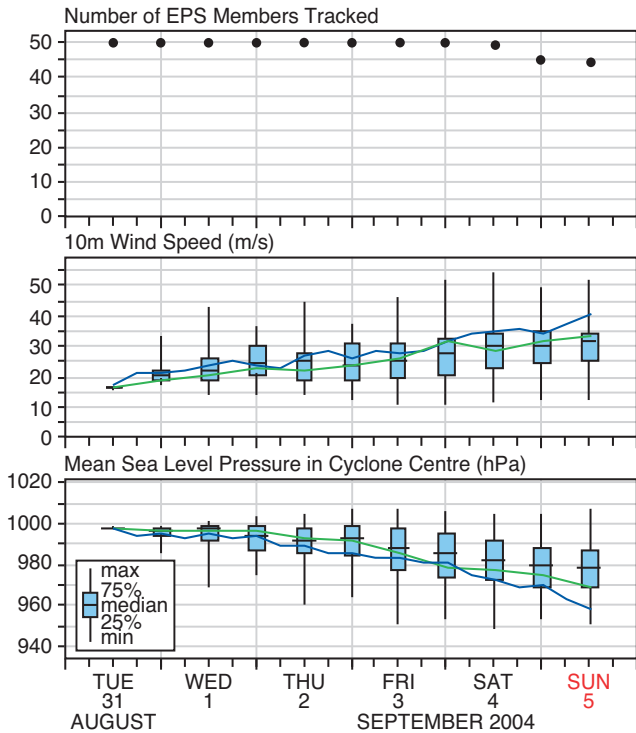
Fig. 4 Lagrangian EPSgram for typhoon Songda. Distribution of 10m wind and mean-sea-level pressure in the middle and bottom panels, respectively. The top panel shows the number of EPS members that were successfully tracked and, therefore, were included in the distribution. High resolution / low resolution unperturbed members are shown by blue / green lines.

the Lagrangian EPSgram shows the EPS distribution associated with a feature (in this case a TC), rather than the EPS distribution at a static grid point. Important information also conveyed on this diagram is the number of EPS members that did keep the TC 'alive' at each forecast step–thus providing a probability that the cyclone will be active at a given time; other distributions are relative only to the sub-sample of active members. Maximum 10 m wind–speed values are computed in the vicinity (445 km) of the TC in each of the forecasts supporting an active one.

Verification

Both the deterministic and probabilistic forecast products described above have been verified, the verification scheme aiming at assessing the performance and systematic errors of the forecast system and at evaluating the benefit of the EPS compared with purely deterministic TC forecasts. Unless stated otherwise, the verification scores are based on the ECMWF TC forecasts from April 2002 to June 2004. These scores are now produced on a routine basis along with the TC forecast products.

Deterministic verification

Deterministic errors have been derived from the TC tracks of the high–resolution operational forecast (T511), the EPS control forecast (T255) and from the mean of all EPS tracks. A limited set of parameters is used for the verification of deterministic forecasts, as explained in Figure 5.
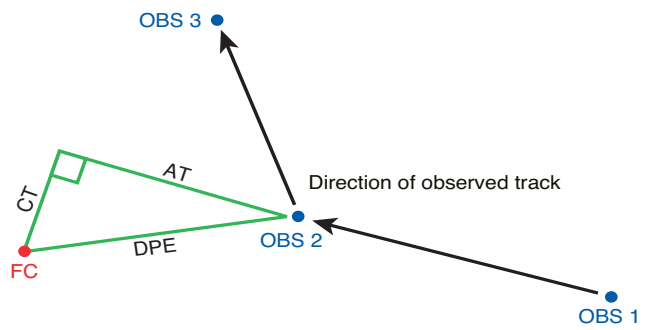

Fig. 5 Diagrammatic explanation of direct position error (DPE), cross-track (CT) error and along-track (AT) error. The DPE values are always positive. The AT errors are positive if the forecast position lies ahead of the observed position along the tropical cyclone track. The CT errors are positive if the forecast position lies to the right of the observed track. Adapted from (*Hemming* 1994).

The distance between the observed and forecast positions is known as the direct position error (DPE). The DPE only indicates how well the cyclone position was forecast. To assess any speed or curvature bias in the forecast, along-track (AT) and cross-track (CT) errors are introduced. The AT error is a measure of the skill of propagation speed in the forecast, while the CT error tells whether the cyclone has recurved too soon or too late in the forecast. Another parameter of the deterministic verification is the core–pressure error (CPE), which applies to the forecast intensity of the cyclone.
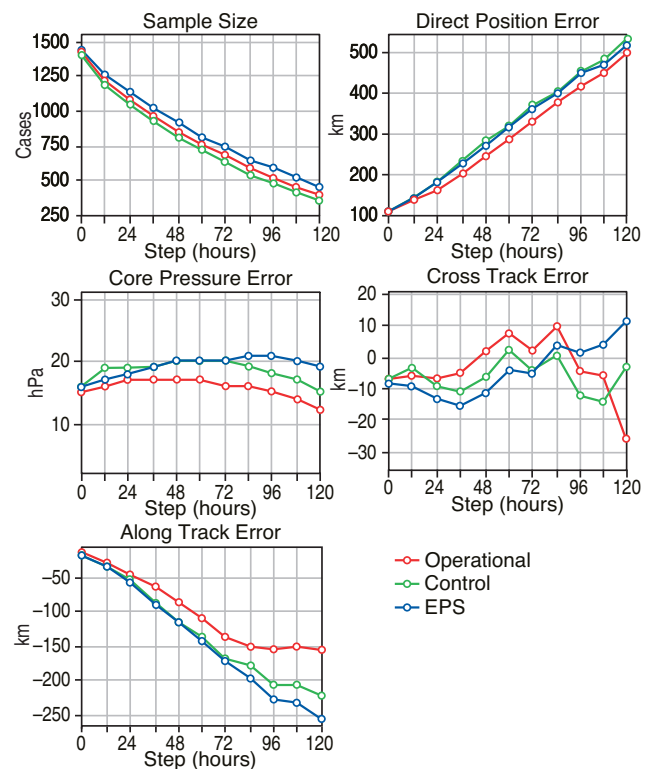

Fig. 6 Sample size and deterministic forecast errors for T511 (operational – red), T255 (Control – green) and the mean EPS (eps – blue) tracks versus forecast time step. All forecasts are from the period 6 April 2002 to 21 June 2004.

Mean values of the deterministic verification parameters versus forecast step are presented in Figure 6, comparing T511 (oper), T255 (ctrl) and mean EPS (eps) tracks (all track positions at a given step are averaged into a single value). Also the total number of forecasts per step is shown.

For the DPE, an almost-linear increase throughout the forecast range is found. At T+120 hours the DPE is close to 500 km. The error in the analysis (step 0) is, on average, close to 100 km, which means that there is a significant weakness in the TC analysis positions. It is evident that the T511 track is always better than the mean of the EPS tracks and the T255 track, though the EPS seems to come slightly closer to the T511 after step T+108. The mean of the EPS tracks will probably perform better than the T511 track later in the forecast range.

Since the CT and AT errors are closely linked (Figure 5), it would provide useful information to evaluate them together. However, this cannot be performed here since all steps represent mean values. The CT errors are relatively small, but it can be argued that there is a tendency for the cyclones to recurve too early in the mid-range, from T+48 to T+84 hours. Later in the range, the CT error becomes almost neutral again, at least with respect to the T511 and the CTRL forecasts. The AT error curves show that that there is a significant slow bias in the forecast, by about 50 km/day. The error is largest in the EPS and CTRL forecasts, growing to around 250 km at T+120 hours, while the T511 seems to saturate at about 150 km from T+84 hours onwards. It is evident that the largest contribution to the DPE comes from the slow bias in the forecast.

The CPE is always positive, which means that both analysed and forecast cyclones are, on average, weaker than observed. Again the EPS and CTRL show weaker performance than the T511, probably because of a smoother field due to the lower resolution. The bias is around 15 hPa in the analysis and increases slightly out to T+60 hours. However, care has to be taken when reading this diagram since the sample size is largest in the first forecast steps, which probably causes the 'hump-shaped' curve. A homogenized sample (only forecasts where all time steps are available) would possibly provide more realistic results, in particular for the CPE. Another limitation to this type of verification comes from the fact that independent observations used here are usually not objective, but rather subjective assessments from human experts making the best interpretation of satellite imagery. This should not, however, hinder the fact that the forecast of TC intensity is still very much a matter for further research and model development.

Figure 7 shows time-series of the DPE at different time steps as seven-month running medians of the monthly-mean values from April 2002 to June 2004. Here it is also evident that the T511 is performing better than the CTRL and mean of the EPS tracks, except for the last months at T+120, where the EPS is performing better. Also, the DPE is currently close to 450 km at T+120, in contrast to the 500 km whole-period mean value (Figure 6). The most positive signal of the time-series is the apparent minimum reached over the early months of 2004. This may be related to some important changes to the physics included in October 2004.
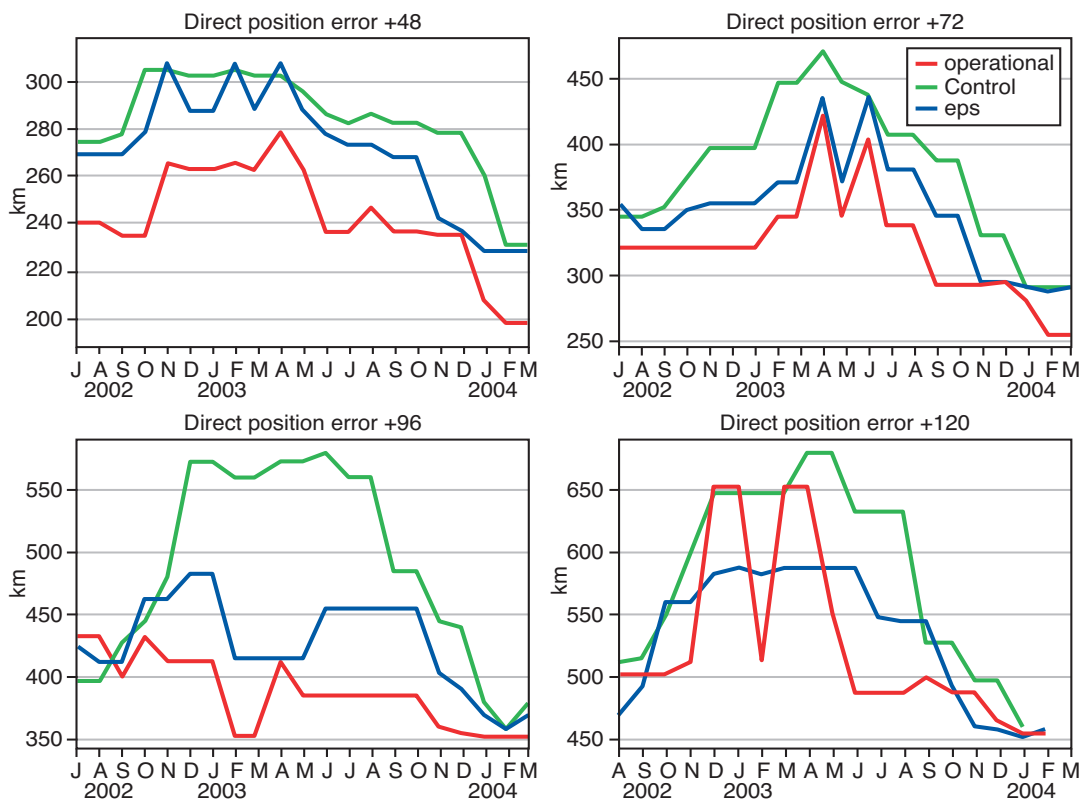

Fig. 7 Seven-month running medians of the monthly-mean direct-position error values for T511 (operational – red), T255 (Control – green) and the mean EPS (eps – blue) tracks at different forecast steps from 2002-04 to 2004-06.
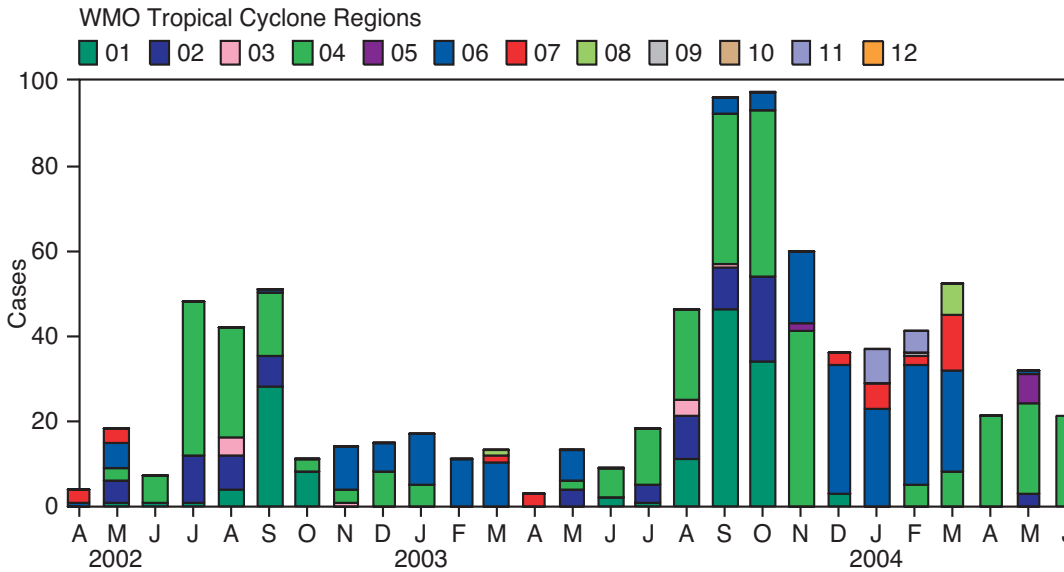
Fig. 8 The number of T511 forecasts at T+48 from April 2002 to June 2004, shown by WMO tropical-cyclone region. WMO regions: 01 – Miami (West Atlantic), 02 – Miami (East Pacific), 03 – Honolulu, 04 – Tokyo, 05 – New Delhi, 06 – La Reunion, 07 – Perth, 08 – Darwin, 09 – Brisbane, 10 – Port Moresby, 11 – Nadi, 12 – Wellington.

The DPE time-series should also be compared with the time-series of sample size in Figure 8, showing the total number of T511 T+48 hour forecasts per month from April 2002 to June 2004. From October 2002 to July 2003 the number of forecasts was relatively small, which corresponds to the period of very large errors seen in Figure 7. As for the DPE at T+48 hours (Figure 6), the level of skill before October 2002 and after July 2003 is almost the same, whereas it improves significantly towards the end of 2003. In Figure 8 the number of forecasts per month is divided into different WMO TC regions. The seasonal variation of the different regions is easily seen, and it is probable that the TC forecast skill would become clearer when the verification is eventually performed for single basins or regions.

Probabilistic verification

For probabilistic evaluation of TC forecasts, the probability of detection (POD) and false-alarm ratio (FAR) has been derived from a standard 2×2 contingency table (Table 2).

Due to the nature of TCs as single events, the correct rejections (Z, not observed and not forecast) is always very high and, moreover, its value is very dependant on the area defined for verification (a global domain, for example, would inflate the number of correct rejections without this reflecting any skill). This implies that the classical ROC diagram, involving the false alarm rate, F/(F+Z), is not very useful for the

purpose of TC evaluation. An alternative way, which does not include Z, is to use instead the false-alarm ratio (FAR), F/(F+H), while still keeping the POD, H/(H+M), as the other measure of quality (Figure 9). In an ideal system there will be no misses and no false alarms, which means that the curve would be standing at the upper left corner and, at the intersection with the diagonal, the frequency-bias index, FBI=(H+F)/(H+M), would be equal to one. In other words, the forecast probability at the intersection represents the 'no-bias threshold' for a user who wants to see the number of warnings he acts upon equal to the number of events that occur (this is, however, not likely to be the optimal threshold). This threshold was around 30% for the 2002-2003 period and slightly less in the last year. For such dramatic events as a TC, the cost of a missed event is likely to be higher than those associated with a false alarm. TC warnings should, therefore, be issued on the basis of probabilities lower than the 'no-bias threshold', while accepting the fact that a significant proportion of them will be false alarms.

The reliability diagram for the strike probability (the probability of a TC passing within a 120 km radius during the next 120 hours.) on the left-hand side of Figure 9 shows a clear improvement in last year's forecasts (March 2003 to April 2004) over the previous year's forecasts. However, the system was still very over-confident in the high-probability range. A 95% probability forecast only verifies in 60% of the cases. This may be due to a lack of spread in the early forecast ranges and also to the slow bias in the forecast tracks. Pre-operational validation tests of the revised targeting and singular-vector computation introduced in October 2004 have shown on a reduced sample of cases (August to September 2004) that the impact obtained (in particular by keeping a more consistent targeting of the cyclone when entering the extratropical transition) was quite positive.

	Observed	Not observed
Forecast	H	F
Not forecast	M	Z

Table 2 Contingency table of events for probabilistic forecast verification. H denotes 'hits', F 'false alarms', M 'misses' and Z 'correct rejections'.
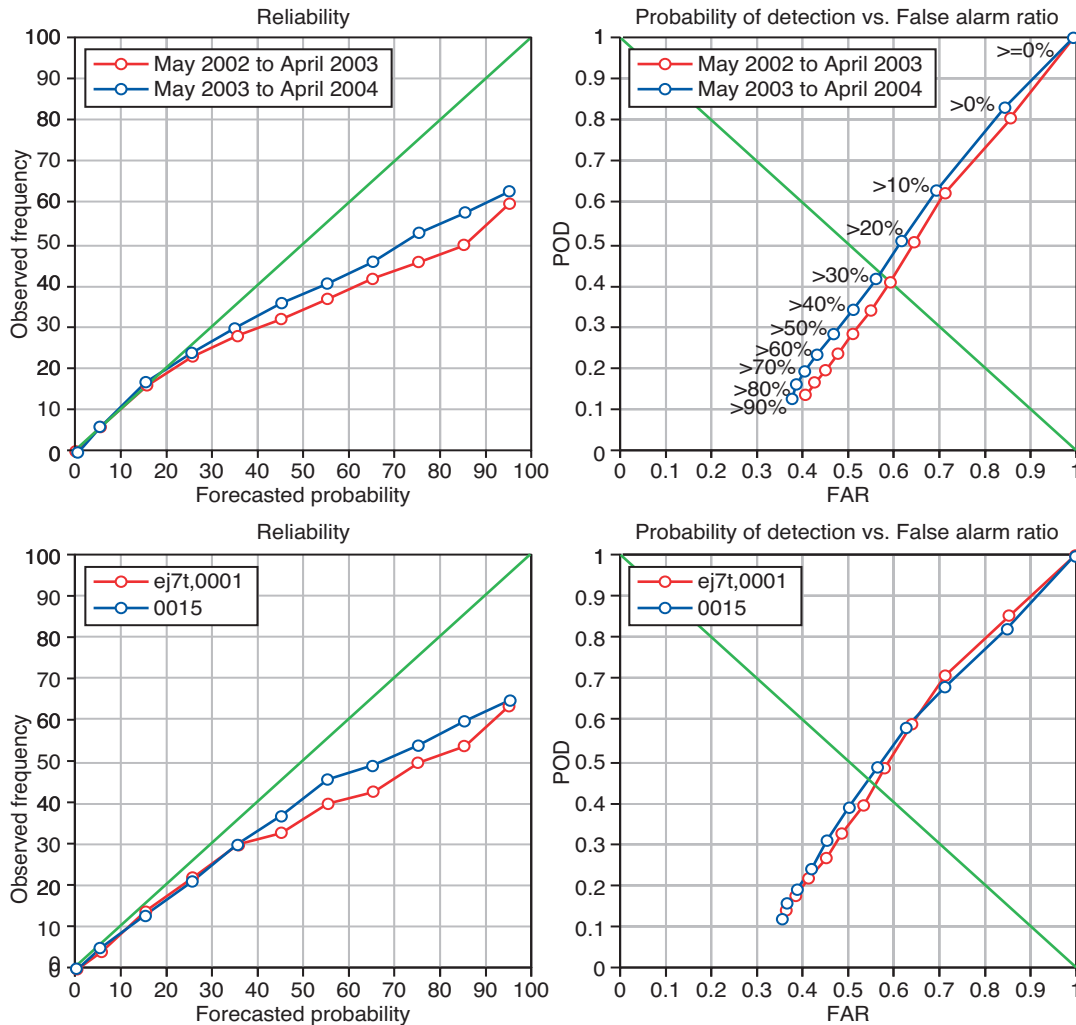
Fig. 9 Reliability diagram (left-hand panels) for the forecast probability that a TC will pass within 120 km during 120 hours of the forecast. The false-alarm ratio (FAR) versus the probability of detection (POD) (right-hand panels) gives a measure of the decision threshold. Values along the curve represent the forecast probability. Upper panels: March 2002 to April 2003 (red) versus March 2003 to April 2004 (blue) ; Lower panels: August to mid-September 2004 (operations in red, pre-operational suite in blue)

An even tougher way to measure the ability of the ensemble to cope with different predictability levels is, for a given forecast range, to measure the relation between the spread and the error. Although the first of these is only an estimate of the expected level of the second over a large number of similar cases, cases when the spread is small should, on average, be associated with smaller errors than when it is larger. Figure 10 illustrates the spread/skill relationship for different forecast steps for the period April 2002 to June 2004. The spread is defined as the standard deviation of the distance between the ensemble tracks and the mean ensemble track. Skill is measured by the distance error between the CTRL track and observed TC positions (*van der Grijn*, 2002). In an ideal forecast system the bins should form a line with unit slope. The best-fit line between the bins has been calculated using linear regression and its slope value is printed in each diagram. It is clear that the relationship between EPS spread and CTRL skill is rather low. Changes introduced in October 2004 have been operating for long enough to provide reliable statistics of the spread/skill relationship.

Operational status and future developments

The generation of tropical–cyclone forecast data (location, wind and pressure) became part of the operational suite in October 2004 (Cy28r3). As a result, these data are archived in MARS using a BUFR template proposed by the Japanese Meteorological Agency (WMO/CBS 2002). These messages will be disseminated soon, in real time, to ECMWF Member States and beyond, on the GTS and to all Meteorological Services within the WMO. These products have been available in graphical format on www.ecmwf.int since June 2004 for ECMWF Member States, and since August 2004 for WMO users.

It is important to note that, as it stands, the system is critically dependant on the good reporting of tropical cyclones on the GTS using BUFR or CREX formats. Because some basins are not covered by such reporting procedures yet, the UK Met Office has kindly agreed to provide ECMWF with its own decoding of unformatted advisory messages from the GTS. This, however, makes it a difficult task to merge information coming from different sources into one single database,
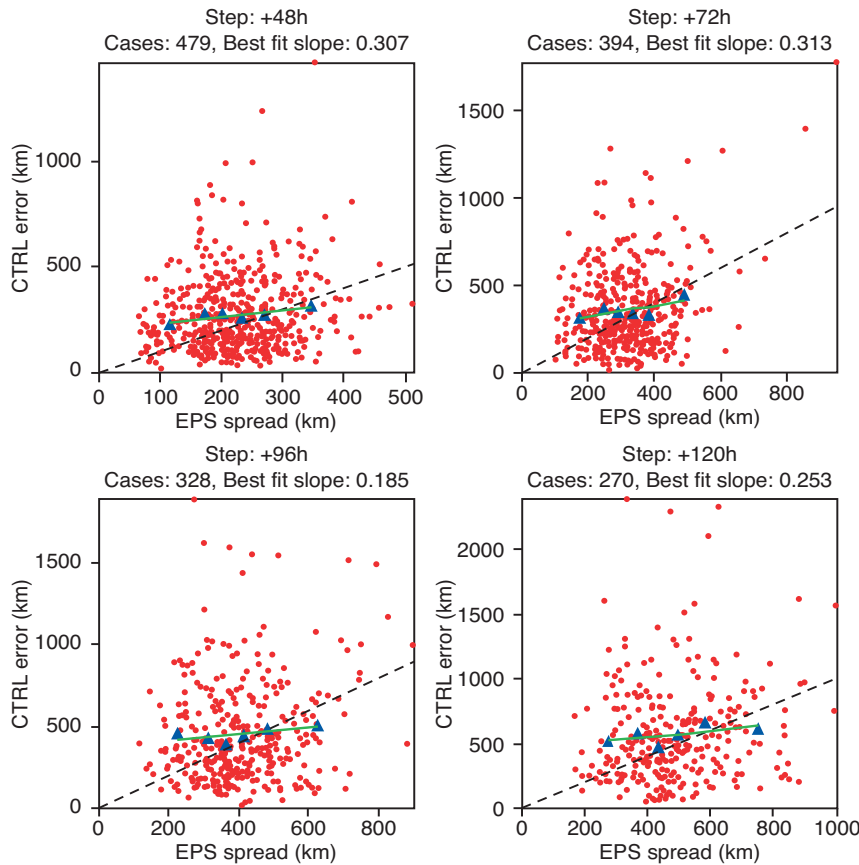
Step: +48h
Cases: 479, Best fit slope: 0.307

Step: +72h
Cases: 394, Best fit slope: 0.313

Step: +96h
Cases: 328, Best fit slope: 0.185

Step: +120h
Cases: 270, Best fit slope: 0.253

Fig. 10 The EPS spread versus the CTRL error at different forecast steps from April 2002 to June 2004. The red dots represent individual forecasts and the blue triangles are bins equally sized with respect to spread distance. The green line is the best-fit line between the bins; in an ideal forecast system this line would have a unit slope (dashed line).

and occasionally it creates naming problems making it difficult to follow the different forecasts for a given TC on the web server.

The most limiting factor in the operational set-up described in this article is that it only accounts for the development and decay of existing TCs. Daily monitoring of the forecasts, both at ECMWF and in other forecast Centres, provides examples of when the model generates tropical cyclones. To explore an automatic detection and tracking of tropical and extratropical cyclones, preliminary tests have used, with some success, the 'feature-tracking' method developed at University of Reading.

On the scientific side, the most challenging aspect of TC forecasting remains to improve the forecasting of their intensity. There are areas that remain to be explored, such as the interactive coupling with the upper boundary layer of the ocean that, within the current resolution constraints, could improve the forecasts. Another difficult issue is to find ways for the data assimilation to cope better with well-organised systems such as TCs; too often in the current configuration new observations weaken rather than strengthen the TC circulations, a situation that suggests poor quality of background-error covariance estimates in such situations.

Although this article focused on forecasting tropical-cyclone activity within the medium range, it is worth mentioning that ECMWF also generates a product giving an indication of whether the next tropical cyclone season will be unusually active or not, based on the seasonal forecasts run once a month with a six-month range (*Vitart et al.* 2002) (www.ecmwf.int/products/forecasts/d/charts/seasonal/forecast/Tropical_storm/). The skill of such

seasonal forecasts is better, however, over the Pacific (the very active 2004 hurricane season that affected the western Atlantic and Caribbean basins in August to September was not indicated by the seasonal forecasts earlier in the year).

FURTHER READING

Van der Grijn, **G.**, 2002: 'Tropical cyclone forecasting at ECMWF: new products and validation'. *ECMWF Tech. Memo 386*, http://www.ecmwf.int/publications/library/do/references/list/14

Heming, **J.**, 1994: Keeping an eye on the hurricane – Verification of tropical cyclone forecast tracks at the UK Meteorological Office. *NWP Gazette*, **1**, 3-8.

Hodges, **K.L.**, 1998: Adaptative constraints for feature tracking. *Mon. Weather Rev.*, 1362-1373

Puri, **K.**, **J. Barkmeijer**, and **T.N. Palmer**, 2001: Ensemble prediction of tropical cyclones using targeted diabatic singular vectors. *Q.J.R. Met. Soc.*, **127**, 709-731

Vitart, **F.**, **D. Anderson** and **T. Stockdale**, 2002: 'Seasonal forecasting of tropical cyclone landfall over Mozambique'. *ECMWF Tech. Memo 387*, http://www.ecmwf.int/publications/library/do/references/list/14

WMO/CBS, 2002: Final report of the meeting of the expert team on data representation and codes, Prague. (available from http://www.wmo.ch/web/www/DPS/Meetings/ET-DRC-PRAGUE-02/report-final.pdf)

Gerald van der Grijn, Jan Erik Paulsen, François Lalaurette and Martin Leutbecher

A snowstorm in north-western Turkey 12–13 February 2004
– Forecasts, public warnings and lessons learned –

The following article from the Turkish Weather Service illustrates the difficult decisions facing forecasters when they anticipate a severe weather event: When should public warnings be issued? Which organisations should be warned? How should they react in the face of a sceptical press? How can they ensure that appropriate evasive actions are taken? The forecast described (based primarily on ECMWF predictions) was very successful, and the reaction of the public and the authorities was much improved over their responses to forecasts of a previous snowstorm a few weeks earlier.

The north-western part of Turkey, especially Istanbul with a population of 10 million, was exposed to a snowstorm between 20-22 January 2004. The Turkish Met. Service had warned all the authorities and people three days before the event. Unfortunately, however, all the necessary actions were not taken as required. This failure caused many people to be affected by the snowstorm and there were four fatalities. The case was much criticised by the media. One important question arose: What will we do if the same thing happens again?

8 February 2004 – Forecasting the new snowstorm

The forecasters at the Forecast Centre started to observe a cold air mass over eastern Europe on 8 February 2004. The ECMWF numerical model indicated clearly that this air mass would affect the north-western Turkey in a few days (Figure 1), and other numerical models confirmed this prediction. There was still enough time to make sure of the accuracy of the forecast, and so it was decided to wait one more day before creating a warning bulletin. The forecasters continued to check the ECMWF 12 UTC forecasts and other Centres' forecasts.

### 9 February 2004 – It is time to prepare warning reports

At the morning briefing of 9 February, actual maps and forecasts from NWP models were analysed carefully (Figure 2). It was unanimously agreed that Turkey would be affected by the very cold air mass in three days. The warning report was prepared and disseminated to the media and authorities, especially to the municipality of Istanbul.

The report focused on:
- the start time of the rain (12 February, afternoon)
- when it will turn into the snow (after 1800 local time)
- how long snow will be effective (two days)
- the fall in temperature (10-15°C drop)
- which areas will be most affected by the snow (north-western Turkey)
- the wind speed and sea state (up to 45-50 knots, 4-5 m wave height)

The General Director of the Met. Service held a press conference to give detailed information about the case. It was almost the first news item on television channels and in newspapers. All the authorities had started to take the necessary actions immediately.

a 11 February 2004 12UTC 500hPa geopotential height / temperature
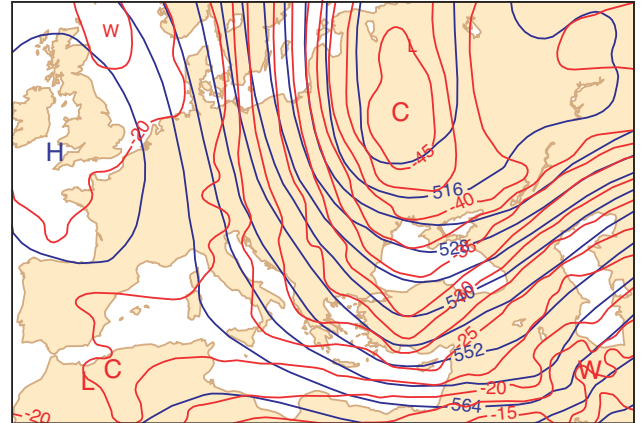
b 12 February 2004 12UTC 500hPa geopotential height / temperature
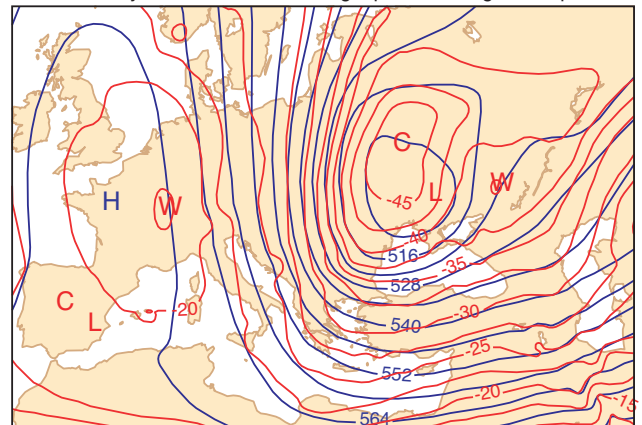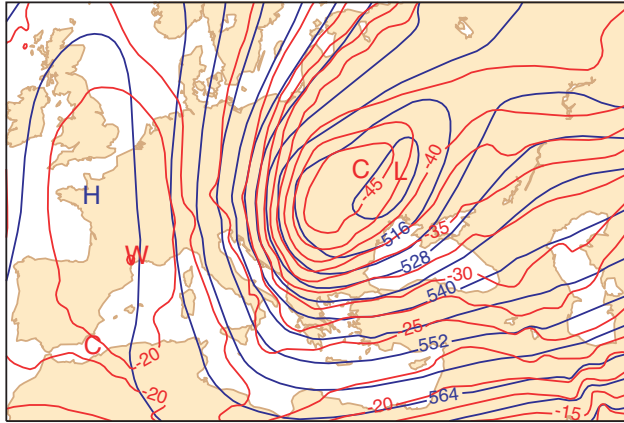
Fig. 1 ECMWF 500 hPa forecasts issued on 8 February 2004 showing the geopotential height and temperature for 1200 UTC on (a) 11 February 2004 and (b) 12 February 2004.

- all the schools were closed for 12 and 13 February
- vehicles to clear the highways were prepared and positioned to key points
- people were warned not to use their cars.
- public places were turned into residences for homeless people

Updating the warnings and waiting for the start of the storm

On 10 and 11 February, there was no significant change in the weather forecast and the Turkish Met Service continued to issue warnings with much more detailed information. However, the weather conditions in Istanbul and western parts of Turkey were clear on 11 February and the temperature was around 10-12 °C. As a result, the meteorological warnings were criticized because of the present clear weather conditions and some speculation had started about the accuracy of the forecasts. However, the forecasters continued to maintain that it would start raining around 1600 local time on 12 February and then turn into snow at around 1800.

a 12 February 2004 12UTC 500hPa geopotential height / temperature

b 13 February 2004 12UTC 500hPa geopotential height / temperature
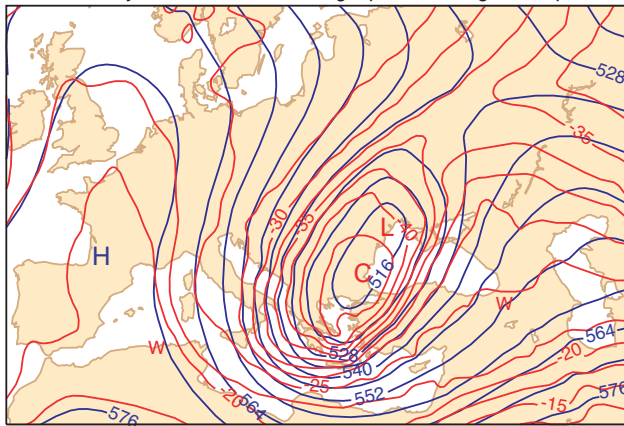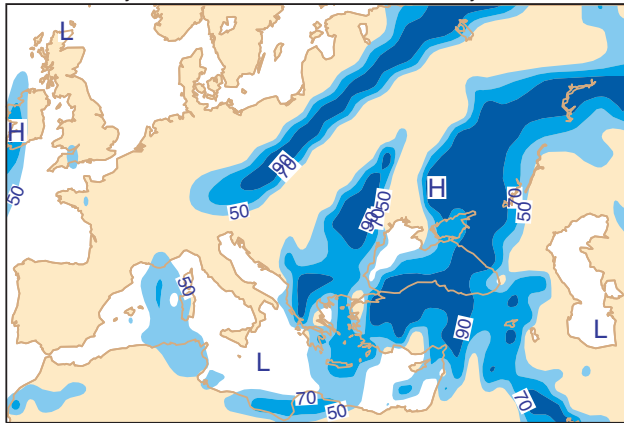
c 13 February 2004 12UTC 700hPa relative humidity

Fig. 2 ECMWF 500 hPa forecasts issued on 9 February 2004 showing the geopotential height and temperature for 1200 UTC on (a) 12 February 2004 and (b) 13 February 2004, and (c) the 700 hPa relative humidity for 1200 UTC on 13 February 2004.

12 February 2004 – The start of the storm

Everybody waited; the sky was still clear, the temperature was around 6-8 °C, the sea was calm and the wind was moderate. At noon the sky was partly cloudy and the wind speed increased to 10 m/s. It started to rain, accompanied by a 18 m/s southerly wind at 1645. It started to snow at 1850 local time and the wind direction changed to north–west with a speed of 18 m/s and the wave heights reached 3 m in Marmara and the western Black Sea. The Dardanelles and Bosphorus were closed to sea traffic after 2200 local time. Ataturk Airport (Istanbul) was closed at midnight.

13 February 2004 – The snow

It continued to snow all day and temperature fell: from a maximum of –2°C in Istanbul to a minimum of –8°C. The snow depth was 40 cm in some areas of Istanbul at the end of the day (and more than 60 cm on the hills). The wind gusts reached 25 m/s . The cold air, snow and wind affected daily life very badly, but most people stayed at home.

Although some problems arose, almost all the highways were open. Transportation in the city continued, but was very slow. Electricity problems occurred in some parts of the city, but they were solved quickly. There was no human loss of life, the biggest gain compared with the previous storm.

14 February 2004 – After the storm

The snow eased in Istanbul and moved to central parts of Turkey. The snow, cold air and strong wind affected central and eastern regions for the next two days, as expected. The snow depth was 130cm in Erzurum (eastern Turkey)

Lessons Learned

- Preparing a perfect warning report is futile if you do not announce it clearly and if it is not understood (and believed) by everyone.
- Very good coordination between the public services and organizations is essential.
- All Governmental and Social bodies must be warned on time; a warning that is not prepared on time is useless.
- The media mostly considers events in metropolitan areas. You have to warn local authorities in rural areas and small cities directly.

The Turkish State Meteorological Service

Planning of adaptive observations during the Atlantic THORPEX Regional Campaign 2003

Nowadays, the oceanic regions are no longer data sparse. Satellite radiances and atmospheric motion vectors provide a good coverage of these areas. This has helped to increase the skill of numerical weather forecasts for the Southern Hemisphere to the level of the Northern Hemispheric skill (*Simmons and Hollingsworth*, 2002).

Nevertheless, most satellite data provide no information on wind and temperature below cloud tops, and clouds are abundant in the baroclinically active regions. Thus, there may be potential to further improve the initial conditions for numerical weather forecasts by complementing the satellite data with in-situ observations in the dynamically most sensitive places.

The philosophy of adaptive observations (or targeted observations) is to economise observational resources by deploying additional observations only in those regions where they are likely to be most important for a specific forecast, i.e. a particular verification region of a few million square kilometres and a specific forecast range of 1-3 days. The process of planning adaptive observations involves several steps. First, verification regions and forecast ranges are selected for which a forecast improvement is desired. This step is referred to here as the case selection. Second, the regions of the atmosphere are predicted where improved initial conditions are likely to yield the largest improvement of the specific forecast. These geographic regions are referred to as sensitive areas. Third, the actual decisions about the deployment of additional observations are made, given the sensitive-area predictions and the operational constraints. The third step has to take place some time before the additional observations are taken. Depending on the procedure for a particular observation type, the required gap between the time of the decision and the observing time is between a few hours and two days – up to two days are required, for instance, to arrange for a research aircraft to deploy dropsondes, because of air traffic control constraints.

The Atlantic THORPEX Regional Campaign 2003 (A-TReC, see also http://www.wmo.int/thorpex/atlantic_ob_system.html) was an international experiment with a special observing period from 13 October to 12 December 2003. The primary goal of A-TReC was to demonstrate that several different observing platforms could be adapted in real time with the goal to improve operational weather forecasts for Europe. A-TReC is the first observation targeting exercise over the Atlantic with an operational flavour. Initial experience on observation targeting for NWP was gathered during the Fronts and Atlantic Storm-Track Experiment (FASTEX) in 1997. Since then, observation-targeting activities took place every year over the eastern Pacific. The Winter Storm Reconnaissance Programme run by the National Centers for Environmental Prediction (NCEP) has had operational status since 2001. In addition, some experience has been obtained with adaptive observations in the context of tropical cyclones in the Atlantic.

The European participation in A-TReC was managed by EUCOS (the EUMETNET Composite Observing System) under the responsibility of the Met Office. The A-TReC operations centre was located at the Met Office in Exeter, and activities were coordinated through two telephone conferences at 09 UTC and 16 UTC daily. ECMWF was involved in the case selection and in the prediction of sensitive areas for A-TReC. Maps of the predicted sensitive areas were made available in real time to A-TReC participants through a web site (now at http://www.ecmwf.int/research/predictability/adaptive_obs/) hosted at ECMWF. In addition, the sensitive-area predictions from Météo-France and the Met Office were transmitted to ECMWF, and were also displayed on the web site in the same graphical format as the ECMWF predictions.

Several people in ECMWF's Meteorological Applications, Data & Services and Meteorological Operations Sections provided the technical support to set up the suites for the real-time sensitive-area prediction, its MARS archive, the web site and the A-TReC observation database.

Additional observations

A-TReC is the first field campaign in which multiple observing systems were targeted in order to improve forecasts for specific weather events. During part of the campaign, up to three research aircraft capable of deploying dropsondes were available: The DLR Falcon was based in Keflavik (Iceland) from 13 to 22 November. The Gulfstream IV from NOAA was operating out of St. Johns (Newfoundland) from 13 November to 11 December. The Citation from the University of North Dakota was based in Bangor (Maine, USA) from 23 November to 12 December.

Additional radiosondes were launched in Europe, Greenland and Canada at 18 UTC on request from the A-TReC observation control centre in Exeter. Further additional soundings were made by selected vessels of the ASAP fleet at 15 UTC and 21 UTC on request from Exeter. Data transmission was activated on additional E-AMDAR aircraft. For all these platforms of the routine observing network, requests were made if additional observations could be obtained close to, or in, the sensitive areas. Moreover, additional drifting buoys were released before A-TReC in the Labrador and Biscay areas. Supplementary atmospheric motion vectors were obtained from GOES-East and Meteosat rapid scans over regions centred on the sensitive areas.

Case selection

The 09 UTC teleconference was dedicated to the case selection. Forecasters from the Met Office, Météo-France and ECMWF (the time difference precluded participation from the US and Canada) joined together to discuss and select relevant meteorological situations potentially affecting Europe or the North American east coast in the coming days. The selection criteria were based mainly on three factors: (a) to address potentially hazardous weather events, (b) to focus on cases in which an enhanced uncertainty was evident, (c) to select cases only in the medium-range with a forecast range between 3 and 5 days. Although the aim was to improve one- to three-day forecast, it was necessary to take into account also the 48-hour notice required by some observation providers.

Every day, each participant prepared a document containing a brief meteorological description and supporting material for an eventual request. The documents were posted on an FTP site hosted by ECMWF ready to be discussed during the morning conference (see Figure 1). Since each Centre based its request on different models, according to its own judgement, it was possible to have a good estimate of the forecast uncertainty. In addition, ECMWF provided a set of operational products on a dedicated web page with particular emphasis on EPS-derived products (ensemble mean, spread, individual forecasts, probabilities, Extreme Forecast Index). Once a decision was reached and a case selected, the verification area, the date and the time were used as input for the sensitive-area computations to be discussed on the same day at the 16 UTC conference.

Decisions from **TReC** (**T**HORPEX **R**egional **C**ampaign) conferences

1. Case selection (morning)

Date and time of meeting: **200311280900 (Friday)**

Team available for consultation:
Chair: Anton Muscat
ECMWF: Federico Grazzini, Alexis Doerenbecher
MF: Jean Ruffie
MO: Richard Dumelow, David Richardson, Steve Stringer

Forecast outlook:

Trough gradually disrupts over Spain and the western Mediterranean during Wednesday and Thursday with a cut off forming over Spain and a ridge building across the UK and northern Europe. ECMWF solutions continue to give some high rainfall accumulations in and around the western Mediterranean during Thursday, Friday and Saturday with the possibility of further Trec events.

Update to existing cases

Case code (fixed)	**Trec_021**
Priority	**low**
Verification region	**Western Atlantic 52N 60W**
Verification time	**200311300000 (Sunday)**
Observation time	**200311281800 (Friday)**

Reason for update:

None. Observations to go ahead as planned at 1800 UTC this evening (Friday)

Case code (fixed)	**Trec_022**
Priority	**High**
Verification region	**Central Europe 45N 07E**
Verification time	**200312011200 (Monday)**
Observation time	**200311281800 (Friday) and 200311291800 (Saturday)**

Reason for update:

ECMWF, MO and MF models showing good general agreement at surface and upper levels across western Europe, especially in vicinity of France. Despite this it was agreed that all observations should go ahead as planned, since the rainfall across southeastern France on Monday 1st December is a high impact event. Priority of Trec_022 increased from Medium to High, due to the high impact nature of the event. Extra observations requested for both Friday (28th) and Saturday (29th) at 1800 UTC, with verification time of Monday 1st December at 1200 UTC. Gulfstream aircraft was due to fly a triangular route from St. Johns this afternoon (Friday) in support with drop sondes but problems with Air Traffic Control at St. Johns may now prevent this.

New case suggestions:

ECMWF and MO suggested that a new case . . .

Fig. 1 Conference log of the 09 UTC conference on 25 November 2003.

Discussions were useful and often instructive, being enriched by different experiences and knowledge from different Centres. Most of the time, agreement on the cases was easily reached in the allocated time of 30 minutes. However, in due course, we noticed that the apparent uncertainty in the forecast at day 3–5 was quite often drastically reduced by the time additional observations were made (one to three days before verification time). This somehow reduced, a posteriori, the need for additional observations in many cases. It would have been appropriate to cancel many of the previously selected cases due to a more predictable situation as the observation time approached. In other words: adaptive observing techniques might be more successful if the time to alert key observation providers could be shortened.

Sensitive-area predictions

In order to select optimal locations for a set of additional observations, one has to be able to quantify the expected impact of additional observations on the forecast uncertainty. To estimate the expected impact, it is necessary to know the statistics of initial-condition errors, how the initial-condition errors change due to the assimilation of additional observations, and about the perturbation dynamics from the assimilation time to the forecast verification time. Approximate techniques for determining the sensitive regions are either adjoint based (singular vectors and adjoint sensitivities) or are based on a linear diagnosis of ensemble forecasts (e.g. Ensemble Transform Kalman Filter; ETKF) – see, for example, *Leutbecher* (2003) and references therein.

The Met Office based their predictions on Ensemble Transform Kalman Filter diagnostics of the ECMWF ensemble. Météo-France and ECMWF based their sensitive-area predictions on singular vectors. These sensitive-area predictions have been archived in MARS:
class=to, stream=seap, expver=11, origin=ecmf/lfpw/egrr
\#   ECMWF, MF, UKMO
NCEP (using the Ensemble Transform Kalman Filter on combined NCEP and ECMWF ensembles) and the Navy Research Laboratory (NRL) (with singular vectors and observation sensitivity) also provided targeting guidance, which was displayed on their own web sites.

ECMWF predictions

All singular-vector computations at ECMWF used a trajectory starting from the 66-hour forecast valid at the nominal observing time for the additional observations (18 UTC). The sensitive-area predictions were ready before 15 UTC, that is, in time for the 16 UTC phone conference and around two days before the targeted observations were taken. Singular vectors were computed in three different configurations to give an indication of how sensitive the predictions are to the choice of the initial time metric and to the representation of dynamics and physics in the tangent-linear model (Table 1). Configurations TE-d42 and TE-m95 used the total-energy metric both at initial and final time whereas configuration H-d42 used the Hessian metric at initial time and the total-energy metric at final time. A dry tangent-linear model at spectral truncation T42 was used in configurations TE-d42 and H-d42. Singular vectors in configuration TE-m95 were computed with a T_L95 moist tangent-linear model.

Configuration	Method	Initial norm	TLM resolution	TLM physics
TE-d42	1	Total energy	T42	Dry
TE-m95	2	Total energy	T_L95	Moist
H-d42	3	Hessian	T42	Dry

Table 1 Singular-vector configurations at ECMWF for A-TReC predictions. Method is the corresponding MARS keyword; for example, use method=3 to retrieve Hessian singular vectors.

The Hessian metric used in configuration H-d42 accounts for the statistics of initial-condition errors as estimated from the variational assimilation scheme. These latter singular vectors are referred to as Hessian singular vectors, as the initial-time metric is the matrix of second derivatives of the variational assimilation scheme's cost function (*Barkmeijer et al.* 1998). A-TReC is the first field campaign in which Hessian singular vectors were used for observation targeting. The initial-time metric depends on the observational coverage of the routine observations that have passed the quality control. This requires the observational coverage at a future time. A reference observation network at 18 UTC on 9 September 2003 was used as proxy for a prediction of the future observational coverage in all Hessian singular-vector predictions of the A-TReC. The reference network provides a reasonable estimate of the data coverage of the land-based component of the routine network (TEMP and SYNOP) and the main air-traffic routes. Observations that are affected by the presence of cloud, i.e. infrared sounder observations and atmospheric motion vectors derived from satellite imagery were removed from the reference network, as their coverage on 9 September 2003 was not representative of the coverage on other dates. Prior to A-TReC, additional experiments were performed showing that the effect of fewer satellite data on the Hessian metric does not affect the overall shape and location of the sensitive region.

Each day during the A-TReC period, calculations were performed for three fixed fairly large verification regions (northern Europe 45°–65°N, 15°W–35°E; southern Europe 30°–50°N, 15°W–35°E; and western Atlantic 30°–65°N, 40°W–85°W) and three fixed verification times (18h, 42h, 66h after the nominal time for the additional observations). These computations used singular-vector configuration TESV-d42, which is the same configuration used in the operational EPS for the extratropical singular vectors. The purpose of these computations was to give a general overview of the sensitive regions and their temporal evolution.

The fixed computations were complemented by more specific ones that used a verification region and a verification time that was selected at the 09 UTC phone conference, depending on the current weather situation. Therefore, these computations were the most valuable for guiding the decisions about where to deploy additional observational resources during A-TReC. For most cases, the specific computations were performed with all three configurations, TESV-d42, TESV-m95 and HSV-d42.

To illustrate the process of taking adaptive observations during A-TReC, two cases are described.
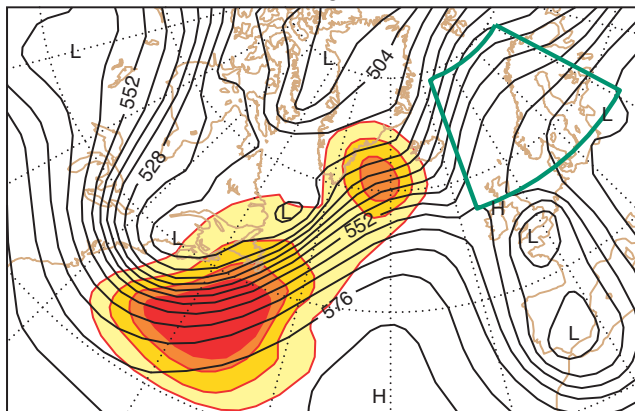
a Prediction based on TE-d42 singular vectors　　　**b** Prediction based on TE-m95 singular vectors
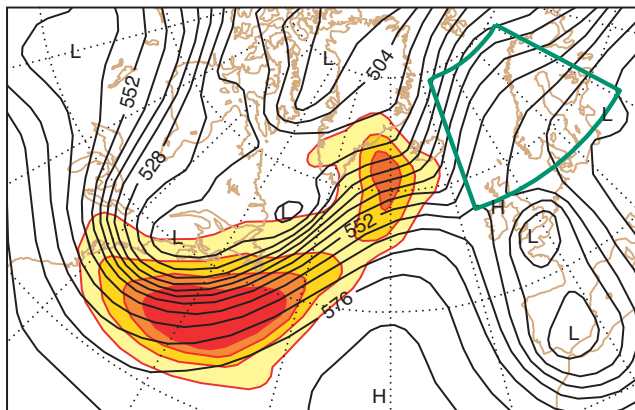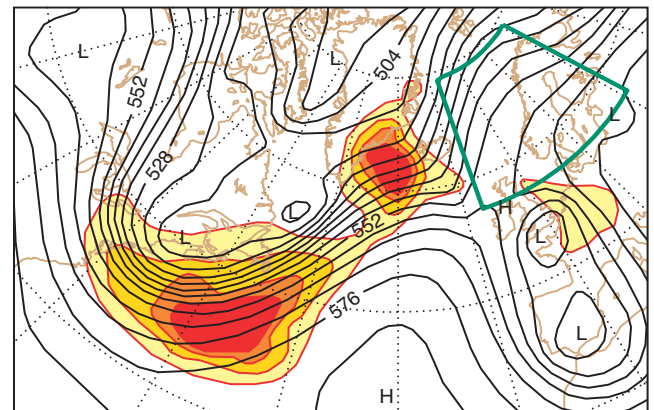
c Prediction based on Hessian singular vectors　　　**d** Prediction based on ETKF diagnosis from Met Office
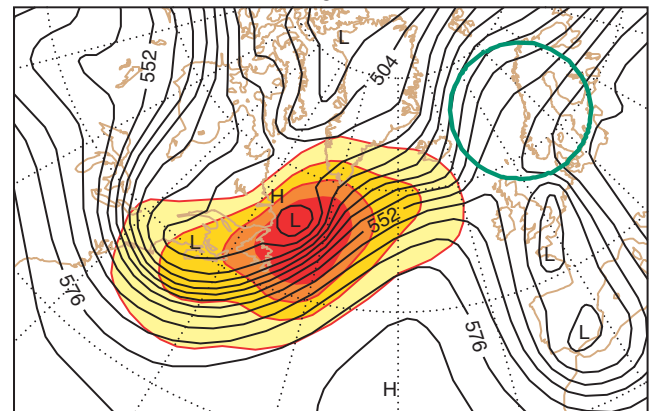

Fig. 2 The sensitive areas predicted by four different techniques for additional observations at 18 UTC on 2 December 2003 to improve forecasts in the region enclosed by the green contour and verifying at 12 UTC on 4 December. Sensitive areas of sizes 1, 2, 4 and 8 × 10^{6} km[2] are shaded; contours are of 500 hPa geopotential every 5 dam. (a) Prediction based on TE-d42 singular vectors, (b) based on TE-m95 singular vectors, (c) based on Hessian singular vectors and (d) based on ETKF diagnosis from the Met Office using the ECMWF EPS.
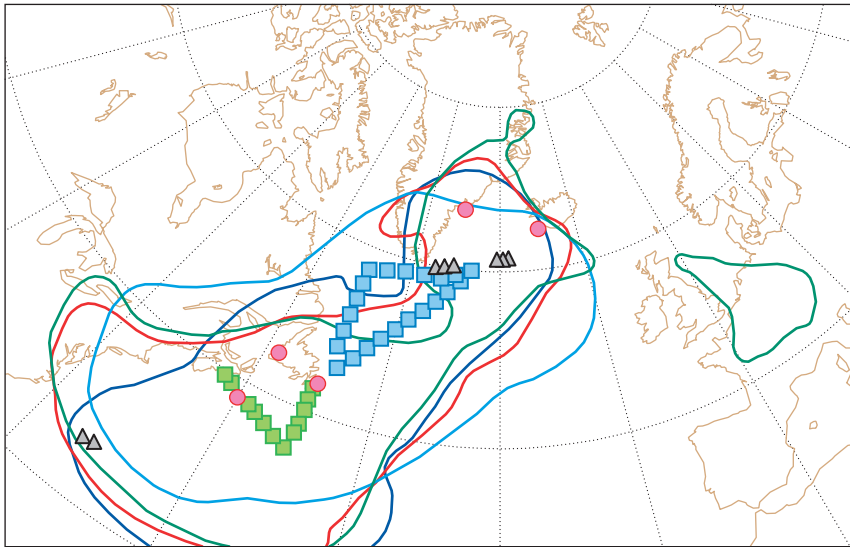
Fig. 3 Targeted observations around 18 UTC on 2 December 2003 in the sensitive areas shown in Figure 2 (squares: dropsonde locations (green – UND *Citation*; blue – NOAA *Gulfstream-IV*); red circles – additional soundings by land radiosonde stations; black triangles – additional soundings from ASAP ships). The contours show the outline of the 8×10^6 km^2 sensitive region as predicted by TE-d42 SVs (red), TE-m95 SVs (green), H-d42 SVs (dark blue) and ETKF (cyan).

The Norwegian storm in early December 2003

The Norwegian Storm was located close to the Norwegian coast at 12 UTC on 4 December 2003. The event is referenced as TREC 024. It was first suggested as a targeting case at the 09 UTC conference on Sunday 30 November 2003. By that time, strong winds and heavy rain were predicted over northern Norway for midday on Thursday 4 December. In the forecasts, the low originated over Newfoundland late on Monday 1 December. It propagated north-east to the north of Iceland and deepened over the Norwegian Sea on Thursday. The centre of the verification area was (65°N, 10°E). This case was selected partly to provide an opportunity for a mission of the Gulfstream IV by the middle of that week. Otherwise, this case was given a low priority.

Sensitive-area predictions with 66-hour lead-time were requested for an observation time at 18 UTC on 2 December and a verification time at 12 UTC on 4 December. This permitted the issue of a 48-hour advance alert for the adaptive observing platforms. This case was confirmed as a 'low priority' case at the 09 UTC conference on 1 December. There was agreement between the forecasts from different Centres. However, the spread in the ECMWF ensemble was enhanced at verification time. Additional sensitivity computations were performed with shorter lead-time (42h) to confirm the predictions from the previous day.

Sensitive-area calculations from the Met Office, ECMWF, NCEP and Météo-France were examined at the 16 UTC conference on Sunday 30 November. Figure 2 shows four of the targeting guidance maps from the ECMWF web site for this case. Panels (a)–(c) show the targeting guidance from ECMWF singular-vector computations and panel (d) shows the ETKF guidance provided by the Met. Office. The different sensitive-area predictions agree well. A consensus sensitive region was defined by the region 70°–55°W and 35°–65°N. This area was confirmed by the predictions on Monday 1 December (the same observation and verification times and verification. area).

The following decisions were taken during the 16 UTC conference on Sunday 30 November: a 48-hour alert for the selected radiosonde stations, the GOES rapid-scan winds (centred on 45°N–50°W), the ASAP ships located in the consensus sensitive region (given above), as well as the AMDAR aircraft. The NOAA Gulfstream IV and the Citation had been warned and given initial guidance (turning points) for their flight tracks.

Figure 3 shows the positions of the dropsondes actually deployed for this targeting case, as well as those of the land radiosondes and the few E-ASAP ships locations. The additional data from commercial aircraft are not shown. The NOAA Gulfstream IV flew north-eastward from St Johns (Newfoundland), the Citation flew from Bangor (Maine) to St Johns. The single-line contours (indicating the boundary of the largest-size target region, 8×10^6 km^2) agree quite well and most of the observations have been deployed inside it.

The US East Coast storm at 12 UTC, 7 December 2003

In the meteorological outlook on Sunday 30 November at the 09 UTC conference a storm, moving north-east and approaching the US east coast in the forecasts, was proposed as possible case. It is referenced as TReC 026. First, the verification date was set to 12 UTC on 6 December with an observation time 18 UTC on 4 December (TReC 026.1). The upper trough moving east across the USA, engaging warm low-level air from the Gulf of Mexico or Caribbean, was assigned low priority, in spite of the potential for heavy rain over eastern USA and a potentially strong cyclogenesis.

The case appeared more interesting during the following days. The case was redefined as TReC 026.2 based on the sensitive-area prediction of 3 December (66 hours lead-time; observation time: 18 UTC 5 December; 42 hours optimization; verification time: 12 UTC 7 December; verification area centred on 40°N, 75°W). TReC 026.2 focused also on the USA snowstorm, but its observation time and verification time matched the critical phase of the cyclogenesis better. Sensitive-area calculations from the Met Office, ECMWF, NCEP and Météo-France were examined at the afternoon conference on 3 December (Figure 4 shows the targeting guidance maps from the Met Office and ECMWF). The targeting guidances from the different techniques disagree considerably in this case. The ETKF sensitivity
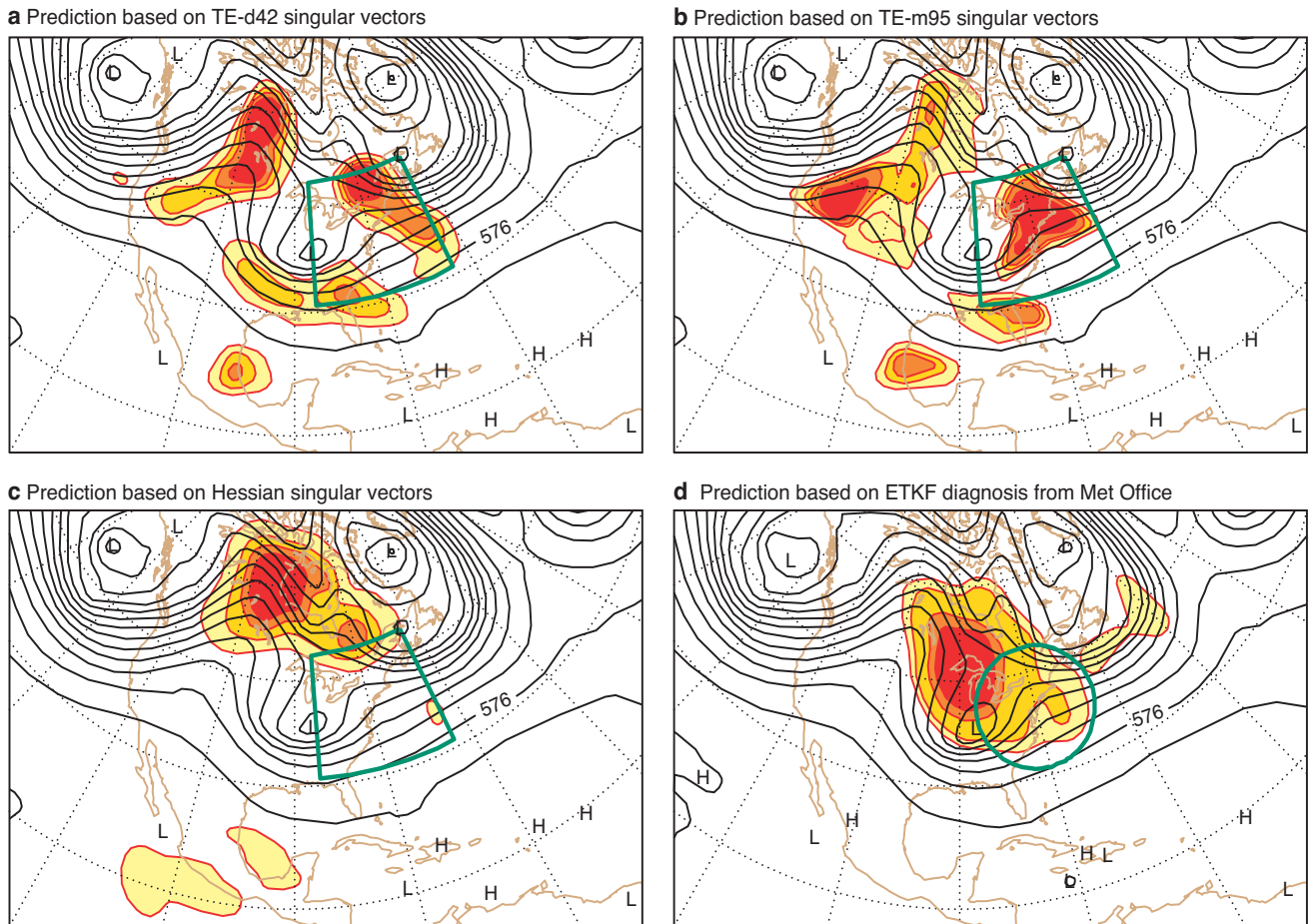
a Prediction based on TE-d42 singular vectors

b Prediction based on TE-m95 singular vectors

c Prediction based on Hessian singular vectors

d Prediction based on ETKF diagnosis from Met Office

Fig. 4 As Figure 2, but for additional observations at 18 UTC on 5 December 2003 and forecasts verifying at 12 UTC on 7 December over a verification region over the east coast of the USA (outlined green).

maximum is over the Great Lakes. This region is not sensitive according to the ECMWF singular-vector based guidance. The TE-d42 and TE-m95 singular vectors highlight three main sensitive regions: western Canada, New England, and offshore from Georgia. The last sensitive area is considered to be important for the low-level flow that was feeding moist air into the system near the coast of the USA. The first two sensitive areas focus on improved initial conditions of the upper-level flow. The Hessian singular vectors account for the high density of the routine network in the USA. They indicate that additional observations are most important over central Canada and Quebec, only. As a consequence, a consensus sensitive region was defined as the domain west of 60°W and north of 30°N. The restrictions on the available observation resources (the remoteness of the airport for the NOAA Gulfstream IV and flight conditions) influenced the choice of the observation deployments.

Air traffic control added difficulties for observing and sampling the region, because of some restrictions on the flight altitude and deployment of dropsondes over land. Eventually, two flights provided 31 dropsonde soundings along the US coast. Figure 5 shows the sounding locations, together with the boundaries of the different targeting guidances. This case highlights problems that are encountered when the guidance from different targeting techniques disagree and

operational constraints further limit the options of taking additional observations.

Comparison of sensitive area predictions

For many A-TReC cases, sensitive-area predictions were obtained with several different methods for the same event, i.e. the same observing time, verification region and verification time. As illustrated in the examples above, there are cases in which all techniques more or less agree where the additional observations are most important in order to improve the selected forecast, and other cases where they disagree considerably. The overall level of agreement between the sensitive-area predictions from different techniques during A-TReC, can be quantified in terms of geographical overlap. For two sensitive areas S_j and S_k having the same size, we define the geographical overlap O_{jk} as the ratio of the area of their intersection to the area of one region

$$O_{jk} = \text{area}(S_j \cap S_k)/\text{area }(S_j)$$

The fraction of cases with a geographical overlap of at least 0.5 is listed in Table 2 for different combinations of techniques and sensitive areas, with an area of 4×10^6 km². Results indicate that the sensitive-area prediction based on total-energy singular vectors from ECMWF (TE-d42) and Météo-France ($T_L 63$, dry TLM) are fairly similar, despite the use of different trajectories and different models. Furthermore, the
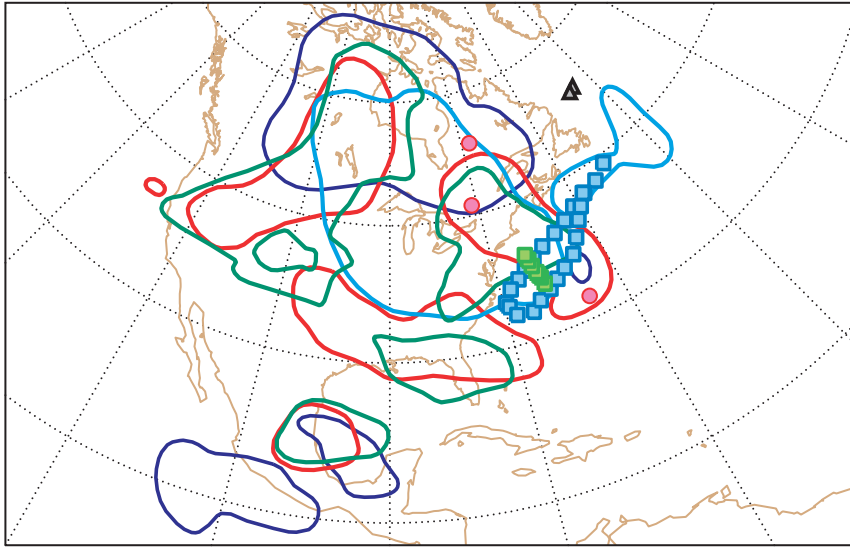
Fig. 5 As Figure 3, but for targeted observations taken around 18 UTC on 5 December in the sensitive areas shown in Figure 4.
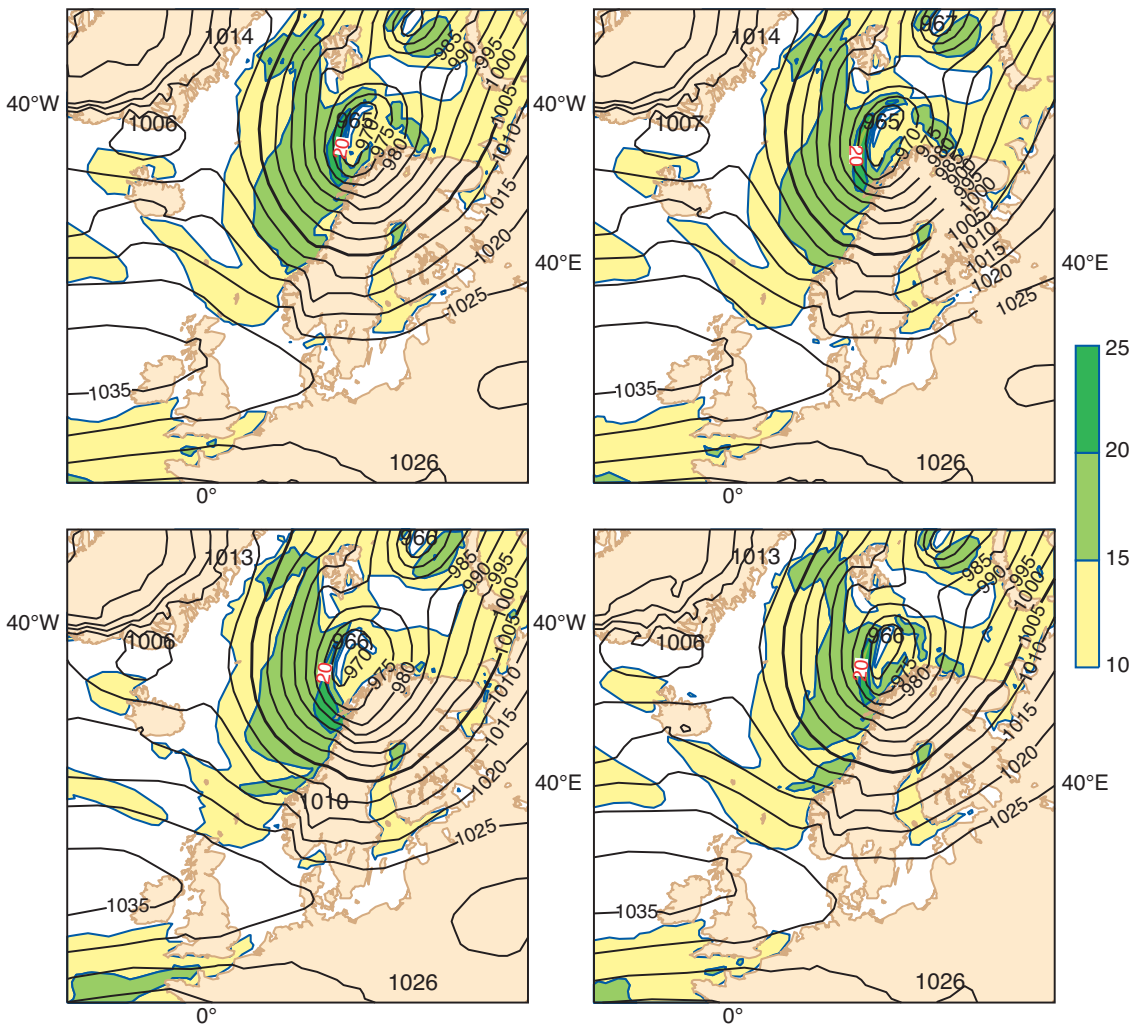

Fig. 6 Mean-sea-level pressure (MSLP) and surface wind speed fields all valid at 12 UTC on 4 December 2003. The MSLP contour interval is 5 hPa, the surface wind speed is shaded starting from 10 m/s, every 5 m/s. The upper-left panel shows the 36-hour forecast from the A-TReC experiment (with extra observations), the upper-right panel shows the 36-hour forecast from the control experiment, the lower left panel shows the analysis (control) and the lower right panel shows the 48-hour forecast from the control experiment. Note the similarity of the two experiments and the consistency of the two subsequent control forecasts, indicating that, at that range, the predictability level was already good.

SAP1	SAP2	Number of cases with overlap ≥ 0.5	
SV TE-d42	SV TE-m95	42 of 43	98%
SV TE-d42	SV H-42	35 of 42	83%
SV TE-d42	SV Météo-France	15 of 16	94%
SV TE-d42	ETKF	31 of 67	46%
SV H-d42	ETKF	32 of 67	48%

Table 2 Fraction of cases with an overlap of the sensitive regions (area 4 x 10^6 km^2) determined with two different techniques (SAP1, SAP2) of at least 0.50.

representation of moist processes in the tangent-linear model and the use of higher spatial resolution have only a fairly minor effect on the sensitive areas in most cases: 98% have an overlap ≥0.5. The fraction of cases with a large overlap between sensitive areas based on total-energy singular vectors and sensitive areas based on Hessian singular vectors is smaller but still high (83%). This highlights the importance of the choice of the initial-time norm in the singular-vector computation for observation-targeting applications.

However, in general, the overlap between any two of the singular-vector based regions is considerably larger than the overlap between one of the singular-vector based regions and the ETKF based region – more than half of the cases have an overlap below 0.5 between the ETKF region and one of the singular-vector based regions. Preliminary results also indicate that the correlation of the forecast-error reduction predicted by the ETKF and the forecast-error reduction in the subspace of the Hessian singular vectors is low for the A-TReC cases. The inconsistency between consecutive forecasts may explain some of the cases with very low overlap because the ETKF was based on an ensemble initialized 12 hours before the singular-vector trajectories. But perhaps the more important difference between the singular-vector techniques and the ETKF technique is the structural difference between transformed ensemble perturbations at a forecast range of two to three days and the initial singular vectors.

Impact of A-TReC observations

The ECMWF Research Department is completing a set of experiments to assess the impact of additional observations released during the A-TReC campaign. A recent version of the ECMWF operational model (model cycle 28r1) has been rerun for the period covering the field campaign with two configurations differing only in the data usage: The A-TReC experiment assimilated observations from the routine observing network plus the extra A-TReC observations, whereas the Control experiment assimilated the observations of the routine observing network only. A preliminary subjective evaluation of the available cases shows little impact of the extra observations, in general. As illustrated in the example related to TREC 24 (Figure 6), by the time the observations were deployed, the forecast has already converged towards a consistent solution. In this case, the impact of the extra observations on the forecast in the verification area (Norway and the Arctic Ocean) was almost negligible. The verification plot shows that the strong cyclone leading to high winds on the Norwegian west coast

had been correctly predicted at the D+2 range. Adding extra observations upstream did not produce any significant change. A detailed inspection of the forecast consistency (between different models and the same models from different base dates) shows that the consistency improved dramatically as the verification time was approached from the day the choice to target the cyclone was made (five days ahead). This behaviour was also present in the EPS spread, as indicated by the comparison of the forecast at ranges D+5 and D+2 (Figures 7 and 8). Comparing the EPS and multi-analysis forecasts[1] at different ranges, it is clear how the uncertainty about the existence, position and intensity of the cyclone reduced from D+5 to D+2.

Discussion and conclusions

Noticeable differences between the targeting guidance based on the ETKF and the singular-vector based guidance were revealed during the A-TReC. Is A-TReC (or field campaigns in general) suitable for determining which technique is superior? One would need to sample both the ETKF target region and the deviating singular-vector based sensitive region with a similar coverage of extra observations. This was not feasible during A-TReC. Moreover, a large sample of cases may be required to estimate forecast-skill differences in the fairly small verification regions.

The cases examined so far already show a high skill in the forecast of the Control experiment, therefore, the impact of the extra observations is expected to be neutral overall. A much larger sample of cases may be required to find noticeable forecast errors associated with hazardous-weather events at a forecast range of up to D+3. The natural suggestion would be to use adaptive observations for the medium-range. However, the linearity assumptions in current adaptive-observation techniques preclude their usage for longer-range forecasts.

The discussion above is related to shortcomings of the procedure adopted for planning adaptive observation deployments. Given the increase of predictability over the 48-hour period between case selection and deployment, it would be appropriate either to shorten the warning time for observation providers or, alternatively, to cancel all those cases that show a sharp reduction in forecast uncertainty as the observation time approaches.

FURTHER READING

Barkmeijer, J., **M. Van Gijzen** and **F. Bouttier**, 1998: Singular vectors and estimates of the analysis-error covariance metric. *Q.J.R. Met. Soc.*, **124**, 1695-1713.

Leutbecher, M., 2003: 'Adaptive observations, the Hessian metric and singular vectors'. Pp. 393-415 in Proceedings of the ECMWF seminar on recent developments in data assimilation for atmosphere and ocean. (http://www.ecmwf.int/publications/library/do/references/list/17334)

Simmons, A.J. and **A. Hollingsworth**, 2002: Some aspects of the improvement in skill of numerical weather prediction. *Q.J.R. Met. Soc.*, **128**, 647-677.

1 Multi-analysis forecasts are computed once a day (12 UTC), running a T255 version of the operational ECMWF model starting from others Centre's global analyses.
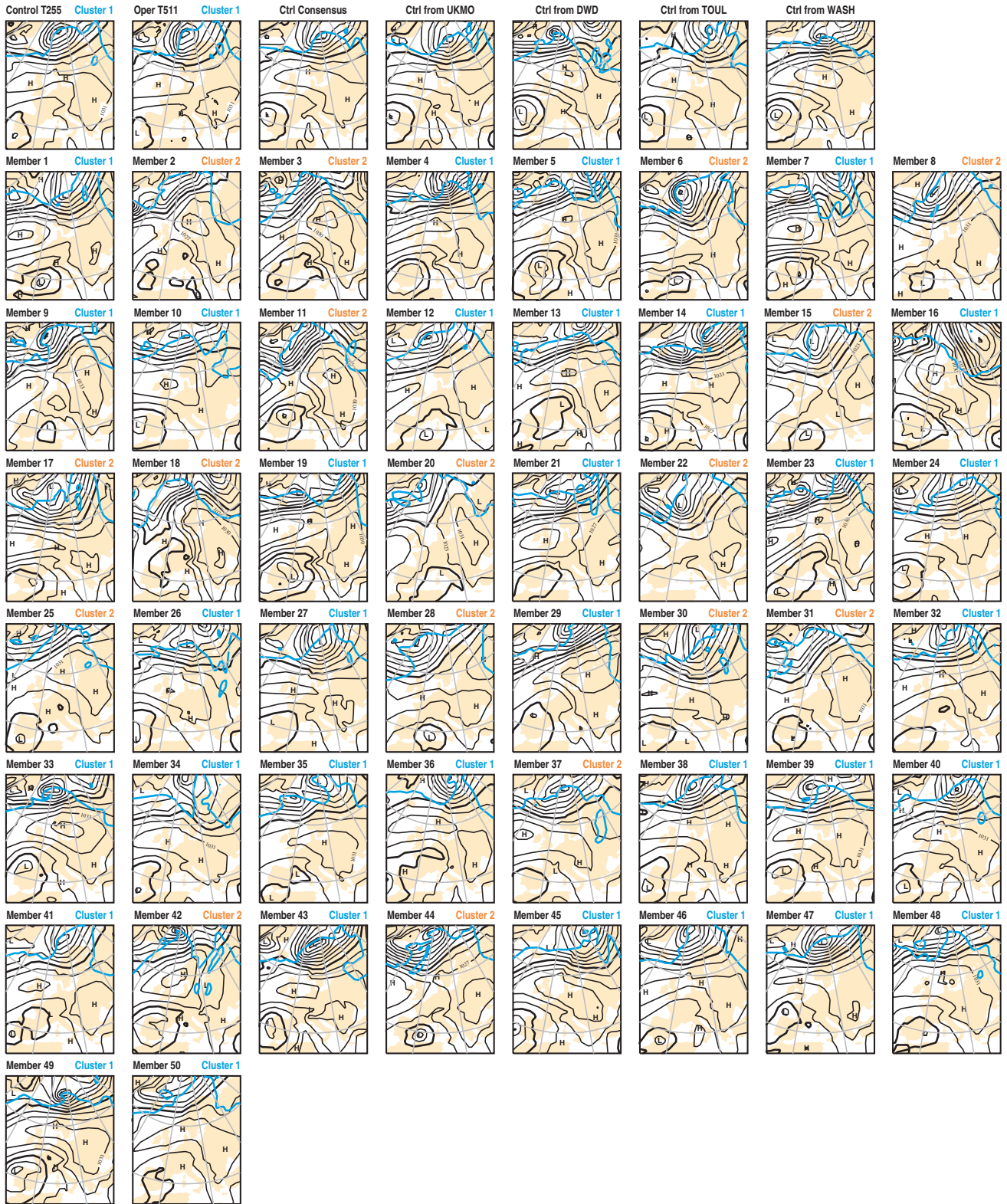
Fig. 7 The T511, the EPS and the multi-analysis member forecasts at D+5 of the mean-sea-level pressure (MSLP) and temperature at 850 hPa. All the forecasts verify at 12 UTC on 4 December 2003. The MSLP contour interval is 5 hPa, and the temperature at 850 hPa is plotted showing only -6C (cyan) and 16C (red) isolines.
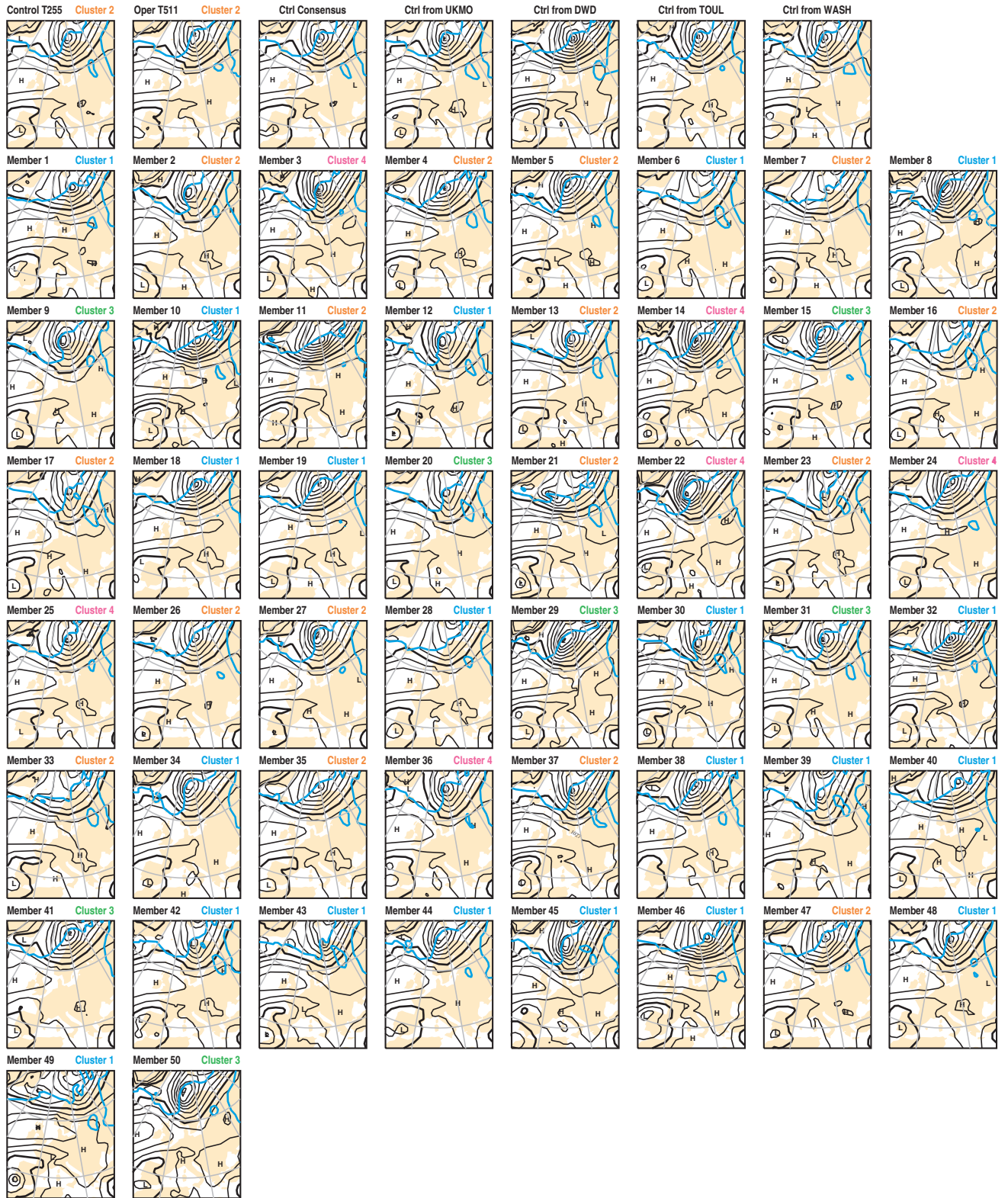
Fig. 8 As Figure 7, but for D+2 forecasts valid at 12 UTC on 4 December 2003.

Martin Leutbecher, Alexis Doerenbecher, Federico Grazzini and Carla Cardinali

Two new cycles of the IFS: Cycle 26r3 and Cycle 28r1

The assimilation and forecasting systems at ECMWF are regularly upgraded to incorporate enhanced assimilation techniques, observational data usage, numerical methods and physical parametrizations. This article describes the scientific content of two recent upgrades (called 'cycles' in the ECMWF jargon) that took place respectively in October 7th 2003 (Cycle 26r3) and March 9th 2004 (Cycle 28r1).

Cycle 26r3

This cycle included a large number of improvements in data assimilation and the use of observations together with improvements in the physics of the atmospheric model.

Data assimilation changes

The New Humidity Analysis

A new and innovative formulation for the humidity analysis (*Hólm et al.* 2002) was implemented operationally as part of Cycle 26r3. Before Cycle 26r3 the 4D-Var humidity analysis was performed in terms of specific humidity, q. The new humidity analysis is based on a transformed relative humidity variable, following the approach of *Dee and DaSilva* (2003). Humidity is in many respects a harder quantity to analyze than wind and temperature, for example. Humidity errors have large variability over short distances and can vary by several orders of magnitude in the vertical. The analysis needs to respect the physical limits due to condensation effects near saturation and the strict limit at zero humidity. In the new formulation error variances are normalized by a factor that depends on the background state; this factor is small in very humid and very dry conditions, and larger for intermediate relative-humidity values. The error standard deviations in terms of either specific or relative humidity are thereby strongly dependent on the atmospheric state. An example with a cold-air outbreak and a cyclone in the North Atlantic is shown in Figure 1.

The new humidity analysis has been implemented within the background constraint of 4D-Var by specifying the background-error statistics in terms of the normalized relative-humidity variable. It has been verified that the new humidity analysis in a broad sense gives the correct weight to all humidity-sensitive radiance data (HIRS, SSMI, Meteosat, GOES, AMSU-B and AIRS) and also to SYNOP 2m-relative humidity and radiosonde specific humidity data. Data impact studies (OSEs) for these main types of humidity data have been carried out (*Andersson et al.* 2004). The OSE results show that the analysis accuracy benefits from these humidity observing systems, and that the main remaining problems are due to humidity biases in both the observations and the model. The next planned changes to the humidity analysis are to introduce data from Meteosat-8★, and to extend (from the current 300 hPa cut-off) the use of the most accurate radiosonde sensors [according to *Nash* (2003) and operational monitoring results (*Garcia-Mendez*, personal communication)] to all levels in the upper troposphere.

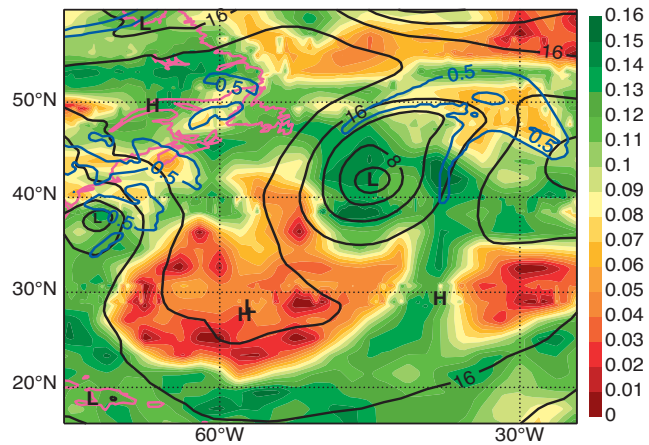★ These changes took place on 28 September 2004 (Cycle 28r3).

Fig. 1 Humidity background error at level 44 (~700 hPa) in terms of relative humidity (shaded, see legend), 15 UTC 24.05.2003. Geopotential at 1000 hPa is contoured in black (4 dm interval) and the blue contour shows cloud fraction = 0.5. The new statistical model for humidity background errors assigns low (orange) relative-humidity error standard-deviations within the cold-air outbreak and within frontal clouds, and high background errors (green) e.g. within the depression.

In the tropics it is quite crucial that the humidity analysis does not cause unwanted changes to the rainfall rate. In recent years there has been a problem with unbalances in the analyses leading to excessive tropical rainfall in the first few hours of forecast. The new humidity analysis has already brought clear improvement to this so-called 'spin-down' problem, and further research in this area is promising. In a sensitivity-experiment modifications were made to limit the humidity analysis increments so that the rate of condensation of the analysis is not larger than the rate of condensation of the first guess, which in effect removes any substantial increases in relative humidity inside clouds. With this modification, tropical rainfall distributions remain nearly constant in time over the first 24 hours of forecasts, as desired. Work in this area is continuing.

Japanese Profilers

Japanese wind profiler data have been monitored operationally for more than a year. The quality of the Japanese network (31 stations at 1.3 GHz) has been found to be consistently good – in some respects better than for the American (32 stations at 404 MHz) and European (16 stations at 50, 400 and 1000 MHz) networks. The standard deviation is low and there are very few outliers. The American profiler data have been used since Cycle 21r2 July 1999 (*Bouttier*, 2001), European since Cycle 25r1 April 2002 (*Andersson and Garcia-Mendez* 2002) and Japanese profilers since Cycle 26r3 October 2003. Because of poorer representativity nearer the ground, none of the profiler stations can be used below 925 hPa, and only four of the Japanese stations are used in the layer 925–850 hPa. Most of the Japanese profilers reach 500, or 400 hPa, but only rarely do they go higher than that.

A test-assimilation was been run for the three-week period from 01.02.2003 to 21.02.2003. The experiment tested the impact of Japanese wind profiler data in the operational context, i.e. full resolution with all available observations. From an accumulation of all twenty-one 12 UTC analysis cycles we found that very few data had been rejected by the automatic quality control checks, confirming the high quality of the data. The results showed some positive impact on analyses and short-range forecasts and the data were thus activated with 26r3.

Use of satellite data

AIRS implementation

The assimilation of satellite observations from the AIRS (Atmospheric InfraRed Sounder) instrument onboard the NASA AQUA spacecraft has become operational with Cycle 26r3, following an extensive monitoring and scientific validation, especially in the area of cloud detection (*McNally and Watts*, 2004). The exploitation of this instrument presented a scientific and technical challenge due to the unique high spectral resolution of this infrared sounder. Substantial efforts were needed in the domain of monitoring and observation handling to be able to cope with such a massive amount of high quality data. The baseline configuration remains conservative in terms of data usage, observation error specification, bias correction, etc. Nevertheless, the operational implementation of this day-1 system constitutes the first operational exploitation of advanced infrared sounders and paves the way for future operational missions (METOP and NPOESS). The impact of AIRS in the assimilation is positive but small, underlining the fact that the system is already heavily constrained by other satellite instruments. However, to assess the intrinsic merit of AIRS as compared to other instruments, an academic study was run that compares the impact of individual instruments in the ECMWF assimilation system when all other radiances are withdrawn. The results are illustrated in Figure 2 for the Southern Hemisphere 500hPa geopotential height forecast anomaly correlation (averaged over 50 cases) at day 3, 5 and 7. The pink (NO-RAD) columns represent the performance of the system when all the radiances are excluded. The AIRS (green columns) expectedly outperforms the classical HIRS infrared instrument (orange columns), but also the AMSU-A microwave instrument (blue column) despite its ability to penetrate clouds. The results are less clear-cut and more contrasted in the Northern Hemisphere (not shown), indicating first that single satellite platforms have limited impact over the NO-RAD system (probably due to a still limited usage of satellite radiances over land and also the importance of the ground based network). The results of this academic study together with the overall small but positive impact of AIRS in the forecasting system were considered very encouraging and led to an operational implementation of this new dataset.

Geostationary radiances and winds

GOES-9, GOES-12 (replacing GOES-8) and Meteosat-5 water vapour channel Clear Sky Radiances (CSR) data have been incorporated in Cycle 26r3, completing the geostation-
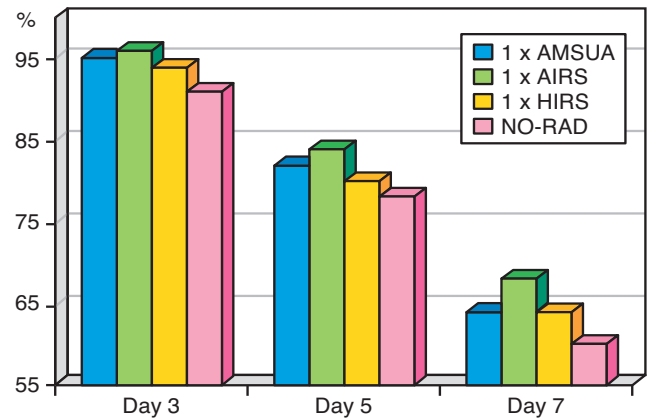

Fig. 2 Southern Hemisphere 500 hPa geopotential height forecast anomaly correlation (averaged over 50 cases) at day 3, 5 and 7 issued from the assimilation experiments where all the satellite radiances have been excluded from the system (NO-RAD), but 1 HIRS instrument on board NOAA 16 (1 x HIRS), but 1 AMSU-A instrument onboard NOAA-16 (1 x AMSUA), but AIRS onboard AQUA (1 x AIRS). *Courtesy T. McNally*.

ary coverage of tropical Upper Tropospheric Humidity (UTH). An Observing System Experiment run for July and August 2003 showed that the impact of the CSR products from the geostationary network is positive for upper tropospheric geopotential height anomaly correlations as well as for wind RMS errors. The data appear to remain unbiased with respect to the model and consistently moisten the upper troposphere in the region of the ITCZ, as previously found with METEOSAT-7. However, increments now seem to be smaller in Cycle 26r3 than found in previous studies; this is likely to be related to the change in analysis humidity variable (as described in the previous section) and the introduction of large amounts of other humidity-sensitive satellite data (see below). As an illustration, the impact of the assimilation of Meteosat-5 on the UTH can be seen by examining the change in RMS first-guess departure of HIRS channel 12 onboard NOAA-16 (water vapour channel sensitive to UTH and used here as an independent verification). An area of reduced RMS first guess departure may be seen in the area where Meteosat-5 is assimilated (see Figure 3).

Note also that after careful checking and tuning, and following studies demonstrating a slight positive impact of the data on the forecasts, Atmospheric Motion Vectors (AMVs) from GOES-12 (in replacement of GOES-8) where also introduced in Cycle 26r3.

Assimilation of MIPAS ozone profiles

Cycle 26r3 assimilation is using MIPAS ozone profiles in addition to ozone layers from SBUV/2 on NOAA-16. The MIPAS data proved to be of very good quality. Their assimilation has had a positive impact on the analyzed ozone field, while the impact on the forecast scores was neutral. The data efficiently correct for model biases, and because of their higher vertical resolution (3–4 km) than data previously used, their assimilation does not lead to problems with the vertical structure of the analyzed ozone field, which were seen
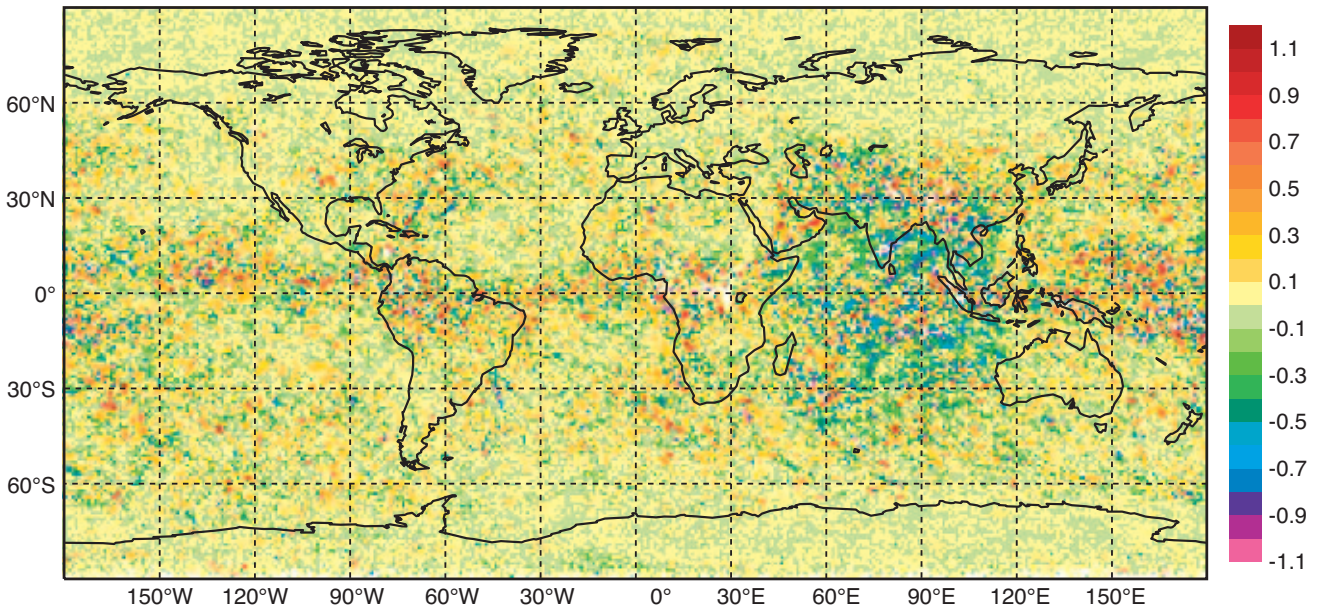
Fig. 3 Difference in RMS first guess departure of HIRS channel 12 onboard NOAA-16 between Meteosat-5 assimilation experiment and control. Negative values indicate areas where the use of Meteosat-5 radiances improves the fit of the model to HIRS channel 12. *Courtesy M. Szyndel.*

when assimilating GOME total ozone or SBUV/2 ozone layers in the presence of a bias. The resulting analyzed ozone profiles agree well with independent ozone sondes, which were not used in the analysis. Figure 4 shows ozone profiles from sondes and assimilation experiments at the Antarctic Neumayer station on 26 August and 11 September 2003. The agreement with the sondes is considerably improved if MIPAS ozone profiles are assimilated.

Unfortunately, at the end of March 2004 ESA decided to switch off the MIPAS instrument because of various anomalies currently under investigation. Current thinking is that MIPAS will return to operations during the second half of 2004 at reduced spectral resolution, but the situation is uncertain at the time of writing. Meantime, only SBUV/2 ozone layers from NOAA-16 are actively assimilated in the operational suite.

Other changes

◆ Benefiting from the new improved humidity analysis, radiances from the AMSUB microwave humidity instrument onboard NOAA-16 and 17 have been operationally

assimilated with Cycle 26r3. Three moisture channels from this sensor have been introduced, providing moisture information at 300–400 hPa. To a large extent, AMSUB data have a consistent influence with that from SSM/I (moistening in the tropics, effect on precipitation) and also show a small positive impact on the forecast skill. Since its operational implementation, a problem in AMSU-B usage over land has been identified and the correction has been implemented.

◆ A fourth AMSU-A instrument (onboard AQUA) has been introduced in the operational system, following clearly positive trial experiments. A redundance of AMSU-A information was probably a key element in the steadiness of the scores after the unfortunate loss of data from NOAA-17 in October 2003.

◆ Cycle 26r3 was also an opportunity for various improvements of the quality control and refinement of the use of the HIRS instrument onboard NOAA-16 and NOAA-17.

◆ Three new wave model parameters have been output in Cycle 26r3. They are connected to the possible presence (in a statistical sense) of freak waves. These are namely the
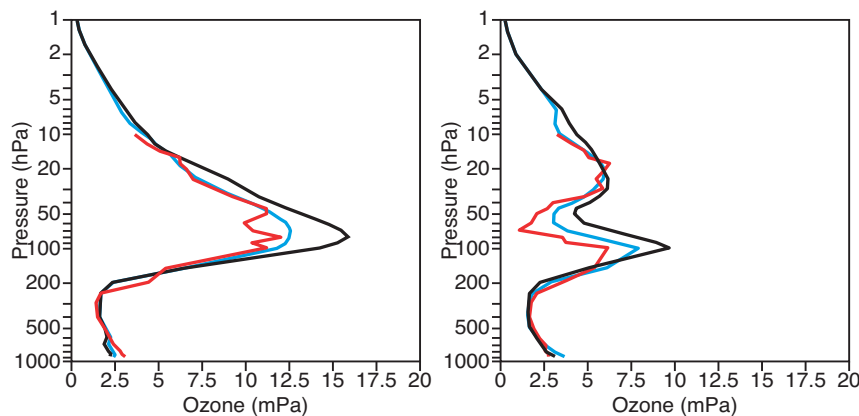

Fig. 4 Ozone profiles in mPa from sondes (thick solid), assimilation experiment without MIPAS ozone profiles (thin solid), and assimilation experiment with MIPAS ozone profiles (dotted) at the Antarctic Neumayer station (71°S, 8°W) on 26 August (left) and 11 September 2004 (right). *Courtesy A. Dethof*

spectral kurtosis, the Benjamin-Feir index and the spectral peakness. The basic theory behind these fields was presented by Peter Janssen in a previous Newsletter article (ECMWF Newsletter 100).

Forecast model modifications

1   The atmospheric forecast model in the IFS plays an important role in the data assimilation. Apart from the full nonlinear model to propagate the state of the atmosphere in time, a tangent linear (TL) and adjoint (AD) version are also used for minimization purposes during data assimilation. The TL and AD models correspond to simplified versions of the full model, and are under continuous development. The purpose is to obtain TL and AD models that represent the full model as realistically as possible but at the same time are computationally efficient. With CY26r3 a significant upgrade of the TL and AD of radiation was introduced. Before this cycle, the TL and AD longwave radiation was simply represented by a constant emissivity on model levels. The new version is much more realistic and includes the effect of clouds. Computational efficiency is achieved by combining the full radiation scheme with precomputed Jacobian matrices and neural networks (*Janisková et al.*, 2002). As expected from a better description of the cloud radiation interactions in 4D-Var, results showed a slight general improvement of the forecasts in terms of anomaly correlation and a significant positive impact for some individual cases.

Fig. 5   Effect of aerosols on model climate for JJA. Errors in the model climate for precipitation (colour shading), wind at 925hPa (arrows) and 500hPa height (contours) are shown with respect to Xie and Arkin precipitation climatology and ERA-40 wind and height fields respectively. The top panel is for the model with the old aerosols; the bottom panel is with the new aerosols. It can be seen that a significant reduction of errors is obtained with the new aerosols over the Atlantic near West Africa. *Courtesy M. Rodwell*.

2   Radiation computations are very expensive and are therefore performed at lower resolution and only at a frequency of one hour during data assimilation and three-hourly during normal forecasts. Before 26r3 the reduced resolution was obtained by sampling one out of four points along latitude lines (except at high latitudes). With 26r3 an interpolation mechanism has been introduced that allows the radiation grid to be completely independent from the model grid. Because the resolution reduction works in North-South direction as well as East-West, the new scheme is more economic for the same resolution reduction. The default radiation grid for the IFS at T511 is T255. The speed-up factor of the radiation computations is 3.5 whereas it was 2.6 in the previous cycle.

3   The annual mean aerosol climatology from *Tanre et al.* (1984) has been replaced by the *Tegen et al.* (1997) monthly values. The impact in data assimilation and 10-day forecasts appears to be small, but a substantial reduction of systematic errors has been observed in the model climate as a result of the reduction of optical depth over the African continent. A substantial reduction is observed in tropical rainfall errors over Africa. Also the associated near surface wind errors over the Atlantic have been reduced (see Figure 5).

4   Three new surface fields have been added to the post-processing and archiving, namely convective available potential energy (CAPE), UV-b radiation, and photosynthetically active radiation. These fields are available from MARS with codes CAPE (GRIB code 59), UVB (57) and PAR (58) respectively. CAPE is an instantaneous field, UV-b and PAR are accumulated during the forecast (see Figure 6 for an example of CAPE). Although ozone is a forecast variable and assimilated in the IFS, model radiation computations are still based on climatological ozone fields. To allow for full interaction between radiation and prognostic ozone, it will be necessary to make some improvements to the ozone model. The full potential of the simulated UV-b will only be available after introduction of interactive ozone.

5   Operational verification of the T511 deterministic forecasts and the T255 EPS control forecasts show a significant difference in NH and SH anomaly correlation. Such a difference is to be expected from horizontal resolution effects, but it was found that part of the difference was due to the time step which is 15 minutes at T511 and 45 minutes at T255. A considerable time step dependence at T255 was traced back to the so-called 'mass flux limiter' in the convection scheme. For numerical stability the mass flux is limited to the CFL criterion which is inversely proportional to time step. It turned out that numerical stability was not compromised by relaxing the limit with a factor 3 for the temperature and moisture equations (applied only for time steps longer than 30 min). This has been implemented in 26r3 and proved to be very beneficial at T255.
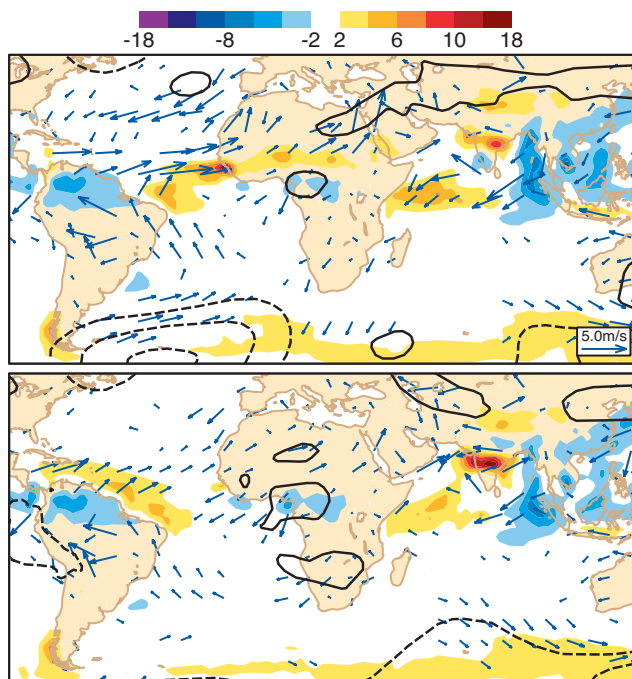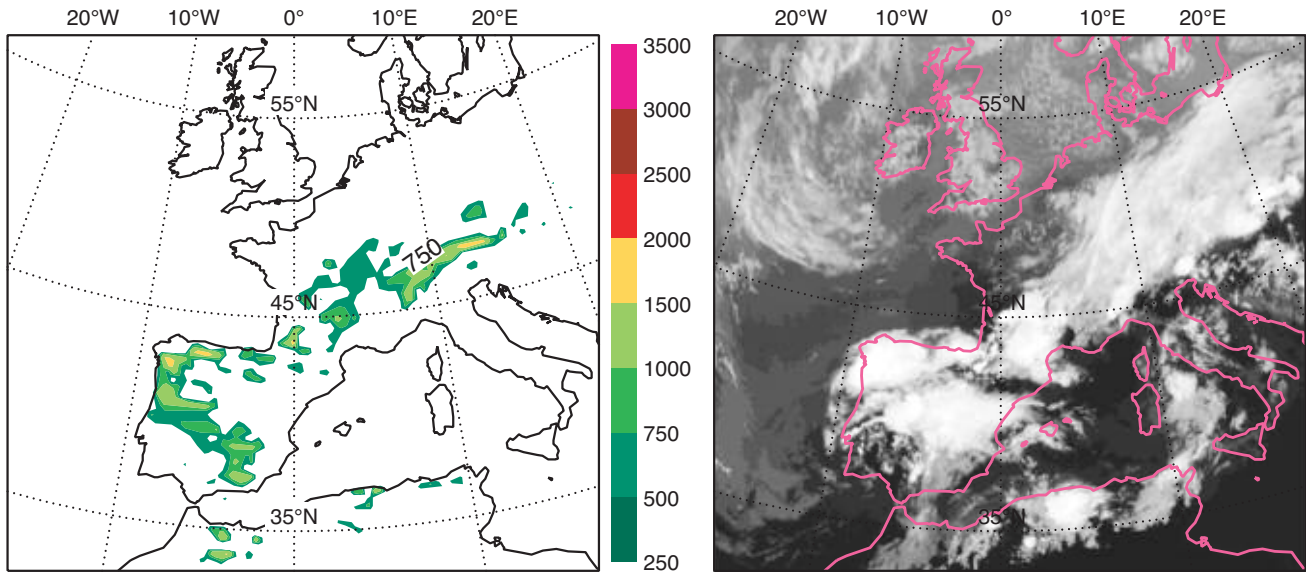
Fig. 6 (Left) CAPE from a 18 hour forecast verifying at 18 UTC 21.05.2004. (Right) A Meteosat IR image for that time. *Courtesy P. Bechtold.*

Overall performance

Such massive and various contributions to the forecasting system warranted a long and extensive testing period. A total of 229 cases were run using Cycle 26r3 and checked against operations. The impact of each individual element has been briefly described here and is further documented in some of the references given below. Only standard performance scores from the whole package are discussed now. Overall, the objective verification showed a substantial improvement of Cycle 26r3 over Cycle 25r4 (the operational system at that time). Figure 7 shows 500 hPa height anomaly correlation for the extratropical Northern Hemisphere (top), Southern Hemisphere (mid) and Europe (bottom), averaged over all forecasts.

At 500 hPa, the conclusion that Cycle 26r3 is better than Cycle 25r4 is statistically significant at confidence levels indicated in the table below, for a t–test applied to the score differences.

Cycle 26r3 turned out to be significantly better than Cycle 25r4 almost everywhere (not shown), and following this overall very good performance, was successfully introduced in operations on 7 October 2003.

Cycle 28r1

This cycle was more modest in terms of atmospheric data assimilation and model changes, but was considered as a major enhancement of the wave assimilation and modelling system.

Days	N. Hemisphere	S. Hemisphere	Europe
3	99.9	99.9	95.0
5	99.0	99.9	95.0
7	95.0	99.8	99.8

Table 1 Statistical significance tests for the 500 hPa height anomaly correlation score difference between Cycle 26r3 and Cycle 25r4 (t-test).
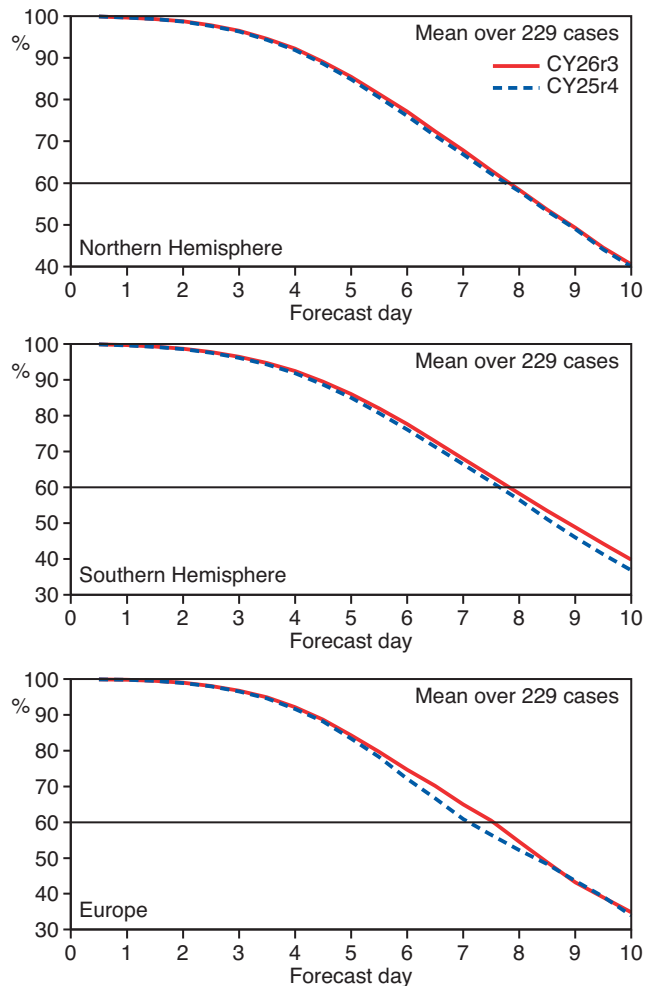
Fig. 7 Anomaly correlation of 500 hPa height for the Northern Hemisphere (top panel), Southern Hemisphere (mid panel) and Europe (bottom panel). Mean scores averaged over 229 cases are shown for 12 UTC forecasts from cycle 26r3 (red solid) and cycle 25r4 (blue dashed) verified against analysis

Data assimilation changes

Snow Analysis

The operational snow depth analysis relies on the short-range forecast, approx. 1500 station observations and a monthly climatology based on observations. The in-situ measurements are used to update the forecast field using a Cressman analysis with empirically derived functions for the spatial weighting. Snow extent derived from the shortwave channels of MODIS (on the American AQUA satellite) showed significant differences when compared to the analysis. A new two-step algorithm (*Drusch et al.* 2004) has been implemented in the analysis to incorporate snow extent derived from multi-spectral satellite imagery (NOAA NESDIS product) in the snow depth analysis. Results are shown for 2 December 2002 in Figure 8. Differences occur over large parts of North America, e.g. to the south of the Great Lakes, and in the Rocky Mountains area.

GOES BUFR winds

The implementation of the GOES BUFR AMVs was also part of Cycle 28r1. The use of this new product allowed common and consistent formats and Quality Indicators for all AMV products (METEOSAT and GOES) used in the assimilation. The distinction between clear and cloudy winds became also possible (allowing for a better quality control) and AMVs from the visible channel were included. Assimilation experiments using these new products showed small but consistently positive impact over both hemispheres.

Atmospheric model changes

The current operational forecast sometimes produces numerical noise in the winter stratosphere when the polar night vortex is displaced off the pole or becomes distorted and breaks up, as is the case during sudden stratospheric warmings. The noise disappears once the vortex recovers its normal shape and position. The computational instability generating this noise is self-limiting and did not lead to forecast failure (see article on 'breakdown of the stratospheric winter polar vortex' by *A. Simmons et al.* in ECMWF Newsletter No 96).

Figure 9 (top panel) shows as an example the 10hPa geopotential height from the operational 12-hour forecast valid on 28 December 2002 at 12 UTC (left panel) and the corresponding map of divergence at model level 11 (~5hPa), plotted at full forecast resolution $T_L 511$ (right panel). The noise in divergence has the appearance of coherent wave trains of quite short wavelengths in the horizontal.
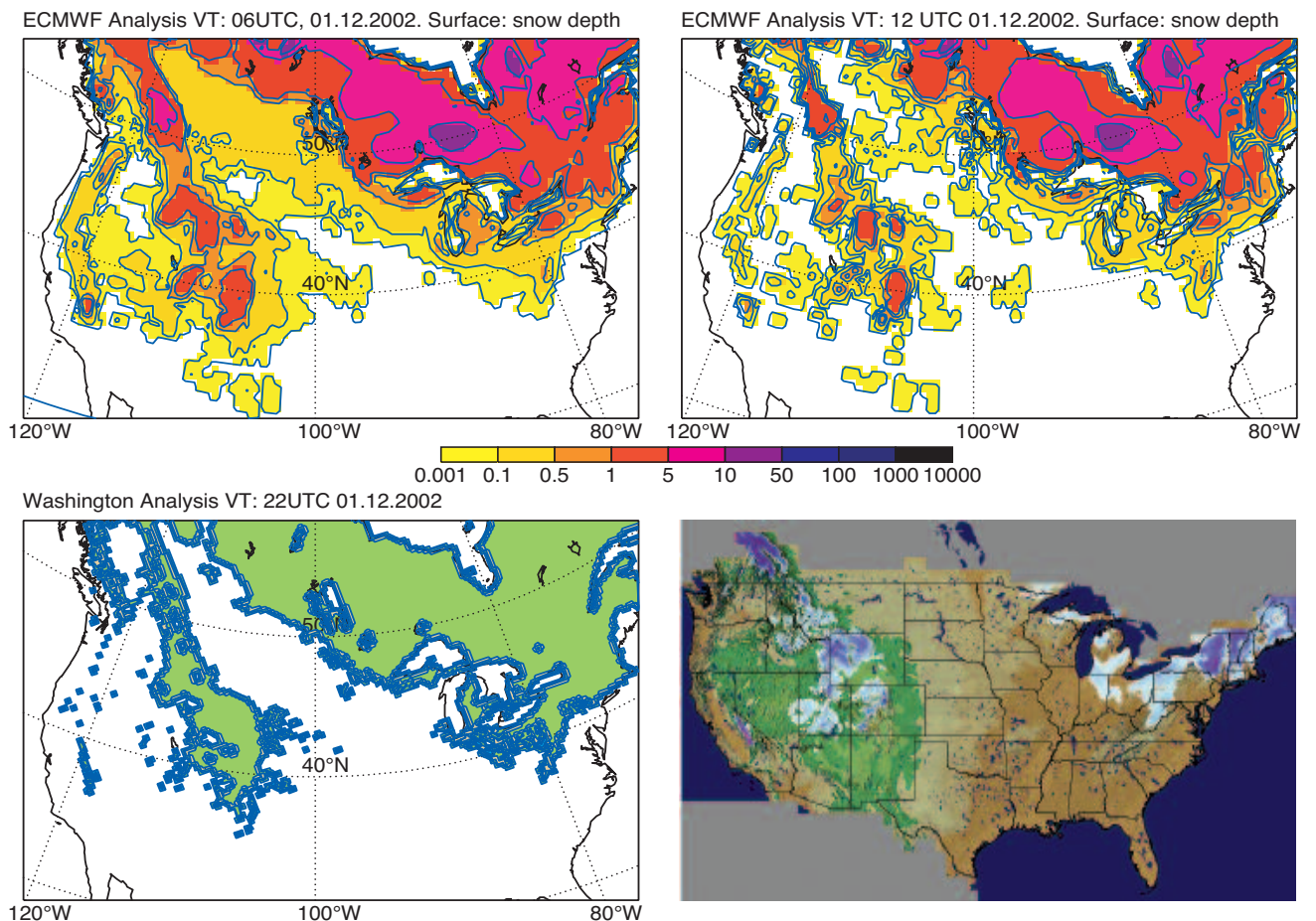
Fig. 8 Validation of the modified snow analysis (top right), which incorporates the use of a satellite-based snow cover product from NESDIS (lower left). Comparison is made with the previous operational snow analysis (top left) and an independent snow analysis (lower right) from the National Operational Hydrological Remote Sensing Center (NOHRSC). *Courtesy M. Drusch and NOHRSC.*

Only a few selected wavelengths seem to be amplified by the mechanism responsible for the generation of this noise. Which wavelengths are amplified depends, among other factors, on the integration time-step. Decreasing the time-step leads to the amplification of progressively shorter waves. The noise disappears when the time-step is chosen small enough so that the amplified waves are too short to be resolved by the models horizontal resolution. At $T_L 511$ the

time-step had to be reduced to 3 min (from 15 min in operations) to achieve a noise-free forecast for the 28 December 2002 case. Such a short time-step clearly cannot be afforded in operations and a different way of suppressing the noise had to be found.

Considering the characteristics of the noise, the process responsible for its generation seems to be as follows: In areas with a large vertical temperature gradient, any horizontal

10hPa geopotential height
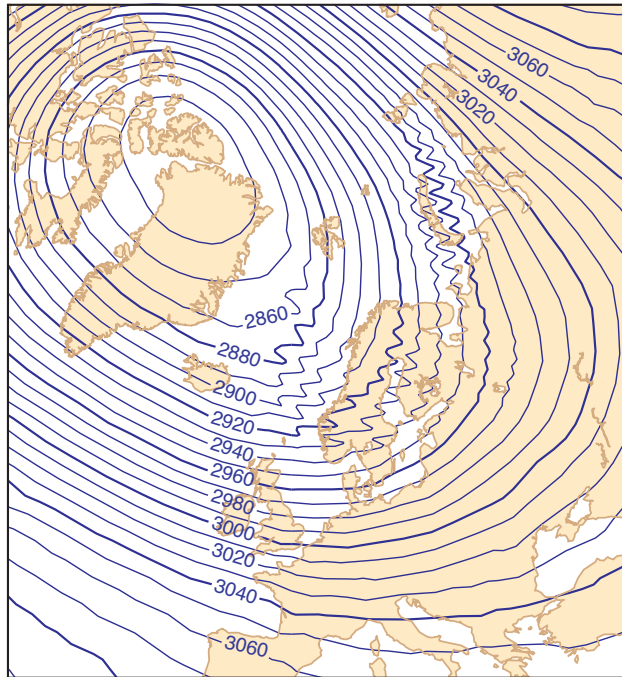
Model Level 11 divergence
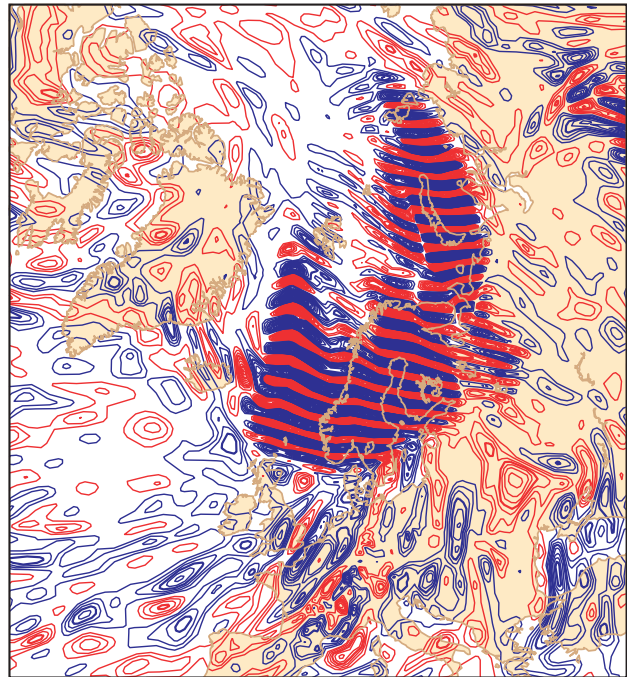
10hPa geopotential height
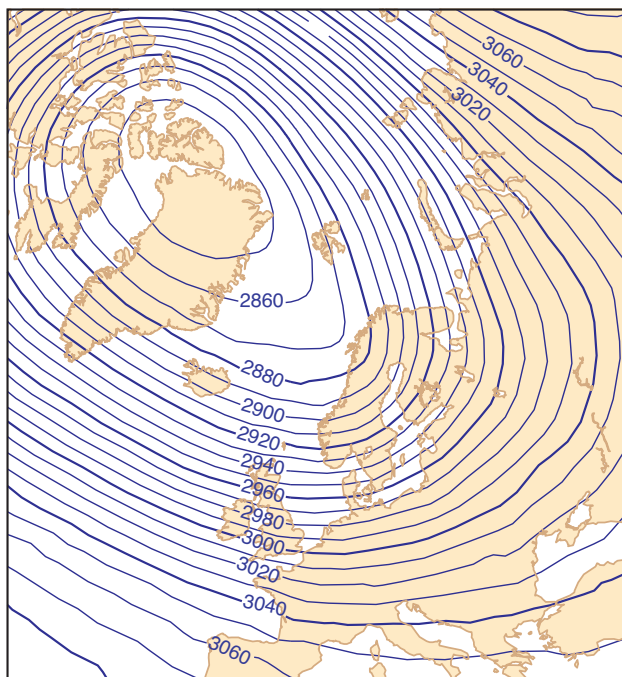
Model Level 11 divergence
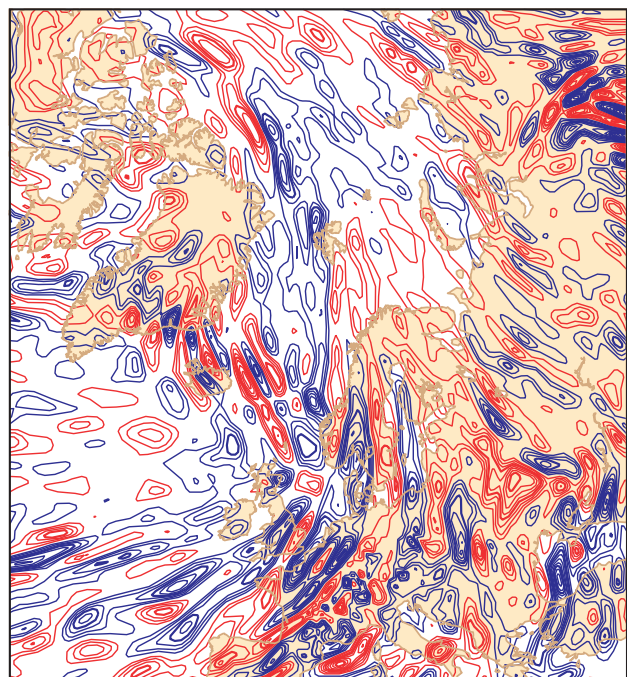
Fig. 9 12 hour forecast of the 10 hPa geopotential height (top right) from initial data of 28.12.2002 at 12 UTC and divergence at model level 11 (~5 hPa) (top left) for the same forecast. Same fields (bottom right and left) when the smoothing procedure is applied (see text for details).

Mean wave height difference for July 2001
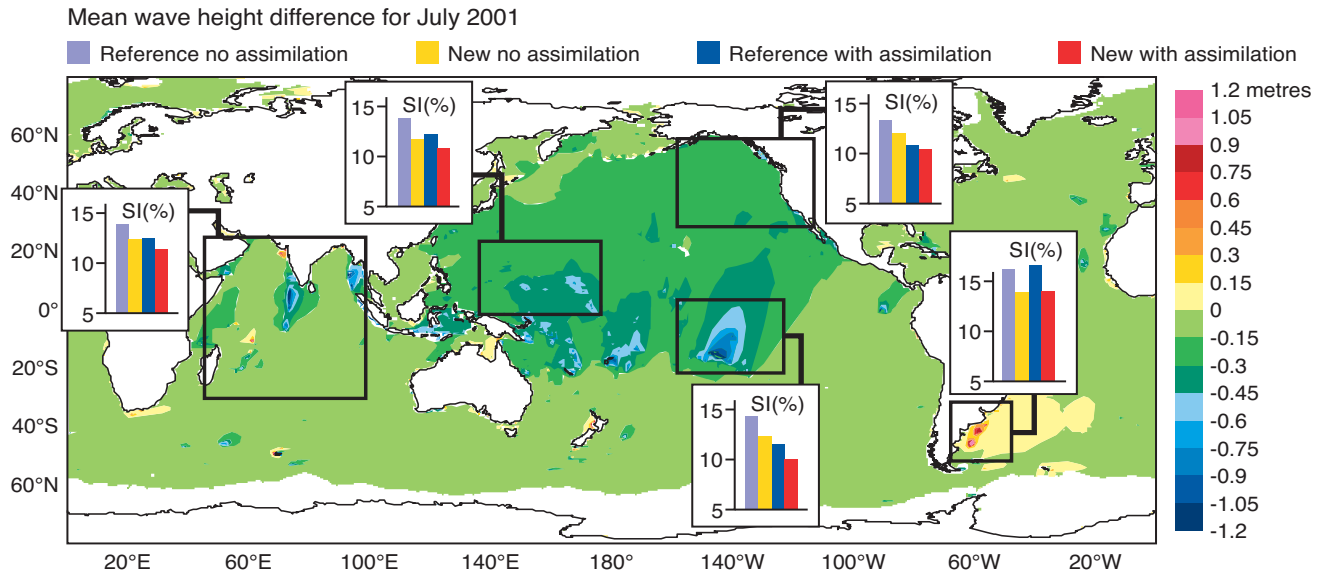
Fig. 10 The colour contours display the mean wave height difference between the new sub-grid bathymetry model and a reference for runs without data assimilation. The new model used the mean bathymetry based on ETOPO2 whereas the reference employed the old bathymetry based on ETOPO5. See text for details.

structure in the vertical velocity will lead, through the vertical advection, to a perturbation in the horizontal temperature field. This perturbation produces a barotropic perturbation of the geopotential field aloft, which will produce a perturbation in divergence at the following time step. This in turn feeds back into the computation of the vertical velocity. This feedback process can lead to resonance for certain waves for which the feedback happens to be in-phase. By applying a low-pass filter somewhere in the feedback loop, the scales of motion which lead to the instability through the feedback will be reduced, and the amplification can be forestalled.

Filtering out the short horizontal scales from the vertical velocity, before it is used in determining the vertical trajectory in the semi-Lagrangian advection in the stratosphere (above ~70 hPa), proved to be sufficient to prevent the development of the noise (*Hortal and Untch*, 2003). Fig 9 (bottom panel) shows the same fields (i.e. 12-hour forecast geopotential at 10hPa and divergence at model level 11 valid at 28 December 2002 at 12UTC) but obtained using a filtered vertical velocity in the semi-Lagrangian advection in stratospheric levels. Clearly the short scale waves with large amplitude that dominate the divergence plot in the top panel have disappeared while the other features have not been affected. This method was also effective in all other noise cases found in the operational forecasts.

Wave model and assimilation changes

Looking at monthly mean analysis wave height increments, especially during the Northern Hemisphere summer (*Bidlot and Janssen* 2003), it appears that there are areas where the wave model first guess is systematically too high or too low. The underestimation in wave heights tends to be located in the active storm track areas or in areas affected by the Indian sub-continent monsoon. It is known that this underestimation is likely caused by under strength model winds. On the other hand, the overestimation for most of the tropical and

northern Pacific cannot be explained in terms of local winds. These systematic overestimations are often present in areas where small island chains exist (French Polynesia and Micronesia in the Pacific Ocean, Maldives Islands and Andaman Islands in the Indian Ocean and Azores and Cape Verde Islands in the Atlantic Ocean).

Hence, it appears that small islands and submerged bathymetric features that are not at all resolved by the coarse wave model grid (55 km) may have a larger impact on the wave climate than it is usually assumed. Although, in the current operational grid, representation of some islands were artificially enhanced to produce the necessary blocking to wave propagation, the results were not very satisfactory. A more appropriate and automatic procedure was introduced in CY28r1 to deal with small islands and reefs.

We have modified the wave propagation scheme to limit the amount of wave energy that can be advected through these sub grid bathymetric features. The WAM model uses a simple first order upwind scheme that requires the knowledge of the wave spectral flux entering a given grid box in the upwind direction. These incoming fluxes are specified by the product of the wave spectral component and the corresponding mean group velocity perpendicular to the upwind grid box facet. However, in reality, if small islands or shallow water features are present, only part of incoming energy will reach the central grid point. With the availability of fine resolution topographic data set such as ETOPO2 (2 minute resolution), it is possible to estimate how much obstruction these features would produce. Note that this data set was also used to derive a new mean bathymetry for the different wave model configurations.

Mean wave height difference between runs with the new bathymetry including the unresolved bathymetry treatment and the reference run for July 2001 is presented in Figure 10. As expected, there is a substantial reduction in the Pacific mean wave height in the lee of the main chains of

islands. As dictated by climatology, the main propagation direction is out of the winter hemisphere and/or in the direction of the trade winds. Other areas where wave height is reduced are also noticeable, in particular in the Indian Ocean. There are also places with increased wave heights. This can be attributed to the new finer bathymetry and how it was used to derive the mean model water depth. Notably, wave heights are much increased on the Argentinean continental shelf and on the South African shelf. Note however that one would have expected wave heights to be lower in the lee of the Aleutian Islands and in the lee of the Lesser Antilles but at these locations, the old grid was manually adjusted to artificially include these islands as land. The new method proves to be a lot more robust in automatically generating the model grid and the attenuation associated with small scales features.

In Figure 10, a comparison between the different model hindcasts and the ERS-2 altimeter wave height data is also given in term of scatter index (normalised standard deviation of the difference). For each set of four bars, the two bars on the left were obtained without assimilation, whereas the two bars on the right were derived from assimilation runs with ERS-2 altimeter wave height data (first guess wave heights were used for the comparison). The beneficial impact

of the change is clearly visible. The inclusion of the sub-grid bathymetry has a tendency to reduce wave heights, resulting in a more negative bias (not shown). The beneficial impact is not only limited to the extra tropics but also around the areas where the largest sub-grid attenuation is taking place. This indicates that the method used here does work well in the far field as well as in the near field. Note also that, the assimilation of altimeter wave heights generally has a positive impact on the wave height statistics. Combining both sub-grid treatment and assimilation yields the best fit to the data.

The WAM model was developed in term of surface stress as expressed by the friction velocity $u\star$. The relation between $u\star$ and the wind speed at a given height (currently 10m) is assumed to be given by the logarithmic profile corresponding to neutral stability condition. The wave model should therefore be forced by surface stresses. However it is usually forced by wind speeds because they are readily available. Hence, these winds should be transformed into their neutral wind counterparts. In the coupled IFS/WAM system, this transformation can easily be achieved on the IFS side by using the atmospheric surface stress and the logarithmic wind profile with the roughness length based on the Charnock parameter. This conversion has been successfully tested. Since
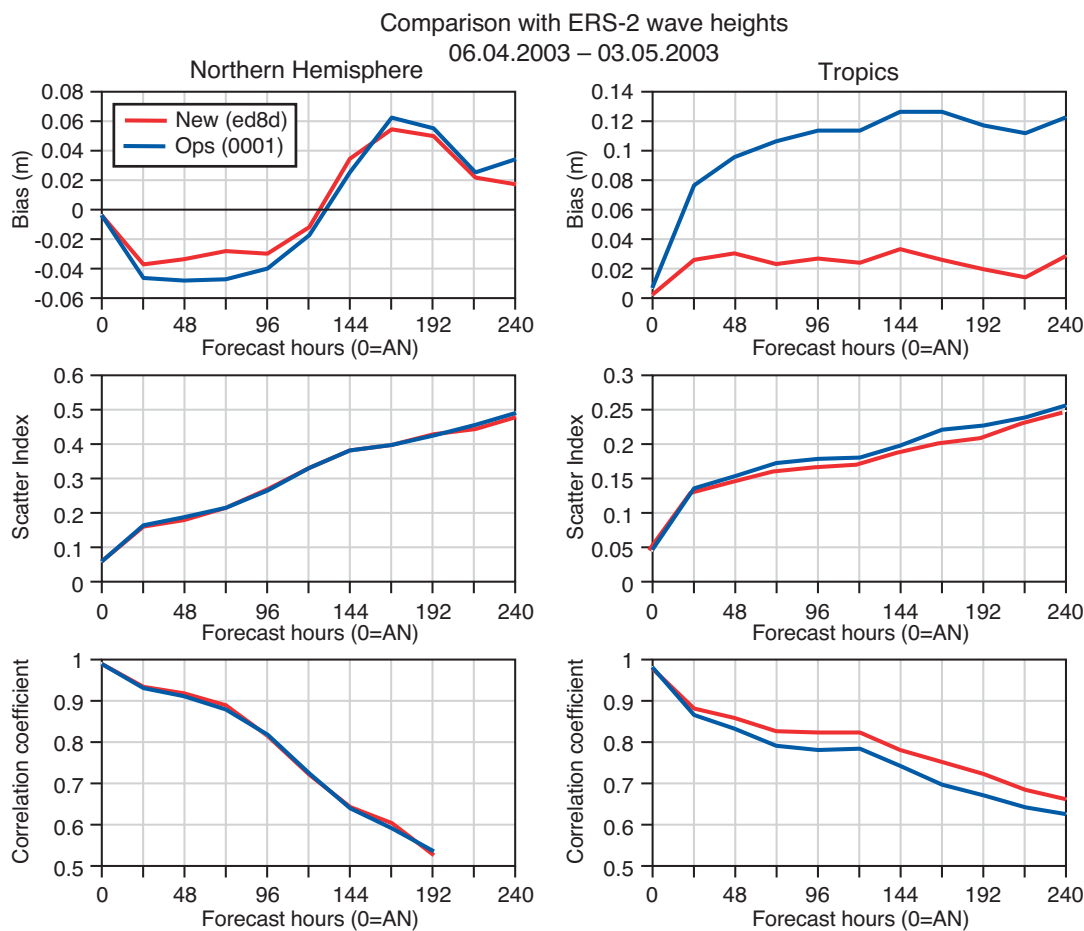

Fig. 11 Wave height scores against ERS-2 altimeter wave heights for the Northern Hemisphere (NH) and the tropics. The reference is operation (0001) and the new model uses neutral winds, unresolved bathymetry and new stress tables.

the global mean impact of using neutral winds was an increase in mean wave height, this change was further tested in combination with the previous change for the unresolved bathymetry because it had the opposite effect on wave height model.

Finally, unrealistic large values of the Charnock parameter were removed following refinement in the stress tables used by the wave model. A bug was also removed in the interpolation of the Charnock parameter from the wave model grid to the atmospheric grid for the current EPS resolution with a minor improvement of the wave model forecasts at that resolution (*Bidlot* 2003).

The three changes described above were combined into a single coupled analysis experiment and compared to operation. Wave forecast scores can be obtained by either comparing the forecasts with ERS-2 data or with the verifying analysis. Figure 11 shows that the new system performs remarkably better in the tropics without any detrimental effect on the Northern Hemisphere when compared to ERS-2 data. A similar conclusion can be reached when the results are assessed against their own analysis (not shown). The usual atmospheric scores are mostly neutral.

Overall impact

Altogether, 99 cases were accumulated to validate the cycle 28r1 package. The relatively small test sample (as compared to the extensive validation of Cycle 26r3) is justified by the overall more modest modifications brought to the assimilation and forecasting system. Confirming the above, Cycle 28r1 showed a large positive impact over operations for the wave height scores. Concerning the atmospheric scores (evaluated through verification of forecasts against analysis and corresponding statistical significance tests) , the impact was overall neutral, with the noticeable exception of the day-3 forecast over Northern Hemisphere and Europe for which Cycle 28r1 was better than the operational suite with a 95% confidence (t-test). Cycle 28r1 was subsequently introduced operationally on 9 March 2004.

Acknowledgements

Jean-Noël Thépaut, Erik Andersson, Anton Beljaars, Mariano Hortal and Peter Janssen

References

Andersson, **E.** and **A. Garcia-Mendez**, 2002: Assessment of European wind profiler data, in an NWP context. *ECMWF Tech. Memo.*, **372**, pp 14.

Andersson, **E**., **E. Hólm** and **J-N. Thépaut**, 2004: Impact studies of main types of conventional and satellite humidity data. Proc. 3rd WMO Workshop on 'The Impact of Various Observing Systems on NWP', Alpbach, Austria, 9-12 March 2004. pp XX. (*In press*).

Bidlot, **J-R.**, 2003: Corrupted Charnock parameter in the EPS configuration. *Research Department Memorandum* **R60.9/JB/0399**.

Bidlot, **J-R**. and **P. Janssen**, 2003: Unresolved bathymetry, neutral winds and new stress tables in WAM. Research Department Memorandum **R60.9/JB/0400**.

Bouttier, **F.**, 2001: The use of profiler data at ECMWF. *Meteorologische Zeitschrift*, **10**, 497-510.

Dee, **D.P.**, and **A.M. Da Silva**, 2003: The choice of variable for atmospheric moisture analysis. *Mon. Wea. Rev.*, **131**, 155-171.

Drusch, **M**., **D. Vasiljevic** and **P. Viterbo**, 2004: ECMWF's global snow analysis: Assessment and revision based on satellite observations. *Journal Appl. Met.* (Accepted)

Hólm, **E**., **E. Andersson**, **A. Beljaars**, **P. Lopez**, **J-F. Mahfouf**, **A.J. Simmons** and **J-N. Thépaut**, 2002: Assimilation and modelling of the hydrological cycle: ECMWF's status and plans. *ECMWF Tech. Memo.*, **383**, pp 55.

Hortal, **M.** and **A. Untch**, 2003: A new interpolation for the vertical computation of the semi-Lagrangian trajectory. *ECMWF RD Memo* **R60.5/MH/0415**, available from ECMWF.

Janisková, **M.**, **Mahfouf**, **J-F.**, **Morcrette**, **J-J**. and **Chevallier**, **F**. (2002): Linearized radiation and cloud schemes in the ECMWF model: Development and evaluation, *Q.J.R. Met. Soc.*, **128**, 1505-1527.

McNally, **A.P**. and **P.D. Watts**, 2003: A cloud detection algorithm for high spectral resolution sounders. *Q.J.R. Met. Soc.*, **129**, 3411-3423.

Nash, **J**., 2003: Review of test results on the accuracy of radiosonde relative humidity sensors. Proc. *ECMWF/GEWEX workshop on 'Humidity Analysis'*, Reading, UK, 8-11 July 2002, 117-123.

Szyndel, **M**., **J-N. Thépaut** and **G. Kelly**, 2004: Developments in the assimilation of geostationary radiances at ECMWF. *EUMETSAT/ECMWF fellowship programme report.* Available from EUMETSAT.

Tanre, **D**., **Geleyn**, **J-F**. and **Slingo**, **J**. (1984): First results of the introduction of an advanced aerosol-radiation interaction in the ECMWF model, in: Aerosols and their climate effects, H.E. Gerber and A. Deepak, Eds., *A. Deepak Publ.*, Hampton, Va, 133-177.

Tegen, **L.P**., **Hoorigl**, **P**., **Chin**, **M**., **Fung**, **I**., **Jacob**, **D.** & **Penner**, **J**. (1997): Contribution of different aerosol species to the global aerosol extinction optical thickness: Estimates from model results, *J. Geophys. Res.*, **102D**, 23895-23915.

25 years since the first operational forecast

The following is John Hennessy's personal account of the early days of computing at ECMWF, and of the difficulties in successfully producing the first operational medium-range forecast 25 years ago.

```
Subject:   The issue of ECMWF's first
           operational forecast
To:        All members of staff
Date:      2 August 1979
From:      J. Labrousse

Last night marked an important milestone in the
development of the Centre's work and activity.
Despite a number of 'technical hitches', a medi-
um-range operational forecast based on data of
12Z, 1 August was completed, and the results
were available in real-time to some at least of
our Member States. Products in chart form (1000
and 500 mb fields for days 0 to 7) were trans-
mitted via facsimile to the Meteorological
Office at Bracknell, who then relayed them to
France and Germany. Copies of the same charts
have also been mailed to the other Member
States. Attempts were also made to send the
products in grid-point form over the low-speed
telecommunications link to Spain.

The Centre has received acknowledgement of and
congratulations on its efforts from both Germany
and France by telex; a translation of these mes-
sages is attached.

I know that many in recent months have been work-
ing very long hours to ensure that our long-
planned goal of beginning operational activity
in the middle of 1979 was achieved, and I would
take this opportunity to express my apprecia-
tion to all staff who have contributed towards
the production of the operational forecasting
system. This is a major step forward and will
be welcomed enthusiastically by our Member
States. There remain the major objectives of
improving the meteorological quality of our
products and our operational reliability, so
that Member States will learn to trust and use
our forecasts in the manner anticipated when the
Centre was established.
```

Memo issued by the Head of Operations

```
Today Deutscher Wetterdienst received the first
products from the Centre, to be used as guid-
ance in medium-range forecasting for the public.
Being fully aware of all the problems the Centre
has had to overcome before this goal was
reached, Deutscher Wetterdienst congratulates
the Director and all staff of the Centre, and
wishes all success for the work to come; it will
be of benefit to all in Europe who are inter-
ested in the weather.
```

Text of message received from Dr. Lingelbach, Director of Deutscher Wetterdienst.

```
We thank you for the reception of the first set
of forecast charts produced by the Centre, and
we express our warm congratulations to you for
the work accomplished.
```

Text of message received from M. Gosset (for M. Mittner, Director of Meteorologie Nationale)

Jean Labrousse, then Head of Operations, sent this memorandum to all staff after completion of the Centre's first operational forecast just over 25 years ago, and messages of appreciation were received from Germany and France – at that time, of course, email was not available. The memorandum itself looks a bit dated today: the use of SI Units had not become standard at ECMWF (mb instead of hPa), Zulu time was still in use (12Z) instead of Universal Time Coordinated (UTC), and there is reference to 'telex' (teleprinter exchange), a now obsolete communication method.

The night of 1–2 August 1979 was certainly historic. I was delighted to be part of it and stayed at ECMWF overnight to be on hand to help with any problems that might arise with the operational suite, particularly with the dissemination; we had never had the opportunity for an end-to-end test with a Member State. The way in which an on-call system might be implemented was far from resolved. All went well to start with. The taxi with the observational data in 'raw' GTS format (character codes of the World Meteorological Organization as transmitted on the Global Telecommunication System) on magnetic tape arrived on time from the United Kingdom Meteorological Office in Bracknell, the preprocessing ran normally and so did the analysis cycles. Problems started with the forecast-model run; it got slower and slower. I had visions of it taking 12 days, which was as long as it took on the CDC 6600 (ECMWF's earlier model-development computer). However, the Systems Section had upgraded the CRAY operating system to level COS 1.3 on 1 August and had informed me of this that afternoon. This was obviously the prime suspect for the problems. At my request the shift leader took a memory dump, dropped the operating system and reloaded the previous version. We restarted the suite, and the rest is history. Initially, although the analysis cycles were run over weekends, forecasts were run only from Monday to Friday. Daily running of the forecast did not begin until 1 August 1980. The forecast run-time then was about five hours. This is a far cry from the 47 minutes 30 seconds for the forecast run for 14 May 1999, which is I believe the fastest ever operational run of the forecast, achieved because we were trying to make up for delays; we ran the forecast on 48 Processing Elements on the Fujitsu VPP5000.

Prior to this, some trial medium-range forecasts had been carried out on a semi-operational basis, using one-day-old data. The first phase of EMOS (ECMWF's Meteorological Operational System) had not yet been completed; this meant considerable manual intervention in running jobs to produce the forecasts. A series of these forecasts was prepared for the

official opening of ECMWF on 15 June 1979, and charts displayed. These trial forecasts 'showed useful skill from a forecaster's point of view'.

The years preceding this first operational run were very busy in designing and implementing system and application utilities. ECMWF staff were in temporary office accommodation in Bracknell until the end of 1978, first in Fitzwilliam House and John Scott House, which housed the CDC 6600 computer, and later also in Brandon House. As well as housing the computer, John Scott House was the venue for the Centre's social gatherings. Staff had to push back the furniture and cardpunch machines to make room for the guests, and then restore everything before leaving at the end of the evening. Despite having three separate buildings, ECMWF did not (unlike now) provide umbrellas for staff moving between buildings, but they did provide heavy-duty plastic bags, complete with the ECMWF name and logo, so that precious line-printer output and plots did not get wet.

ECMWF's first Invitation to Tender, ITT(76)1, was issued in mid-July 1976 for 'the acquisition and installation of a powerful computer system'. The ITT makes very interesting reading nowadays. The volume of observational data to be handled could be as high as 4 megabytes a day, the ten-day forecast was to be run in 10 hours and the volume of data (observations, analyses and forecast) to be archived was estimated at 32 megabytes per day. Among the test programs to be executed by computer vendors were tests for card reader, card punch and line printer. As a result of this ITT, the CRAY-1 and CDC Cyber 175 were selected, but no telecommunication system. The CRAY-1 was the only machine capable of running the forecast model in the required time, but was not designed for stand-alone operation, and so the Cyber 175 front-end kept all the permanent files and did the general housekeeping.

A separate ITT was issued in July 1977 for the telecommunication system and a graphical display system. A temporary installation of a limited configuration of the CRAY and Cyber systems was made at Rutherford Laboratory (some 50 kilometres away)–the CRAY-1 in November 1977 and the Cyber 175 in January 1978–with the machines being run by the Centre's operators. Remote Job Entry terminals in Fitzwilliam House and John Scott House were connected to the Cyber 175 and it was possible to submit jobs to both the CRAY-1 and the Cyber. The line printer in Fitzwilliam House was notorious for building up a large charge of static electricity and it was quite common for users to touch it with a coin to minimize the shock before attempting to remove the paper. As the link between the CRAY-1 and Cyber systems was not developed at this time, CRAY jobs submitted to the Cyber were staged to magnetic tape. At intervals these jobs were manually transferred to the CRAY-1 via the tape unit on the CRAY operator station. A regular courier service also ran between Rutherford and Bracknell to take jobs with large numbers of cards and bring back large amounts of printed output and plots. It was a relief when the Cyber was moved to Shinfield and a new CRAY-1 was delivered there also, with a fully linked system being put together towards the end of 1978. On 12 November the

operators working at Rutherford came to Shinfield and, as many had only spoken to each other on the telephone and had not met before, many people recognised each other only when they spoke.

The telecommunication system finally arrived in early 1979. It was known as the Network Front End Processor (NFEP). Software was developed by Service in Informatics and Analysis and the hardware was a Regnecentralen RC 8000 computer. The NFEP interfaced to the Cyber 175 by emulating a CDC Remote Job Entry terminal. For lines to Member States the communication protocols were based on the (then new) CCITT Recommendation X25 and the IFIP proposal. Following installation there were further delays in doing the provisional acceptance tests, as there were problems in the modules in medium-speed line connections. There were also delays in the provision of the actual circuits themselves. The complete computer system then consisted of three different machines with three different operating systems, three different word lengths, three different byte lengths and two different character sets, all communicating with each other in a number of different ways.

While all this was going on, work was also in progress on the various components of EMOS–ECMWF's Meteorological Operational System. The cornerstone of EMOS was the design and development of the Supervisor, known now as SMS–Supervisor Monitor Scheduler. Today's SMS is a far cry from the original in its implementation, but the fundamental principles have not changed, with families, tasks, events and messages all defined in the original SMS. SMS ran at a system control point on the Cyber 175 and this enabled it to communicate with other suite (user) jobs. Events and messages were communicated between the CRAY-1 and Cyber by means of file transfers. Control of SMS was by the Control Display Program (CDP), a command-line interface to a teletype terminal. Only the operational suite was controlled by SMS, whereas nowadays SMS is used to control and run research experiments as well. SMS has been developed from a Teletype, a line-mode system running one suite on two machines, to an X-based system capable of controlling multiple suites running on many machines.

As you will have gathered, the data acquisition system initially consisted of magnetic tapes delivered by taxi from Bracknell. The original plan was that ECMWF would use decoded and quality-controlled observational data from up to three national meteorological centres, the data to be transmitted in a compact form on 4800 bps lines. Each national centre would send two thirds of the data on the GTS, so that ECMWF would receive two copies of all observations. No decoding or quality-control programs would be needed at ECMWF and this would avoid 'duplication of effort'. Later this plan was amended, and the input observational data were designated to be received from Bracknell and Offenbach in raw GTS format. Early 1980 saw the data arrive in near real-time over a 2400 bps line from Bracknell, and later in the year from Offenbach as well. Files of observations contained up to 250 bulletins; less than 250 occurred when 20 minutes had elapsed since the previous transmission. On the NFEP, a batch job was prepared for the Cyber

with the observation file attached as input. On the Cyber, this job added the new bulletins to those already received– I say add, but initially this was not possible. The existing file of bulletins had to be read and written to a new file, and it was to this new file that the new data were then written. All observations at this time were in WMO character codes. As the volume of satellite data increased, compressed binary codes became essential, but the GTS used character-oriented protocols. A method was devised to transmit binary data over the line from Washington. The six least significant bits of each 8-bit character were used to transmit a 6-bit segment of binary data in a series of pseudo-ASCII characters. This started in 1984 and was used for many years until replaced by BUFR–coded data.

The preprocessing system decoded and quality controlled the observations. These were interesting decoding programs based on programs from the French National Meteorological Service. The incoming observations were in ASCII (CCITT Alphabet No. 5), but the Cyber had its own Display Code characters in six-bit bytes and so a lot of bit manipulation was necessary, the ASCII characters being stored in 12 bits (2 bytes) on the Cyber. Most of the code was in assembler language but some was in Fortran 66, a language that had no character type. This came only with Fortran 77 and the second generation of decoding programs was written entirely in Fortran 77, the first programs in the Centre in that language. The quality-control programs were adapted from those of the Swedish Meteorological and Hydrological Institute. A rudimentary 'reports data base' held the decoded and quality-controlled observations in a compact format, and from this database extractions were made for the analysis cycles.

Post-processing of the forecast model output generated dissemination products for the Member States. At that time there was not the flexibility for specifying required products that there is today. ECMWF had a fixed catalogue of products, with fixed areas and resolutions. Initially only products up to seven days were disseminated. The format of products was either the WMO GRID code or a compact bit-oriented grid code designed at ECMWF-no GRIB or BUFR machine-independent formats were available in those days. This ECMWF bit code continued for many years, and it was not until just before operations were switched to the Fujitsu VPP700 in 1996 that the last dissemination products in this code were issued. Files of analysis and forecast data were sent to the NFEP for onward transmission to the Member States. The NFEP had to distinguish between batch-job outputs and dissemination files. All dissemination files had unique names involving date/time, but all started with NBO. The NFEP software looked at file names and when a file with a name starting with NBO (Not Batch Output) was encountered the first one or two records of the file was read to ascertain where to send it and what the transmission filename was. Country addresses were simply a single letter. A batch job, on punch cards, provided the repeat dissemination facility, with the operators having to punch two cards, one with country address letter and the other with the product catalogue numbers. An interesting event occurred in September 1991 when the Americans received forecasts from ECMWF for 2091. GRIB Edition 1, with century of data included in the headers, was used for the first time and the trans-Atlantic software interpreted century as the first two digits of the year!

An archive system was developed to store the operational data, both observations and fields, and to make it available to general users. The data were stored on magnetic tapes on the Cyber in a compressed format. A general-purpose retrieval procedure called GETDATA was provided to access the data on the Cyber. The early archives had a number of gaps; we discovered that one of the programs storing the data occasionally ran into difficulty. Unfortunately, when it did it printed a message saying that the archiving had not completed fully and then issued a stop command instead of an abort. Consequently nobody was aware of the failure when it occurred.

As GETDATA began to show its age, a data-handling project was set up in 1982 and this produced MARS (Meteorological Archival and Retrieval System) based on CFS (now HPSS). This was essentially 'client/server architecture' before the name had been invented–indeed client/server architectures did not appear in any great numbers until the late 1980's. We are all familiar today with 'predictive-texting' for mobile telephones, but from day–1 the MARS language also had such predictive ability. Not everybody found the transition to MARS a smooth one. One Member State user wrote "The phrase 'user-friendly' was not uppermost in my mind as I read the MARS User Guide (perhaps it is friendly for Martians)". The author has wisely remained anonymous. – "The MARS system, as it exists now, is a giant step backwards from GETDATA (which is far from perfect anyway)". I admit to being the author.

It was a totally different working environment in the early years. All documentation had to be handwritten (with hand-drawn diagrams) before being given to the secretaries for typing. There were no desktop terminals or word processors. All programs were written in FORTRAN or assembler language. FORTRAN had a fixed format, a maximum of six characters for variable names and no lower-case letters were allowed. The program code had to be hand written on special forms before putting it into an input tray at Computer Reception for punching onto cards. Inevitably there were always errors in the punch cards due to poor handwriting and not sticking to the conventions for Z and 7 and letter O and zero. It was quite normal to have several attempts at running jobs before all punching errors were eliminated.

There was a very significant improvement in productivity in programming when the 'alphanumeric VDUs ' became generally available. The introduction of the VDUs was gradual, and at the start of 1979 only 12 were in use with one 'graphical VDU' supported. Using VDUs, some EMOS documentation was produced by typing the text as comments in a FORTRAN program, doing a compilation and listing and trimming the resulting line-printer output which had a page-width of 132 characters.

Twenty-five years is a long time, especially in computing and related areas. Today, ECMWF's supercomputers are roughly equivalent to 20,000 CRAY-1 systems. Changes

elsewhere have been equally dramatic. Telecommunications (with modems the size of suitcases) have come from one 50-baud line to the Regional Meteorological Data Network (RMDCN) combining ECMWF's network with that of WMO in Europe with also a very fast connection to the INTERNET. The volume of observational data has increased enormously, largely due to more and more satellite data, and now stands at about 2 gigabytes per day. My recollection is that on the first night we disseminated 27 products. Now the volume and number of products disseminated to Member States, the GTS and others via the INTERNET stands at about 33 gigabytes and more than 2 million individual products. Graphical output was from one electrostatic plotter, now there are colour three-dimensional plots and movies, all available on the office desktops as well as on hard copy and the World Wide Web. Printing has also been revolutionized from a simple line printer (upper-case letters only) to colour, double-sided printing, with the ability to include graphics as well as text. There have been staggering changes in 25 years. Will the next 25 years bring as many changes as have occurred since the pioneering days?

John Hennessy

61st Council session on 13–14 December 2004

Chaired by Anton Eliassen, the ECMWF Council held its 61st session in Reading on 13–14 December 2004. The Council approved a 2% increase in the Budget 2005 giving the Director flexibility to implement it. Other main results of this session were:

Amendments to the ECMWF Convention

The Council unanimously adopted recommendations of the Policy Advisory Committee for amending the Convention with regard to the issue of languages at the Centre. This proposal does not alter the amendments to the Convention already adopted at Council's 60th session in June 2004.

To formally adopt the Amending Protocol, Council will convene an extra-ordinary session in April 2005. Thereafter, the official ratification process in the ECMWF Member States will start.

Co-operation Agreements

The Director was authorised by Council to conclude a Co-operation Agreement with the Republic of Lithuania and to sign Agreements with the European Space Agency (ESA) and the Convention on Long-Range Transboundary Air Pollution (CLRTAP).

Regional Meteorological Data Communications Network

The Council agreed on the extension of the RMDCN contract with Equant to March 2009. Amendments to the contract will allow for a migration from Frame Relay to Multi Protocol Label Switching as well as a doubling of the access capacity for current RMDCN members. A new standard connection of 768 kbps (at present 384 kbps) will be provided to each ECMWF Member State.

Computing

The Director was authorised to extend the current contract with IBM to cover supply of an enhanced High Performance Computing Facility until March 2009. This will result in the installation of a Phase 4 of the IBM system in Spring 2006 with an aggregated sustained performance of 4.5 teraflops.

Four-Year Programme

The Council unanimously adopted the four-year programme of activities. Its main goals are:
◆ continue to extend the skill of both deterministic and probabilistic medium-range forecasts at the rate of one day per decade;
◆ extend the range of reliable forecasts of severe weather over land and sea towards day 4 and day 5;
◆ develop a unified Ensemble Prediction System merging the medium-range EPS and the monthly forecasting system;
◆ continue the development of a multi-model seasonal/long-range prediction system;
◆ improve the timeliness and reliability of product dissemination, and the availability of the computer facilities to the Member States.

Products of the Centre

The Council decided that
◆ a Member State, on a case-by case basis, may delegate to ECMWF the provision of real-time products with the understanding that the licensing will remain with the Member States;
◆ ECMWF can respond directly to any requests for real-time products from outside the ECMWF territory;
◆ the Director may allow, on a case-by-case basis, for research and education the cross border re-distribution of archived data to registered users.

Scientific Advisory Committee

Prof. M. Ehrendorfer from Austria and Prof. H. Kelder from The Netherlands were appointed members of the Scientific Advisory Committee for a first term of four years. Dr. L. Cavaleri from Italy was appointed for a second term.

MARS reaches one Petabyte

On 17 October 2004, the Centre's meteorological archive (MARS) reached the symbolic size of one Petabyte(*) of primary data, for a grand total of 8.6 billion meteorological fields. MARS contains mainly model outputs, from operational runs, research experiments and projects, such as the ECMWF 40-year reanalysis, ERA-40 (see

ECMWF Newsletter 101 Summer/Autumn 2004). Past studies have shown that the size of the Centre's archive is proportional to the power of its supercomputer. At the current rate of growth the next significant milestone of one Exabyte should be reached in 2019.

(*) 1 Petabyte represents 1024 Terabytes or 2^{50} bytes.

Baudouin Raoult

ECMWF Calendar 2005

Feb 7-Mar 11 – Computer User Training Course

Feb 7-8	COM SMS	Introduction to SMS/XCDP
Feb 21-25	COM INTRO	Introduction for new users/ MARS
Feb 28-Mar 1	COM MAG	MAGICS
Mar 2-4	COM MV	METVIEW
Mar 7-11	COM HPCF	Use of supercomputing resources

Mar 1-4   Workshop on TIGGE (THORPEX Interactive Grand Global Ensemble)

Mar 14-May 25 – Meteorological Training Course

Mar 14-18   Use and Interpretation of ECMWF Products *(and see June 6-10)*

Apr 4-8   Predictability, diagnostics and seasonal forecasting

Apr 11-21   Parametrization of diabatic processes

May 4-13   Data assimilation and use of satellite data

May 16-25   Numerical Methods, adiabatic formulation of models

April 18-19	Finance Committee	74th
April 19-20	Advisory Committee on Data Policy	6th
April 21-22	Policy Advisory Committee	22nd
April 22	Council (Extra-ordinary session)	62nd

May 17-18	Security Representatives' meeting
May 19-20	Computer Representatives' meeting
June 6-10	Use and interpretation of ECMWF Products *(and see March 14-18)*
June 6-10	Workshop – Representation of sub-grid processes using stochastic-dynamic models
June 13-14	Council 63rd
June 15-17	Forecast Products – Users Meeting
Sept 5-9	Seminar – Global Earth-System Monitoring
Oct 3-5	Scientific Advisory Committee 34th
Oct 5-7	Technical Advisory Committee 35th
Oct 10-14	Use & interpretation of ECMWF products – Meteorological Training Course for WMO Members
Oct 17-18	Finance Committee 75th
Oct 19-20	Policy Advisory Committee 23rd
Nov 8-11	ECMWF/NWP-SAF Workshop on bias estimation and correction in data assimilation
Nov 14-18	10th Workshop on Meteorological Operational Systems
Dec 6-7	Council 63rd

ECMWF publications

(see http://www.ecmwf.int/publications/library/ecpublications/)

Technical Memorandum

451   **Benedetti**, **A**., **P. Lopez**, **E. Moreau**, **P. Bauer**: Verification of TMI-adjusted rainfall analysis of tropical cyclones at ECMWF using TRMM Precipitation Radar observations. *October 2004*

450   **Cardinali**, **C**., **S. Pezzulli** & **E. Andersson**: Influence matrix diagnostic of a data assimilation system. *October 2004*

449   **Shutts**, **G.**: A stochastic kinetic energy backscatter algorithm for use in ensemble prediction systems. *August 2004*

448   **Benedetti**, **A**., **P. Lopez**, **P. Bauer** & **E. Moreau**: Experimental use of TRMM precipitation radar observations in 1D+4D-Var assimilation. *August 2004*

446   **Yeung**, **L.H.Y.** , **E.S.T. Lai**, **Q.C.C. Lam**, **P.K.Y. Chan**, & **P. Cheung**: Performance and application of ECMWF EPS forecasts in the prediction of heavy rain and high winds in Hong Kong. *July 2004*

445   **Isaksen**, **L**., **M**. **Fisher** & **E. Andersson**: The structure and realism of sensitivity perturbations and their interpretation as 'key analysis errors'. *August 2004*

444 **Drusch**, **M.**, **E.F. Wood**, **H. Gao** & **A. Thiele**: Soil moisture retrieval during the Southern Great Plains Hydrology Experiment 1999: A comparison between experimental remote sensing data and operational products. *June 2004*

443 **Drusch**, **M.**, **D. Vasiljevic** & **P. Viterbo**: ECMWF's global snow analysis: Assessment and revision based on satellite observations. June 2004

442 **Meetschen**, **D.**, **B. van den Hurk**, **F. Ament** & **M. Drusch**: Optimized surface radiation fields derived from METEOSAT imagery and a regional atmospheric model. *July 2004*

441 **Ricci**, **S.**, **A.T. Weaver**, **J. Vialard** & **P. Rogel**: Incorporating state-dependent temperature-salinity constraints in the background error covariance of variational ocean data assimilation. *June 2004*

440 **Bourke**, **W.**, **R. Buizza** and **M. Naughton**: Performance of the ECMWF and the BoM ensemble systems in the Southern Hemisphere. *May 2004*

ERA-40 Project Report Series

17 **Kållberg**, **P.**, **A. Simmons**, **S. Uppala** & **M. Fuentes**: The ERA-40 archive. *September 2004*

Contract Reports to the European Space Agency

Janisková, M: Impact of EarthCARE products on numerical weather prediction. July 2004

Dethof, A: Monitoring and assimilation of MIPAS, SCIAMACHY and GOMOS retrievals at ECMWF. November 2004

Watts, **P.D.**, **A.P.** **McNally**, **J-N**. **Thépaut**, **M. Matricardi**, **R.J. Engelen** & **N. Bormann**: Measurement of seasonal CO_2 fluctuations from space. *October 2004*

Workshop Proceedings

ECMWF workshop on assimilation of high spectral resolution sounders in NWP. *28 June-1 July 2004*

Ninth workshop on meteorological operational systems. *10-14 November 2003*

Seminar Proceedings

Recent developments in numerical methods for atmospheric and ocean modelling. *6-10 September 2004*

New items on the ECMWF web site

MARS Archive Parameter Data

A database of all meteorological parameters that are in use at ECMWF and stored in our MARS data archive is now available.

http://www.ecmwf.int/services/archive/d/parameters

High Performance Computing Workshop 2004

The biennial High Performance Computing in Meteorology workshop was held in October at ECMWF. It featured presentations from meteorological and research institutions around the world and computer manufacturers such as Cray, IBM, Intel, Fujitsu, NEC and SGI.

http://www.ecmwf.int/newsevents/meetings/workshops/2004/high_performance_computing-11th/

ECMWF High Performance Networking Workshop

ECMWF held the workshop for High-Performance Technology in Local Area Networks on in September. The objective of the workshop was to bring together users and vendors of high-performance networking and interconnect technologies and share thoughts on the technology deployments, trends and future directions with European focus.

http://www.ecmwf.int/newsevents/meetings/workshops/2004/High_Performance_Networking/

ECMWF/ELDAS Workshop

The closing workshop for the European Union project ELDAS (Development of a European Land Data Assimilation System to predict Floods and Droughts) was held in November at ECMWF

http://www.ecmwf.int/newsevents/meetings/workshops/2004/ELDAS_Land_surface_assimilation/

EU Research projects

Two new European Union project web sites are available on the ECMWF Web Site under both the Framework 5 and 6 Programmes.

– ECMWF is hosting Research Theme 1 (RT1) of the ENSEMBLES project, coordinated by Paco Doblas-Reyes at ECMWF which will be the development of the Earth System Model. The ENSEMBLES project, co-ordinated by Dave Griggs, Director of Climate Research at the Met Office, aims to develop an ensemble prediction system for climate change based on the principal state-of-the-art Earth System models developed in Europe, validated against gridded datasets, to produce for the first time, an objective probabilistic estimate of uncertainty in future climate at the seasonal to decadal and longer timescales.

http://www.ecmwf.int/research/EU_projects/ENSEMBLES/

– The HALO project, coordinated by Tony Hollingsworth at ECMWF, will coordinate the architecture and system integration for the interacting parts of the Atmosphere, Land and Ocean thematic integrated projects (IP) in GMES, the Global Monitoring for Environment and Security initiative. Presentations from the HALO workshop, held in November, are available.

http://www.ecmwf.int/research/EU_projects/HALO/

Index of past newsletter articles

This is a list of recent articles published in the ECMWF Newsletter series.
Articles are arranged in date order within each subject category. Articles can be accessed on the ECMWF public web site

http://www.ecmwf.int/publications/newsletter/ index.html

Useful names and telephone numbers within ECMWF

Telephone number of an individual at the Centre is:

International: +44 118 949 9 + three digit extension
UK: (0118) 949 9 + three digit extension
Internal: 2 + three digit extension

e.g. the Director's number is:
+44 118 949 9001 (international),
(0118) 949 9001 (UK) and 2001 (internal).

E-mail
The e-mail address of an individual at the Centre is:
firstinitial.lastname@ecmwf.int

e.g. the Director's address is: D.Marbouty@ecmwf.int

For double-barrelled names use a hyphen
e.g. J-N.Name-Name@ecmwf.int

Internet web site
ECMWF's public web site is: http://www.ecmwf.int

	Ext
Director	
Dominique Marbouty	001
Deputy Director & Head of Administration Department	
Gerd Schultes	007
Head of Operations Department	
Walter Zwieflhofer	003
Head of Research Department	
Philippe Bougeault	005
ECMWF switchboard	000
Advisory	
Internet mail addressed to Advisory@ecmwf.int	
Telefax (+44 118 986 9450, marked User Support)	
Computer Division	
Division Head	
	050
Computer Operations Section Head	
Sylvia Baylis	301
Networking and Computer Security Section Head	
Matteo Dell'Acqua	356
Servers and Desktops Section Head	
Richard Fisker	355
Systems Software Section Head	
Neil Storer	353
User Support Section Head	
Umberto Modigliani	382
User Support Staff	
John Greenaway	385
Norbert Kreitz	381
Dominique Lucas	386
Carsten Maaß	389
Pam Prior	384
Computer Operations	
Call Desk	303
Call Desk email: cdk@ecmwf.int	
Console – Shift Leaders	803
Console fax number ☎ 44 118 949 9840	
Console email: newops@ecmwf.int	
Fault reporting – Call Desk	303
Registration – Call Desk	303
Service queries – Call Desk	303
Tape Requests – Tape Librarian	315
Software libraries (eclib, nag, etc.)	
John Greenaway	385

	Ext
ECMWF library & documentation distribution	
Els Kooij-Connally	751
Meteorological Division	
Division Head	
Horst Böttger	060
Applications Section Head	
Alfred Hofstadler	400
Data and Services Head	
Baudouin Raoult	404
Graphics Section Head	
Jens Daabeck	375
Operations Section Head	
François Lalaurette	420
Meteorological Analysts	
Antonio Garcia Mendez	424
Federico Grazzini	421
Anna Ghelli	425
Meteorological Operations Room	426
Data Division	
Division Head	
Adrian Simmons	700
Data Assimilation Section Head	
Erik Andersson	627
Satellite Section Head	
Jean–Nöel Thépaut	621
Reanalysis Project (ERA)	
Saki Uppala	366
Probability Forecasting & Diagnostics Division	
Division Head	
Tim Palmer	600
Seasonal Forecasting Head	
David Anderson	706
Model Division	
Division Head	
Martin Miller	070
Numerical Aspects Section Head	
Mariano Hortal	147
Physical Aspects Section Head	
Anton Beljaars	035
Ocean Waves Section Head	
Peter Janssen	116
Education & Training	
Renate Hagedorn	257
GMES Coordinator	
Anthony Hollingsworth	824